Project Number: 248267
Project acronym: BuNGee
Project title: Beyond Next Generation Mobile Networks

BuNGee Deliverable: D4.1.2

Simulation Tool(s) and Simulation Results

Due date of deliverable: <30/04/2012>
Actual submission date: <07/06/2012>

Start date of project: January 1, 2010	**Duration**: 30 months
Lead Participant: University of York **Contributors:** See page 3 **Release number:** 1.0 **Keywords:** BuNGee, System-level Simulation, 1Gbps/km^2, Capacity Density, Architecture, Multi-Beam Directional Antenna, RRM, MIMO, MBA-MIMO, Cognitive Radio	
Project co-funded by the European Commission within the Seventh Framework Programme (2007-2013)	
Dissemination Level: Public	

The research leading to these results has received funding from the European Community's Seventh Framework Programme (FP7/2007-2013) under grant agreement n 248267

Executive Summary

This report describes the work on Task 4.1 of the BuNGee project 'Deployment/System Simulation'. The system-level simulation models the main features of the BuNGee system based on the proposed BuNGee Architecture as detailed in D1.2 [1] as well as the advanced techniques developed in other BuNGee work packages. The results of the system-level simulation are provided in this report as an indication of the system performance.

The details of the simulator are provided in this report. A two layer simulator has been developed to capture the features of BuNGee's two-hop system architecture. The first layer models the self-backhaul link between HBS and HSS. The second layer models the access link between ABS and MS. The modelling of the BuNGee system is a very complex task that needs to address a range of issues in the physical, MAC and network layers. A modularized structure is used in designing the simulator to maximize the flexibility of the simulator and its compatibility with future developments. A number of modules are developed to model different aspects of the system, including a location function, traffic function, propagation function, MIMO function and RRM function. The assumptions that have been made are also described in this report.

The scenario, system assumptions and deployment topologies used are derived from the BuNGee system specification described in BuNGee deliverable D1.2 [1]. The multi-HBS backhaul network propagation environment has been simulated by UCL as part of WP2 and the results are provided to the system-level simulation. A number of WINNER II propagation models are applied to estimate the path loss between entities in the access network and the path loss between backhaul entities and access entities [2]. The 3D antenna patterns of the HBS antenna, HSS antenna and ABS antenna are provided by CASMA [3]. Collaboration has been carried out at UY between WP2 and WP4 to develop a MIMO-Truncated Shannon Bound function, and the MIMO techniques proposed by WP2 are incorporated into the system-level simulation.

Two RRM approaches are simulated in the system-level simulation: the frequency planning proposed by Alvarion and a basic cognitive radio approach. In an outdoor MS only scenario, an overall throughput density above 2Gbps/km^2 can be achieved using Multi-Beam Assisted MIMO and fixed frequency plan. Under the same outdoor MS only assumption, a 1.05 Gbps/km^2 throughput density is achieved by using point-to-point MIMO with frequency planning. In addition we consider a scenario in which users are uniformly distributed throughout the coverage area at ground level. This is highly pessimistic since most users within buildings are likely to be close to the street, and many will be on higher floors where the signal is much stronger. In this pessimistic case the overall throughput may be reduced to 0.85Gbps/km^2. A basic cognitive radio approach has also been modelled where a spectrum sensing function is assumed at the receiver. The cognitive radio approach is able to reduce the RRM complexity by completely removing the requirement for frequency plan. The basic cognitive radio is able to significantly reduce the system delay in the indoor+outdoor MS scenario while achieving a similar 0.85Gbps/km^2.

It is clear that the 1Gbps/km^2 target can be achieved and the RRM complexity can be reduced by applying the advanced techniques developed in BuNGee. The throughput density can be increased even further, to as high as 2Gbps/km^2 even in a pessimistic case, by applying Multi-Beam Assisted MIMO. Even in the worst case scenario where the majority of the MS are deployed indoors with no means of dedicated indoor coverage, the overall achievable throughput density of approximately 0.85Gbps/km^2 can still be achieved. Moreover, the QoS of the system can be significantly improved by applying cognitive radio techniques. If dedicated approaches are assumed to provide indoor coverage, e.g. femto-cells, the 1Gbps/km^2 can be reached even in the worst case scenario. Thus, the system-level simulation results thus give strong evidence that the 1 Gbps/km^2 throughput density target can readily be achieved by the BuNGee project.

Contributors

(list to be established by the lead contractor together with the technical coordinator)

Participant #	Participant short name	Name of the Contributor	E-mail
5	UY	Tao Jiang	tj511@ohm.york.ac.uk
5	UY	Peng Li	pl534@ohm.york.ac.uk
5	UY	Chunshan Liu	cl563@ ohm.york.ac.uk
7	UCL	Nizabat Khan	nizabat.khan@uclouvain.be
5	UY	David Grace	dg@ohm.york.ac.uk
5	UY	Alister Burr	agb1@ohm.york.ac.uk
7	UCL	Claude Oestges	claude.oestges@uclouvain.be

Table of Contents

List of Tables

List of Figures

List of Acronyms

Abbreviation / acronym	Description
ABS	Access Base Station
CR	Cognitive Radio
DL	Downlink
HBS	Hub Base Station
HSS	Subscriber Station connected to HBS
MIMO	Multiple Input Multiple Output
SISO	Single-input single-output
MMSE	Minimum Mean Square Error
MS	Mobile Subscriber
LOS	Line of Sight
NLOS	Non-Line of Sight
OFDMA	Orthogonal Frequency-Division Multiple Access
QoS	Quality of Service
RRM	Radio Resource Management
SINR	Signal to Interference-plus-Noise Ratio
SISO	Single Input Single Output
TDD	Time Division Duplex
UL	Uplink
ZF	Zero-Forcing
SIC	Successive interference cancellation
AMC	Adaptive modulation and coding
STBC	Space time block code
CDF	Cumulative Distribution Function
INR	Interference to Noise Ratio
MBA	Muti-Beam Assisted

1. Introduction

The system-level simulation in WP4 models the BuNGee architecture and its surrounding environment. The D4.1.2 system-level simulation serves as an indication of the BuNGee system capacity. A two layer simulator has been developed to capture the features of BuNGee's two-hop system architecture. The first layer models the self-backhaul link between HBS and HSS. The second layer models the access link between ABS and MS. These two layers are connected together by a channel usage table and the aggregated traffic at HSS for downlink and ABS for the uplink. A 3D (user, time, frequency) channel usage table is designed to track the frequency utilization information in the simulation. The entities that are transmitting on the same frequency can be obtained by examining this table, and then the interference can be determined by using appropriate propagation model.

The modelling of BuNGee system is a very complicated task that needs to address a range of issues in the physical, MAC and network layers. A modularized structure is used to design the simulator to maximize its compatibility. A number of modules are developed to model different aspects of the system, including a location function, traffic function, propagation function, MIMO function and RRM function. A number of assumptions have also been made to enable the modelling of some advanced techniques, e.g. MIMO and Cognitive Radio techniques. The details of these assumptions are available in section 2.

The square topology is modelled. The backhaul network propagation environment has been simulated by UCL and the results are provided to the system-level simulation. WINNER II B1, WINNER II B4, WINNER II C2 and WINNER II C4 propagation models are also applied to estimate the path loss between the various links in the system [2]. The antenna patterns of the HBS antenna, HSS antenna and ABS antenna are provided by CASMA [3]. Collaboration has been carried out at UY between WP2 and WP4 to develop a MIMO function, and the MIMO techniques proposed by WP2 are incorporated into the system-level simulation. The details of how these elements have been modelled are given in section 3.

Two approaches are simulated in the system-level simulation: the frequency planning proposed by Alvarion and a basic cognitive radio approach. Section 4 gives the results and the analysis of the performance and the conclusions are given in section 5. A full list of parameters and the lookup tables for the backhaul network propagation are provided in the appendix.

2. Assumptions

2.1 System Scenarios and Parameters

A Manhattan-grid environment is used in the final system-level simulation. A multi-HBS square-cell topology is applied as in Figure 2-1. There are 16 streets both East-West (E-W) and North-South (N-S), and that forms a 15×15 block area. The HBS antennas are placed above rooftop in the centre of their cell and 5 HBS form a 9 square-cell deployment environment in this case. The total service area is 1.82 km^2 (1.35km × 1.35km). In order to utilize the received signal power estimation results obtained from UCL's ray-tracing based channel model for the backhaul network [4], the physical environment of the service area has been defined jointly with WP2 (UCL in particular).

The HBSs and ABSs/HSSs are indexed as shown in Figure 2-1. HBS beams are indexed clockwise from 1 to 64 as illustrated also in Figure 2-1. Appropriate modification has been made to extend UCL's ray-tracing results to a 64 HSS and 64 HBS beams scenario by taking advantage of the symmetric feature of the service area. The details are given in the propagation section.

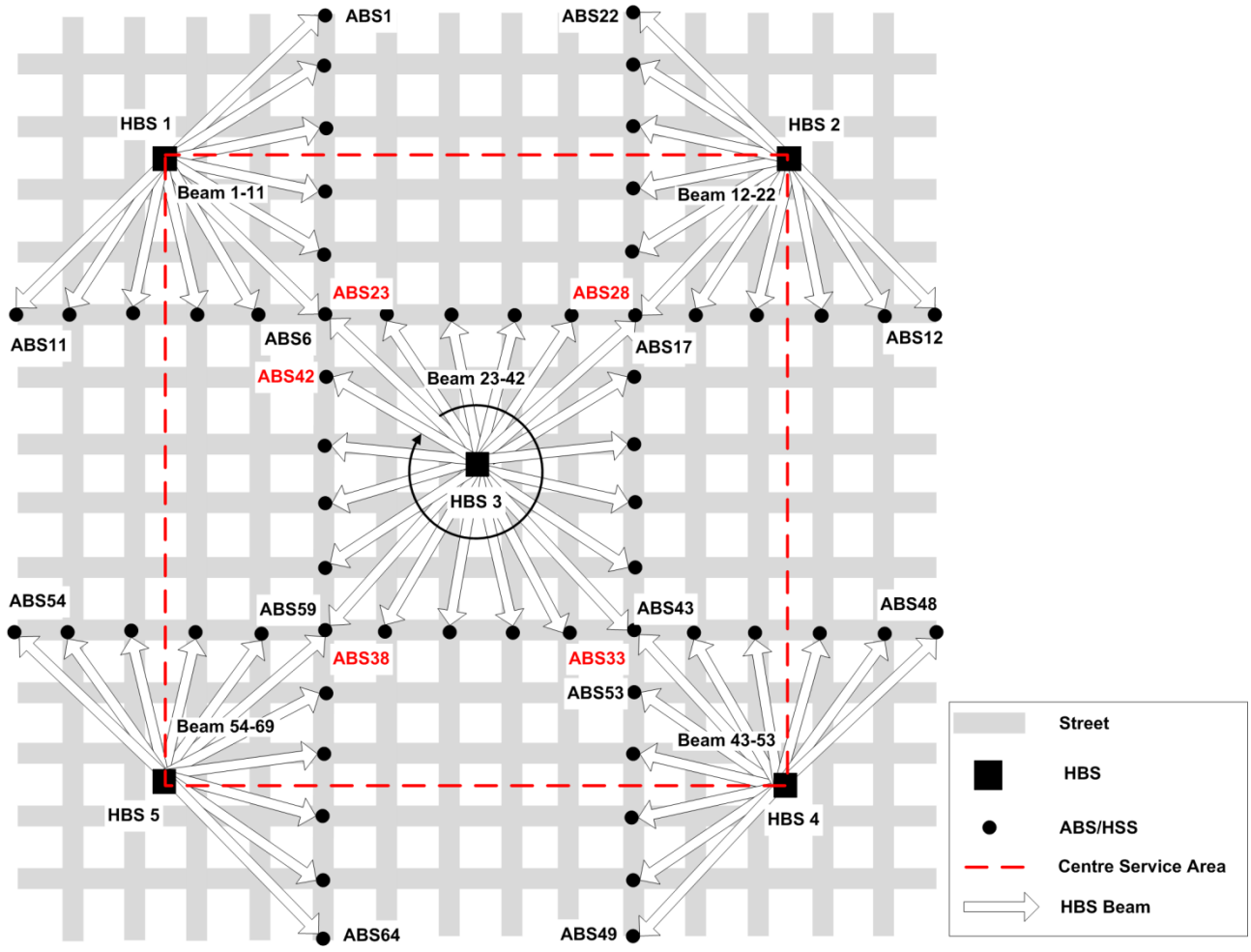

Figure 2-1: Simulation Setup

1500 MSs are distributed uniformly either over the entire service area or on the streets depending on the modelling scenarios. These MSs are service by all 64 ABSs placed outdoor at street level. MSs are associated to the best available ABSs in terms of SNR levels. The user density is about 800 MSs per 1km^2 in this case, which complies with the requirement of Work Package 1 [5]. However, only the MSs placed in the highlighted centre service area are taken in to account when measuring throughput density, in order to give a more representative interference environment of a larger system.

2.2 Propagation Models

A number of channel models have been used to calculate path loss in the system-level simulation. The ray-tracing based channel model developed at UCL is used to estimate the path loss between the HBS and HSS. The detailed descriptions of the ray-tracing tool and the ray-tracing results can be found in D2.1 [4]. WINNER II [2] provides a comprehensive set of channel models that are capable of covering the propagation environment of the access network of BuNGee. In this simulation, WINNER II B1 is used to calculate the path loss between the ABS and MS that is located outside of a building block. The path loss between ABS and MS inside of a building block is estimated by using WINNER II B4. The propagation between backhaul entities and access entities are obtained by using WINNER II C2 for outdoor MS, WINNER C4 for indoor MS.

In the final system level simulation a number of WINNER II LOS probability models [2] are applied to improve the accuracy of the path loss modules of the simulator. It was assumed in the Interim Simulation (D4.1.1 [6]) that as long as BSs and MSs were placed on the same streets, the paths between them were clear LOS. This assumption is clearly too optimistic so that the LOS probability models are introduced.

2.2.1 Backhaul Network Propagation Models

Interference is one of the main difficulties that beyond next generation wireless networks will encounter. Therefore, understanding the nature and characteristics of the interference is critical in these inherently interference-limited networks. This section firstly briefly describes the enhanced ray-tracing tool. Then, some possible interference scenarios of BuNGee architecture have been identified and subsequently modelled and characterized in terms of received power/pathloss.

2.2.1.1 UCL Multi-HBS Ray-Tracing Results

Ray-tracing simulations have been performed to calculate received power at the HSS receiver antennas, for multi-HBS interference scenario [4]. In this interference scenario, 5 HBSs are placed as transmit antennas such that they cover a total of 225 building blocks. A total number of 72 beams are utilized in this multi-HBS scenario. On the receiver side, 64 HSSs are distributed according to a square topology. These HSSs are directed towards their respective HBS in the simulations. Details of this multi-HBS interference scenario are presented in Figure 2-2, where both HBSs and HSSs are numbered in clockwise fashion according to the needs of subsequent work. However, beams of utilized antennas are numbered in an anti-clockwise direction. This multi-HBS interference scenario becomes very complex due to the large number of blocks and dense HSS antenna deployments. Therefore, UCL has extracted results for two representative base stations:

- HBS5 (12 beams, corner case)
- HBS3 (12 beams, middle case)

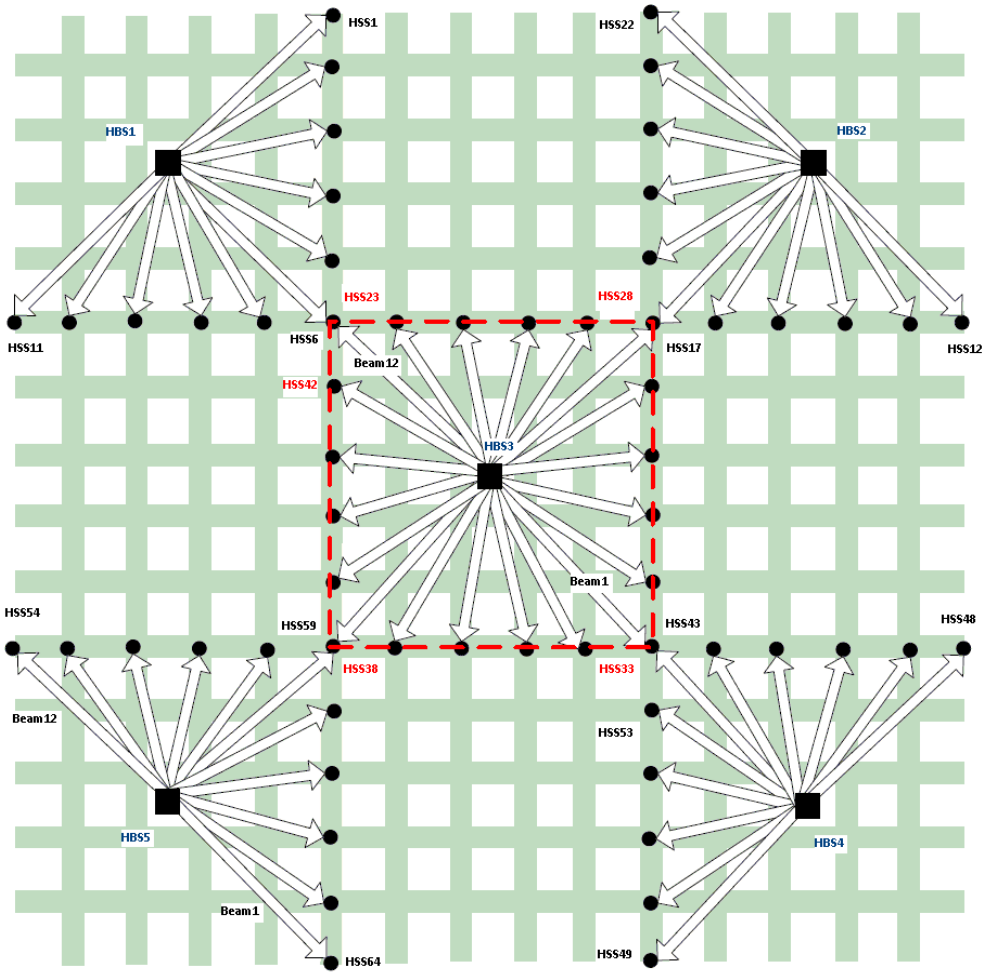

Figure 2-2: Multi-HBS interference scenario with square topology for HSS deployment

The corresponding results for all other HBSs can be evaluated by exploiting the symmetric properties of the defined scenario. Furthermore, only 12 beams of the above mentioned base stations have been utilized for the sake of simplicity. The effect of each beam has been evaluated separately in terms of received power at each HSS antenna. Furthermore, diffuse scattering has also been not been applied in these simulations, to keep the complexity manageable. So it should be kept in mind that received powers at each HSS location will perhaps slightly increase after including the diffuse scattering components. All simulation results are extracted with +45 polarized transmit antenna and -45 polarized receive antenna. Co-located corner HSSs (23, 28, 33 and 38) of HBS3 are simulated twice for their respective antenna directions.

Results

There are in total two categories of HBSs in the deployment scenario (as shown in Figure 2-2): the centre case (HBS3) and the corner case (HBS1, HBS2, HBS4, HBS5). Thus simulation results for two representative HBSs (the centre case HBS and the corner HBS) are sufficient in terms of understanding the propagation environment of the backhaul network.

HBS5 (Corner Case)

Simulation results are divided into five tables each representing a coverage area from HBS1-to-HBS5. All results are compiled in tabular form and presented in Appendix I (from Table 6-2 to

Table 6-6). Generally, it can be reported that interference from immediate neighbouring HBS antenna beams is high at some HSSs locations. For example, there is significant interference from HBS5 antenna beams at some HSSs in the cell area of neighbouring HBS1, HBS3 and HBS4. Importantly, it increases considerably when HSSs of those cell areas are facing towards HBS5.

In Table 6-2, the received powers at HSS8 and HSS9 from Beam7-10 of HBS5 are relatively higher. These relatively higher received powers are highlighted in the table and can be termed as interference to HBS1 cell area. This is probably due to straight streets towards above mentioned HSS locations. However, the coverage area of HBS2 seems safe from interference of HBS5 (12 beams) mainly due to larger distance and building obstructions. The corresponding simulation results of HBS5 for HBS2 are presented in Table 6-3.

Simulation results for the HBS3 coverage area are given in Table 6-4. This seems to be mostly affected by the neighbouring HBS5 transmit antenna beams. It can be observed that a number of HSSs receive higher powers and are highlighted in Table 6-4. It is mainly due to the central HBS5 beams 4-9, which are directed towards HBS3 coverage area.

In Table 6-5, received powers in the coverage area of HBS4 are presented. Similar to HBS1, only HSS51 and HSS52 have relatively higher received powers due to street canyon effects and are highlighted in Table 6-5. Finally, in

Table 6-6, the received powers at HSS54-HSS64 for the coverage area of HBS5 are shown. These intended received powers are relatively quite high as expected and cannot be described as interference.

HBS3 (Middle Case)

As for HBS5, simulation results of only 12 HBS3 beams (Beam1-to-Beam12) are extracted. Results are divided into five tables each corresponding to five respective HBS cell areas, as in the previous case. Again, all results are compiled in tabular form in Appendix I. Generally, it can be reported that HBS3 introduces significant interference to some HSSs in the cell area of the neighbouring HBS. For example, two HBS3 beams (Beam11 and Beam12) interfere with HSS1-HSS6, apparently due to the street canyon effect. Similarly, two HBS3 beams (Beam1 and Beam2) affect HSS43-HSS48, and are highlighted in blue in all tables.

The relatively higher received powers at HSS1-HSS6 from the two HBS3 beams (Beam11 and Beam12) are highlighted in Table 6-7. These are mainly due to the fact that both beams are directed towards HBS1. In

Table 6-8, the interfering beams (Beam5-Beam8) of HBS3 and corresponding HSSs in the HBS2 cell area are highlighted. The intended received powers at HSS23-HSS33 from the HBS3 beams are presented in Table 6-9, and these are high values as expected. However, simulated 12 beams also affect (in terms of interference) the other half of the cell area of HBS3. In Table 6-10, the interfered HSSs which mainly arise from two beams of HBS3 (Beam 1 and beam 2) are highlighted. Lastly, the received powers in HBS5 coverage area are presented in Table 6-11, which are negligibly low in terms of interference from HBS3 beams.

2.2.1.2Extended Ray-Tracing Results

Due to the large number of building blocks and dense HSS antennas deployment scenario, UCL's results are only available for HBS 5 and half of the beams of HBS3. Therefore, in order to make the results available for all 5 HBS (64 HBS beams), appropriate modification is required by taking advantage of the symmetric property of the service area. Furthermore, the frequency plan proposed by Alvarion assumes only 1 HBS beam per 1 HSS. Thus, a square cell with a total of 20 HSSs only requires 20 HBS beams. However, UCL's ray-tracing simulation assumes 6 HBS beams per 90° sector, which in turn assumes 24 beams per HBS. Thus, the beams which have the potential to cause more interference to others (beam 6 or beam 7 in each 180° sector) are dropped to fit with the frequency plan. The following actions have been carried out:

1. Drop beam 6 of HBS5 and beam 6 of HBS3 from UCL's results tables (Table 6-2 to Table 6-11)
2. Mapping HBS5 results (Table 6-2 to Table 6-6) to HBS1, HBS 2, HBS4
3. Mapping HBS3 12-beam results (Table 6-7 to Table 6-11) to the other 12 beams of HBS3
4. Reorder HBS beams (HBS1-HBS5) clockwise to comply with Figure 2-1

The tables of the propagation results for HBS1-HBS5, which are used in the final system level simulation, are provided also in Appendix I (Table 6-12 to Table 6-17).

2.2.2 Access Network Propagation Models

WINNER II [2] provides a comprehensive set of channel models that are capable of modelling the propagation environment of the access network of BuNGee and the propagation between backhaul and access entities. In this simulation, WINNER II B1 is used to calculate the path loss between the ABS and MS that is located outside of a building block [2]. The path loss between ABS and MS inside of a building block is estimated by using WINNER II B4 [2]. The propagation between backhaul entities and access entities are obtained by using WINNER II C2 for outdoor MS, WINNER C4 for indoor MS. Two WINNER II LOS probability models are also applied to estimate the probability of LOS links between outdoor entities [2].

2.2.2.1 WINNER II B1 – Urban Micro-Cell

The propagation environment investigated by WINNER II in an urban micro-cell scenario is quite similar to BuNGee access networks' propagation environment [2]. A Manhattan-grid layout is considered and all BS and MS antennas are assumed well below the rooftops of the surrounding buildings. All ABS and MS are assumed to be outdoor as illustrated in Figure 2-3. Both LOS and NLOS cases have been considered, allowing for temporary blockage of the LOS, for example by large vehicles. The LOS and NLOS path loss are calculated as follows:

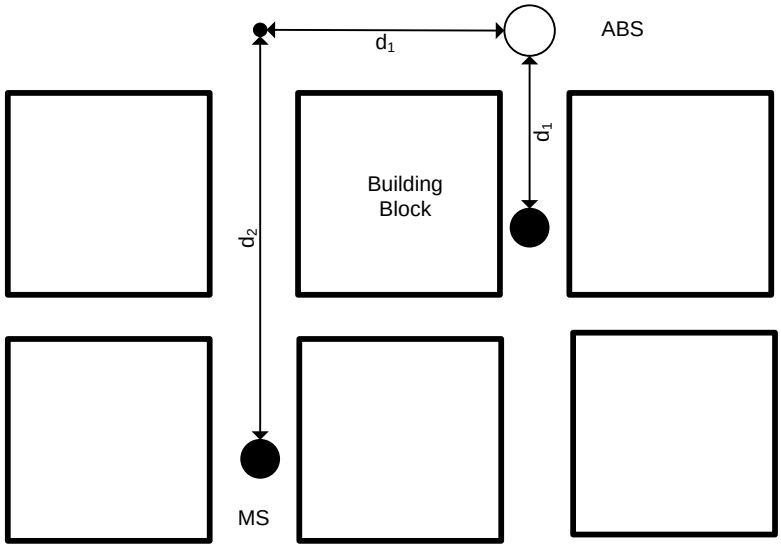

Figure 2-3: WINNER II B1 Path loss Calculation

LOS

If the MS and ABS path is clear LOS, and the LOS distance d_1 between them is less than the breakpoint distance d'_{BP} ($10m<d_1<d'_{BP}$), then the path loss can be calculated by:

$$PL = A\log_{10}(d_1) + B + C\log_{10}(f_c/5.0) + X \quad (2\text{-}1)$$

where

$$A = 22.7, \quad B = 41.0, \quad C = 20 \quad (2\text{-}2)$$

f_c is the carrier frequency in *GHz.*

The breakpoint distance d'_{BP} is defined as:

$$d'_{BP} = 4h'_{BS}\, h'_{MS}\, f_c/c \quad (2\text{-}3)$$

where h'_{BS} and h'_{MS} are defined in equation (2-4), (2-5) respectively.

$$h'_{BS} = h_{BS} - 1 \quad (2\text{-}4)$$

$$h'_{MS} = h_{MS} - 1 \quad (2\text{-}5)$$

h_{BS} is the ABS antenna height and h_{MS} is the MS antenna height. c = 3.0x10^8 *m/s* is the propagation velocity in free space.

If $d'_{BP} < d_1 < 5km$, then the path loss can be obtained as:

$$PL = 40.0\log_{10}(d_1) + 9.45 - 17.3\log_{10}(h'_{BS}) - 17.3\log_{10}(h'_{MS}) + 2.7\log_{10}(f_c/5.0) \quad (2\text{-}6)$$

NLOS

If the MS and ABS are not on the same street, then the path loss can be calculated by:

$$PL = \min(PL(d_1, d_2), PL(d_2, d_1)) \quad (2\text{-}7)$$

where

$$PL(d_k, d_l) = PL_{LOS}(d_k) + 20 - 12.5n_j + 10n_j \log_{10}(d_l) + 3\log_{10}(f_c/5.0) \quad (2\text{-}8)$$

and

$$n_j = \max(2.8 - 0.0024d_k, 1.84), \quad (2\text{-}9)$$

PL_{LOS} is the path loss of B1 LOS and $k, l \in \{1,2\}$, d_1 and d_2 are distance between the entities along the street as it is shown in Figure 2-3.

2.2.2.2 WINNER II B4 – Urban Micro-Cell Outdoor to Indoor

The layout considered in WINNER II B4 [2] is also an urban micro-cell. The only difference is that WINNER II B4 only considers the path loss between on street BSs and in building MSs. Therefore, in this simulation the path loss between ABS and in building MS is obtained by using WINNER II B4 propagation model. The scenario is shown in Figure 2-4.

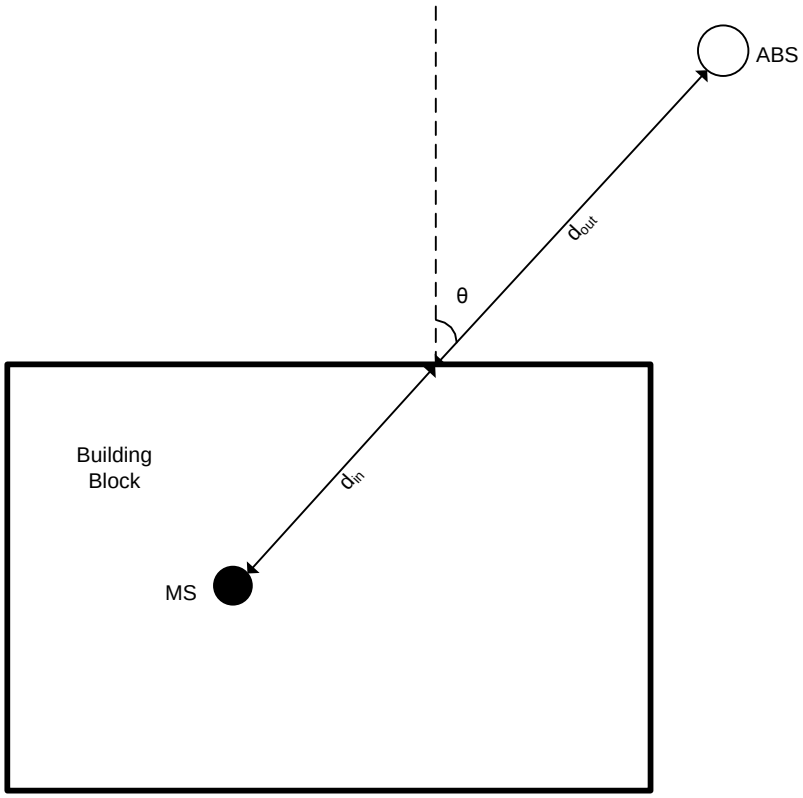

Figure 2-4: WINNER II B4 Path loss Calculation

The path loss in this case can be calculated by:

$$PL = PL_b + PL_{tw} + PL_{in}$$
$$\begin{cases} PL_b = PL_{B1}(d_{out} + d_{in}) \\ PL_{tw} = 14 + 15(1 - \cos(\theta))^2 \\ PL_{in} = 0.5 d_{in} \end{cases} \quad (2\text{-}10)$$

where PL_{B1} is the B1 path loss, d_{out} is the distance from the ABS to the penetration point on the wall, and d_{in} is the distance from that point to the mobile terminal. θ is the angle between the wall and the wireless link.

2.2.3 Propagation Between Backhaul Network and Access Network

2.2.3.1 WINNER II C2 – Urban Macro-Cell

As indicated in [2] the WINNER II C2 model is applicable to a typical urban macro-cell scenario where an MS is located at street level and fixed base station is placed over the roof-top. Either a Manhattan-grid type regular building block layout or an irregular building layout can be considered by using WINNER II C2. The path loss can be obtained by:

LOS

If 10 <d<d'_{BP} the LOS path loss can be obtained as:

$$PL = A\log_{10}(d) + B + C\log_{10}(f_c/5.0) + X \quad (2\text{-}11)$$

Where

$$A = 26, \quad B = 39, \quad C = 20 \quad (2\text{-}12)$$

d is the distance between BS and LOS MS, f_c is the carrier frequency in *GHz.*

If d'_{BP} <d<5*km* the LOS path loss can be obtained as:

$$PL = 40.0\log_{10}(d) + 13.47 - 14\log_{10}(h'_{BS}) - 14.0\log_{10}(h'_{MS}) + 6.0\log_{10}(f_c/5.0) \quad (2\text{-}13)$$

NLOS

The path loss of NLOS links can be calculated by:

$$PL = (44.9 - 6.55\log_{10}(h_{BS}))\log_{10}(d) + 34.46 + 5.83\log_{10}(h_{BS}) + 23\log_{10}(f_c/5.0) \quad (2\text{-}14)$$

h_{BS} is the BS antenna height and h_{MS} is the MS antenna height. d is the distance between BS and MS, f_c is the carrier frequency in *GHz.*

2.2.3.2WINNER II C4 – Urban Macro-Cell Outdoor to Indoor

WINNER II C4 is provided to calculate the path loss between outdoor BS and indoor MS [2]. The difference between WINNER II C4 and WINNER II B4 we mentioned previously is that the BS antenna is placed above

rooftop. Thus, there will be a long LOS distance for BSs to the signal penetration point on the walls of the building blocks. The outdoor propagation environment of C4 is similar to C2 and the indoor environment is similar to WINNER II A1. The path loss can be obtained by:

$$PL = PL_{C2}(d_{out} + d_{in}) + 17.4 + 0.5d_{in} - 0.8h_{MS} \quad (2\text{-}15)$$

where PL_{c2} is the path loss function of WINNER II C2. If the signal path from BS to the penetration point on the wall is LOS then the WINNER II C2 LOS function is used, otherwise WINNER II C2 NLOS function is used.

2.2.4 LOS Probability Models

Appropriate LOS probability models are required in order to accurately model the physical environment between outdoor BS and outdoor MS. In the final system level simulation a number of WINNER II LOS probability models [2] are applied to improve the accuracy of the path loss modules of the simulator. The following WINNER II probability models are used to determine the existence of NLOS or LOS path between outdoor BSs and MSs:

LOS Probability between ABS and MS

Probability estimation for WINNER II B1:

$$P_{LOS} = \min(18/d, 1) \cdot (1 - \exp(-d/36)) + \exp(-d/36) \quad (2\text{-}16)$$

LOS Probability between HBS and MS

Probability estimation for WINNER II C2:

$$P_{LOS} = \min(18/d, 1) \cdot (1 - \exp(-d/63)) + \exp(-d/63) \quad (2\text{-}17)$$

2.3 BuNGee Antennas

A number of directional antennas have been designed by Cobham Antenna Systems (Microwave Antennas) (CASMA), including the 24-beam directional HBS antenna, ABS directional antenna and HSS directional antenna. The utilization of the directional antenna is key to BuNGee's system design as BuNGee's aggressive spectrum reuse introduces a high level of interference. Sophisticated directional antennas are able to significantly reduce the interference in the system.

The 24-beam HBS directional antenna has gains between 19 dBi and 21 dBi for different beams. A 13 dBi directional antenna is applied at the HSS and pointed towards the largest power ray direction as it suggested in [4]. Two 17 dBi antennas are assumed at each ABS pointing in two opposite directions either E-W or N-S along the street and in parallel to the ground. The azimuth angle and the elevation angle are calculated between entities, and the 3D antenna patterns provided by CASMA are used for obtaining the appropriate antenna gain. The 3D antenna patterns of HBS beams, ABS antenna and HSS antenna are illustrated by Figure 2-5, Figure 2-6 and Figure 2-7 respectively.

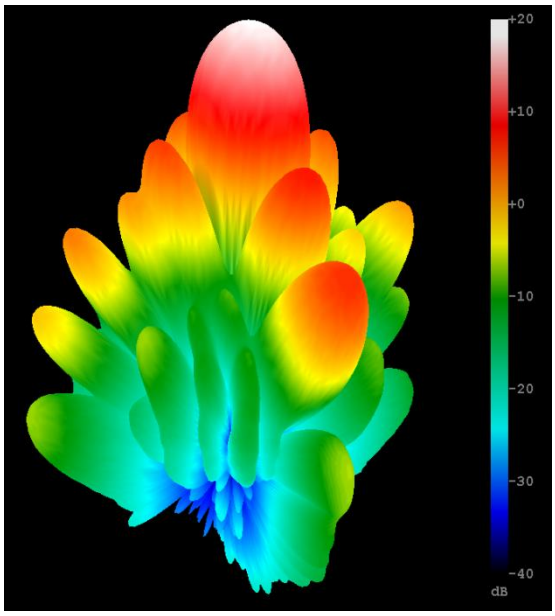

Figure 2-5: 3D HBS antenna pattern (one beam)

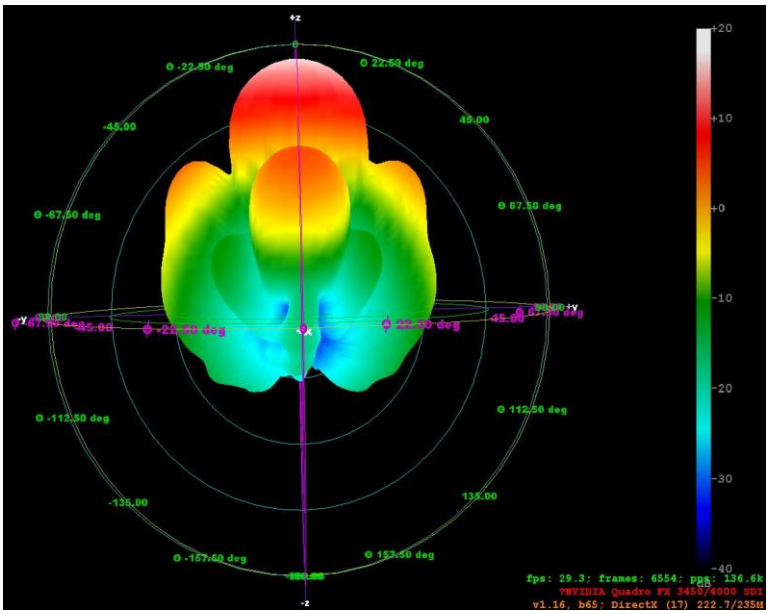

Figure 2-6: 3D ABS antenna pattern

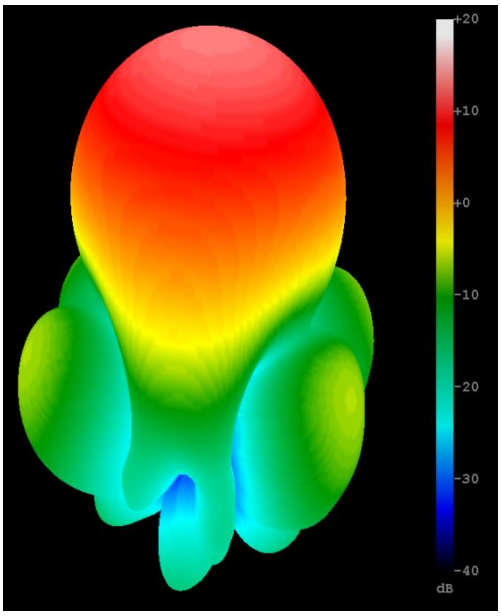

Figure 2-7: 3D HSS antenna pattern

2.4 Traffic models

A file-transfer based traffic model has been used in this simulation to generate traffic for both DL and UL. The interarrival time of transmissions follow a negative exponential distribution and the file size follows Pareto distribution. The probability density function of Pareto distribution is defined as:

$$p_X = \alpha \cdot (x_m^{\alpha} / x^{\alpha+1}) \qquad for\, x \geq x_m \tag{2-18}$$

where the mean value of the distribution can be obtained by:

$$E(X) = \alpha x_m / \alpha - 1 \tag{2-19}$$

Retransmission is assumed such that file transmissions that are initially blocked will backoff for a random time. The mean backoff time is set equal to the mean interarrival time of files in the simulation. Again, a fairly basic backoff strategy is used because it has very limited impact on the system capacity. Moreover, this approach is likely to show the lower bound system capacity which is useful in terms of understanding the system capacity of BuNGee.

2.5 MIMO-Truncated Shannon Bound

Advanced BuNGee MIMO techniques developed in WP2 have the potential to significantly improve the link capacity. The achievable data rates of both the backhaul network and the access network of BuNGee can be significantly enhanced by using multiple antennas and suitable signal processing techniques at the hub base stations (HBSs), access base stations (ABSs) and mobile stations (MSs). According to our considered scenario, HBSs and ABSs will have dual polarized antennas which can act as an antenna array and MSs are assumed to be equipped with at least two antennas each. Multiple antennas can be used for spatial multiplexing that has the potential to achieve approximately a two-fold increase of the achievable rates. Therefore in the present evaluation we assume that the backhaul and access links (HBS-ABS and ABS-MS) are 2x2 MIMO channels.

In order to evaluate the performance of the backhaul and access links we have to take into account the effects of the MIMO channel. In SISO channels the achievable throughput is a deterministic function of the

pathloss, shadowing and small-scale fading; this can be evaluated in a straightforward and rapid manner through the generation of the suitable random variables. However, in MIMO channels, when spatial multiplexing techniques are employed, the Shannon capacity of a MIMO channel is determined by [7]:

$$C = \max_{tr(\mathbf{R}_{ss})=N_T} \log_2 \det\left(\mathbf{I}_{N_R} + \frac{1}{\sigma_v^2} \mathbf{H}\mathbf{R}_{ss}\mathbf{H}^H \right). \quad (2\text{-}20)$$

where $\mathbf{R}_{ss}$ is the auto correlation of received signal vector **r**. The above assumes that the MIMO channels are deterministic. In general, however, the throughput is no longer a deterministic function but changes randomly, because the random channel matrix **H** means that its channel capacity is also randomly time-varying due to the respective channel coefficients (a 2x2 MIMO channel consists of four channel coefficients).

The required signal processing techniques, either at the receiver or the transmitter side, involves matrix inversions (such as MMSE/Zero-Forcing) or tree searching (such as sphere decoding). The resulting performance depends strongly on the properties of channel matrix, mainly the matrix rank and condition.

Consequently, for a wireless link of a given average quality (determined by the pathloss and shadowing), the achievable rate follows a distribution. However, it is not a deterministic function of the strength of the respective channel coefficients. Therefore the capacity cannot be evaluated rapidly with the use of a single function in the simulation environment. Instead for each iteration it is required that a 2x2 channel matrix is generated whose four coefficients have identical average SINR, but with different small-scale fading values (although following the same statistical distribution). The generation of four random variables per wireless link together with the required matrix inversions significantly increases the simulation complexity and running time. This is especially true for a system level simulation which is required to consider a network with many MIMO links among HBSs, ABSs, and MSs. Therefore we have investigated computationally efficient ways of evaluating the capacity of MIMO wireless links without the requirement of detailed channel coefficients, using only a statistical distribution. In the following sections we introduce the Truncated Shannon Bound and the MIMO signal processing techniques involved in BuNGee system simulation.

2.5.1 Truncated Shannon Bound

For a system which may contain many different nodes such as HBSs, ABSs and MSs, the number of channel links rises rapidly with the number of nodes. It is clearly not feasible to carry out a full-scale Monte Carlo simulation to evaluate the throughput of every link in the system. The introduction of multiple antenna elements at both transmitter and receiver has made this process significantly more complicated. First, it is no longer sufficient simply to consider the aggregate interference experienced by a specific link and quantify it as a simple SINR, since the direction of the interference becomes important. And secondly, the link capacity can no longer be treated as a deterministic function of any SINR, even in the absence of interference, since capacity is a function of the channel matrix **H** (see eq. capacity), which must be treated as random.

In order to address this problem, similar to [8], in BuNGee, we use a two-step process: a system-level simulation to evaluate the signal to interference-plus-noise ratio (SINR) of each link, taking into account path loss, shadowing and slow fading of the signal. Thereupon a link-level function could be applied to evaluate the capacity of the links. This could be based on the (1) Shannon bound, or on (2) closed-form expressions for BER *versus* SNR, or (3) a look-up table obtained by simulation. In all these cases, once slow Rayleigh fading has been taken into account, this function can be treated as deterministic. (Fast Rayleigh fading can be included in the average BER function).

In order to reduce our simulator's complexity we have developed a stochastic based methodology, which maps each value of average link SINR to a statistical distribution of achievable rates. Our simulator tracks the average SINR value for each considered wireless link; average SINR does not depend on the properties of MIMO channels, but solely on the pathloss and shadowing realization of the useful and the interfering links. For a useful range of average SINR values we drew offline the empirical distributions of the achievable capacity. Therefore in our actual simulation for every generated value of average SINR, the attained throughput takes a value from the empirical throughput distribution. This accelerates and simplifies the general numerical evaluation of the throughput of the BuNGee wireless links. In order to guarantee highly

accurate results we need to ensure that the empirical throughput distributions, that are generated offline for a range of average SINR values, are truly representative of the achievable throughput.

Generally, MIMO throughput distributions depend on the following factors:

1. The employed capacity bound;
2. The number of antenna elements;
3. The signal processing method;
4. The nature of small-scale fading;
5. The level of antenna correlation.

The Truncated Shannon Bound

For evaluating the performance of the schemes presented above we consider the TSB which is representative of the rates that can be achieved by SISO links, given an adaptive modulation and coding (AMC) codeset. According to the TSB, the throughput of any link can be expressed as

$$C_{TSB}(\gamma) = \begin{cases} 0 & \gamma < \gamma_0 \\ W\alpha \log_2\left(1+\gamma/\gamma_{sh}\right) & \gamma_0 \le \gamma < \gamma_{max} \\ C_{max} & \gamma_{max} < \gamma \end{cases} \quad (2\text{-}21)$$

In practice there is an upper limit to the throughput, C_{max}, set by the throughput of the highest rate coding/modulation, and a lower limit γ_0 on the SNR below in which the throughput is zero, set by the required SNR of the lowest rate scheme. Hence the curve should be truncated at these points, as shown in Figure 2-8, as well as further scaled to account for the average throughput, leading to the TSB.

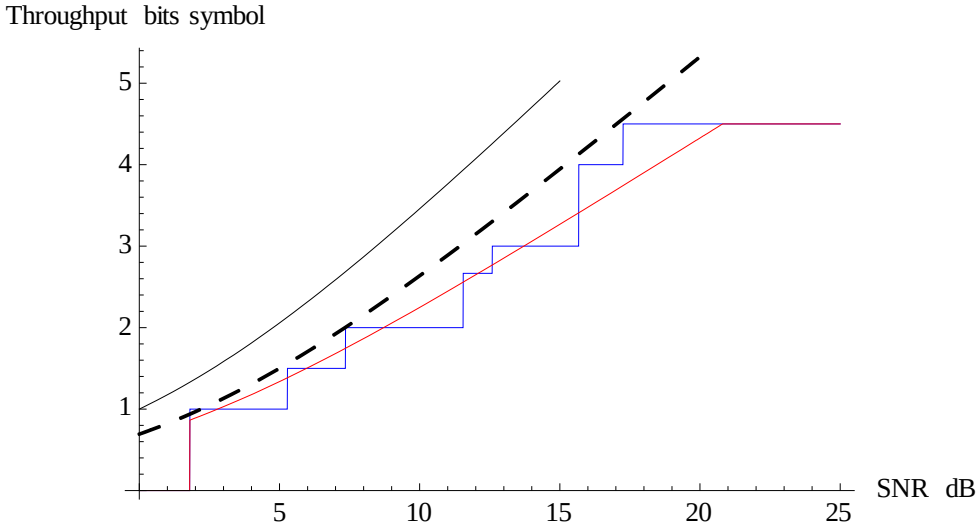

Figure 2-8: Throughput function of a set of coding/modulation schemes (stepped blue) compared with Shannon bound (solid black), shifted/scaled Shannon bound (dashed black), and truncated Shannon bound (red).

A question here is what the shift and scaling parameters to be used in the TSB to optimally approximate the actual throughput function for an arbitrary set of coding/modulation schemes? This is verified by ensure the average throughput given by the TSB is as close as possible to the average throughput obtained by using the true throughput function, given that the link SINR is random, so that the average should be taken over its distribution. Mathematically we can therefore write:

$$\int_{s_0}^{\infty} C_{TSB}(s)\, p(s,\bar{s})\, ds \equiv \int_{s_0}^{\infty} C_{thr}(s)\, p(s,\bar{s})\, ds = \bar{C}(\bar{s}) \quad (2\text{-}22)$$

where C_{TSB} denotes the TSB function, $s = 10log_{10}(\gamma)$ and $\bar{s}$ denote respectively the instantaneous SNR and the average SNR, both in dB, $p(s,\bar{s})$ denotes the probability density function of the instantaneous SNR (in dB) on a given link, C_{thr} denotes the true throughput function, and $\bar{C}(\bar{s})$ denotes the average throughput as a function of average SNR. The parameters of the TSB are to be chosen to fulfil this identity, as far as possible with any likely SNR distribution.

We can approximate the PDF with arbitrary accuracy as the sum of a set of rectangular functions: that is, the distribution can be treated as a mixture distribution of uniform distributions, provided the range *d* of the support of these PDFs is less than that of the actual distribution. We write:

$$p_{ap}\left(s,\bar{s}\right)=\sum_{i=1}^{n_p}a_i u\left(s,\bar{s}_i,\delta_i\right) \tag{2-23}$$

where:

$$u\left(s,\bar{s},\delta\right)=\begin{cases}0 & s\le\bar{s}-\delta\\ \dfrac{1}{\delta} & \bar{s}-\delta<s<\bar{s}+\delta\\ 0 & s\ge\bar{s}+\delta\end{cases} \tag{2-24}$$

Then:

$$\begin{aligned}\bar{C}\left(\bar{s}\right)&=\int_0^\infty\sum_{i=1}^{n_p}a_i u\left(s,\bar{s}_i,\delta\right)C_{TSB}\left(s\right)ds\equiv\int_0^\infty\sum_{i=1}^{n_p}a_i u\left(s,\bar{s}_i,\delta\right)C_{thr}\left(s\right)ds\\&=\sum_{i=1}^{n_p}a_i\int_{\bar{s}_i-\delta/2}^{\bar{s}_i+\delta/2}C_{TSB}\left(s\right)ds\equiv\sum_{i=1}^{n_p}a_i\int_{\bar{s}_i-\delta/2}^{\bar{s}_i+\delta/2}C_{thr}\left(s\right)ds\end{aligned} \tag{2-25}$$

and hence average capacities will match provided that:

$$\int_{\bar{s}_i-\delta/2}^{\bar{s}_i+\delta/2}C_{TSB}\left(s\right)ds\equiv\int_{\bar{s}_i-\delta/2}^{\bar{s}_i+\delta/2}C_{thr}\left(s\right)ds,\forall\bar{s}_i \tag{2-26}$$

The comparison is shown in Figure 2-9 for *a* = 0.65 and zero shift.

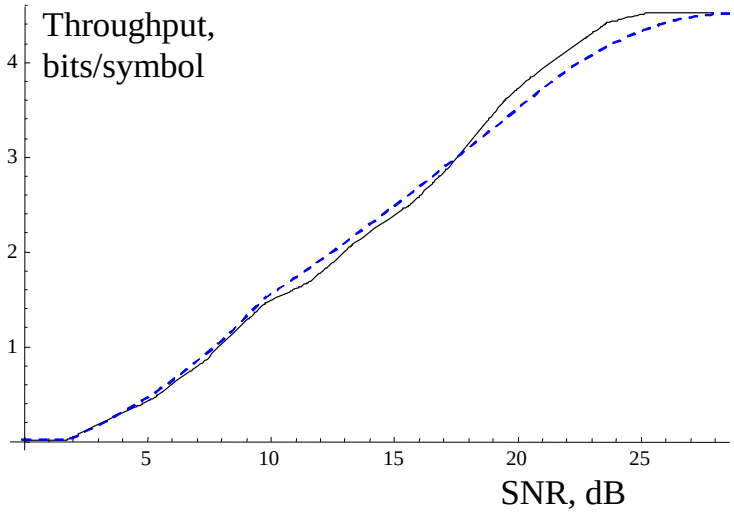

Figure 2-9: Average throughput against average SNR for TSB, a = 0.65, shift 0 dB (dashed line) compared with actual throughput function (solid)

2.5.2 Point-to-Point MIMO Link Capacity Estimation

In order to apply the aforementioned TSB to MIMO systems, we may have to separate the spatially multiplexed data streams at the receiver side. This can be done by introducing MIMO signal processing techniques such as detection and/or precoding algorithms at receiver and/or transmitter, respectively.

We consider the capacity estimation of a MIMO link, and develop a stochastic model for it which can readily be used in a system-level simulation. Since the capacity is in fact random, depending on the MIMO channel matrix, for Monte Carlo simulation at the system level, we need to generate random instances of the capacity which follow the statistics of the capacity of the typical link, making use of parameters for the link which can be obtained from the system-level simulation. The most important such parameter is the signal to noise-plus-interference ratio (SINR) encountered at the receiver of the link. We will see, however, that in many cases this single parameter does not fully define the link capacity distribution: it may depend on other factors such as the *balance of noise and interference*, the *number of interferers* and their *directions*.

In SISO systems we can directly apply the TSB, as described in the previous section, to estimate the throughput as a function of SINR, which can then be expressed in closed form. In MIMO systems the process is not usually as straightforward. Here we consider a class of schemes in which linear or non-linear processing is used at the receiver and/or transmitter to provide one or more streams over which conventional AMC can be used. This is a broad class, encompassing space time block codes (STBC), spatial multiplexing using both linear receivers (MMSE or ZF) and non-linear (successive interference cancellation – SIC), and precoding. The TSB can then be applied **based on the SNR experienced on each stream**, and an aggregate link throughput can thus be obtained.

MIMO Link TSB Estimation

It is difficult in general to obtain the distribution of the stream SNR in closed form for most schemes, especially for realistic channel models, and hence in general **link-level Monte Carlo simulation** has to be used to estimate the distribution of stream SNR and hence of throughput. This should then be stored in an offline look-up table from which random instances of link throughput can be drawn.

A convenient format for this look-up table is the cumulative distribution function (CDF) of throughput, defined as:

$$F_C\left(\tilde{C},\bar{s}\right)=\Pr\left[C\le\tilde{C}\middle|\bar{s}\right]=\int_0^{\tilde{C}}p\left(C,\bar{s}\right)dC \tag{2-27}$$

where $\bar{s}$ denotes the average SNR in dB. This is a monotonically increasing function within the range [0, 1]. We may then generate a random variable $f \in [0,1]$ with uniform distribution, and use it to look up $\tilde{C}$ such that $F_C(\tilde{C},\bar{s})=f$. The PDF of $\tilde{C}$ is then given by:

$$\begin{aligned} p_{\tilde{C}}\left(\tilde{C}\right)&=\operatorname*{Lt}_{\delta C\to 0}\left[\frac{\Pr\left[\tilde{C}\in\delta C\right]}{\delta C}\right]=\operatorname*{Lt}_{\delta C\to 0}\left[\frac{\Pr\left[F_C\in\delta F_C\right]}{\delta C}\right]\\ &=\operatorname*{Lt}_{\delta C\to 0}\left[\frac{\delta F_C\,p\left(F_C\right)}{\delta C}\right]=\frac{dF_C}{d\tilde{C}}=p_C\left(\tilde{C}\right)\end{aligned} \tag{2-28}$$

Hence the random variable $\tilde{C}$ has the required distribution. Since this CDF is in general also a function of the average SINR $\bar{s}$, a two-dimensional look up table is required. If other factors such as INR, etc, are also significant, then a larger number of dimensions may be required. However, if the effect of such factors is not large, or if their distributions are separable from that of SINR, a good approximation is obtained by averaging over them.

MIMO Signal Processing

In our present evaluation we focus on the uplink (MS-ABS, ABS-HBS link), although similar concepts can be applied in the downlink. In order to exploit MIMO channels for increasing throughput through spatial multiplexing we consider some well-known signal processing techniques, namely, linear detection and successive interference cancellation (SIC) detection.

In the case of linear detection, a beamforming matrix, which is a form of a channel matrix inverse, is applied to the received signals in order to minimize the interference between the transmitted data streams, and hence the symbol estimates are obtained via

$$\hat{\boldsymbol{s}} = Q(\boldsymbol{\Omega}^H \boldsymbol{r}_k), \tag{2-29}$$

where $Q(\cdot)$ denotes the quantization operation. The beamforming matrix can be designed according to either the Zero-Forcing (ZF) or the Minimum Mean Square Error (MMSE) criterion. ZF completely eliminates inter-stream interference, and the beamforming matrix takes the form of the Moore-Penrose pseudoinverse of the channel matrix. The ZF beamforming matrix is given as bellow,

$$\boldsymbol{\Omega}_{ZF} = \arg\min_{\Omega_{ZF}} \{\mathbf{s} - \boldsymbol{\Omega}_{ZF}^H \boldsymbol{H}\boldsymbol{s}\}, \tag{2-30}$$

where **r** is the received vector and $\boldsymbol{\Omega}_{\mathrm{ZF}}$ is ZF filter. Although ZF can eliminate interference, it gives rise to noise enhancement when the channel matrix is ill-conditioned. Although MMSE beamforming allows some inter-stream interference, it achieves an optimal trade-off between noise enhancement and interference and results in higher performance than ZF. The cost function of MMSE filtering is given as follows

$$\boldsymbol{\Omega}_{\mathrm{MMSE}} = \arg\min_{\boldsymbol{\Omega}_{\mathrm{MMSE}}} \{\mathbf{s} - \boldsymbol{\Omega}_{\mathrm{MMSE}}^H \mathbf{r}\}, \tag{2-31}$$

where **r** is the received vector and $\boldsymbol{\Omega}_{\mathrm{MMSE}}$ is MMSE filter.

Detection performance can be further improved if it is performed using successive interference cancellation (SIC), i.e., the detected symbols are detected in succession and their interference successively stripped off the remaining received signal by interference cancellation. This frees the signal from some interference components and can enhance the achieved capacity. The conventional SIC algorithm computes the N_Rx1 MMSE filter corresponding to each layer's data stream as

$$\boldsymbol{\omega}_k = (\bar{\mathbf{H}}_k \bar{\mathbf{H}}_k{}^H + \frac{\sigma_v^2}{\sigma_s^2}\mathbf{I})^{-1}\mathbf{h}_k. \tag{2-32}$$

where $\bar{\mathbf{H}}_k$ denotes the matrix obtained by taking the columns *k*, *k*+1,…*K* of channel **H**. In this algorithm, the procedure uses nulling and symbol cancellation to successively detect the desired symbol for each data stream $\hat{s}_k$, *k*, *k*+1,…*K*.

$$\hat{s}_k = Q(\boldsymbol{\omega}_k^H \boldsymbol{\varepsilon}_k), \tag{2-33}$$

These detected symbols construct decision vector $\hat{s} = [\hat{s}_1, \hat{s}_1, \ldots, \hat{s}_K]^T$.

The successively cancelled received vector in the *k*-th stage is $\boldsymbol{\varepsilon}_k$. The received vector after the cancellation of previously detected *k-1* symbols is

$$\begin{cases} \boldsymbol{\varepsilon}_k = \mathbf{r}, & k = 1, \\ \boldsymbol{\varepsilon}_k = \mathbf{r} - \sum_{j=1}^{k-1} \mathbf{h}_j \hat{s}_j, & k \geq 2. \end{cases} \tag{2-34}$$

After subtracting the detected symbols from the received signal vector, the remaining signal vector is processed either by an MMSE or ZF filter for the symbol estimation for the following streams.

The performance of SIC based detection is inferior to that of the optimal maximum-likelihood solution. The probability of detection error of such a detector is generally limited by the remaining interference and the effect of error propagation [9]. Several state-of-the-art solutions [10-11] are proposed to enhance the performance of SIC based detection and achieve a close to optimal performance while maintaining the low complexity of traditional SIC detectors.

For the present evaluation, in order to clarify the description of TSB of MIMO systems, we assumed linear MMSE detection which results in a good trade-off between performance and complexity.

2.5.3 Multi-Beam Assisted MIMO

In BuNGee, the HBSs can create multiple fixed narrow beams with the use of an antenna array fed by a Butler matrix. The signal at the i^{th} beam for uplink can be represented as the combination of signals from different ABSs:

$$\mathbf{y}_i = \mathbf{H}_{ij}\mathbf{s}_j + \sum_{k \neq j} \mathbf{H}_{ik}\mathbf{s}_k + \mathbf{n}_i \tag{2-35}$$

where $\mathbf{s}_j$ is the transmit signal of the j^{th} ABS, $\mathbf{H}_{ij}$ is the 2x2 channel matrix between the i^{th} beam and the j^{th} ABS and $\mathbf{n}_i$ is noise. Each beam can be assigned to serve a unique ABS. In such a scenario, however, the throughput of one ABS may severely be restricted due to the interference from other beams using the same frequency band, i.e., the middle term in (2-35). Frequency planning can somehow mitigate the interference and increase the throughput by avoiding using the same frequency at strong interference ABSs and thus reducing the middle term in (2-35).

Further improvement can be attained by adopting the idea of multi-beam assisted MIMO processing. Unlike single beam processing where one beam only serves one specific ABS, in multi-beam assisted MIMO processing, the beams are serving all the ABSs in the cell simultaneously. The detection is carried out by jointly processing the signals received by all the beams. The signal vector can be written as:

$$\mathbf{y} = \mathbf{H}\mathbf{s} + \mathbf{n} \tag{2-36}$$

where $\boldsymbol{y} = [\boldsymbol{y}_1^T, \dots, \boldsymbol{y}_N^T]^T$, $\boldsymbol{s} = [\boldsymbol{s}_1^T, \dots, \boldsymbol{s}_N^T]^T$, $\boldsymbol{n} = [\boldsymbol{n}_1^T, \dots, \boldsymbol{n}_N^T]^T$ and the channel matrix of the MIMO system is

$$\mathbf{H} = \begin{bmatrix} \mathbf{H}_{11} & \cdots & \mathbf{H}_{1K} \\ \cdots & \mathbf{H}_{ij} & \cdots \\ \mathbf{H}_{N1} & \cdots & \mathbf{H}_{NK} \end{bmatrix} \tag{2-37}$$

MIMO processing techniques, such as the linear detection and SIC, can be directly applied. The only difference is that the size of the MIMO channel matrix changes from a set of 2x2 matrices $\mathbf{H}_{ij}$ to a single larger 2Nx2K matrix **H**. The multi-beam MIMO processing provides significant improvement on the system performance because all the received signals carry useful information for detection and the interference within the cell in single beam processing is exploited.

2.6 Radio Resource Management

Two radio resource management strategies have been simulated in the system-level simulation, the fixed frequency planning proposed by Alvarion [12] and basic cognitive radio based dynamic sub-channel assignment approaches.

2.6.1.1Frequency Planning

The details of the multi-HBS frequency plan are shown in Figure 2-10. At the HBS side, 4 different channels are used for each group of 4 neighbouring beams in the order channel 1 to channel 4. ABSs located at the top and bottom of each cell are designed to serve N-S streets, and ABSs on the left and right serve the E-W streets. The two ABS beams pointing in opposite directions should use two different channels and neighbouring ABS beams use two different channels. ABSs that serve N-S streets use two different channels from those that serve E-W streets. The frequency plan of the top-left corner cell is identical to the bottom-right cell. The frequency plan of the top-right corner cell is identical to the bottom-left cell. Note that in order to avoid possible strong interference at the co-located corner HSSs, the frequency plan of the centre-cell HBS beams follows an order (Green, Yellow, Blue, Red) different from all other edge cells (Green, Red, Blue, Yellow).

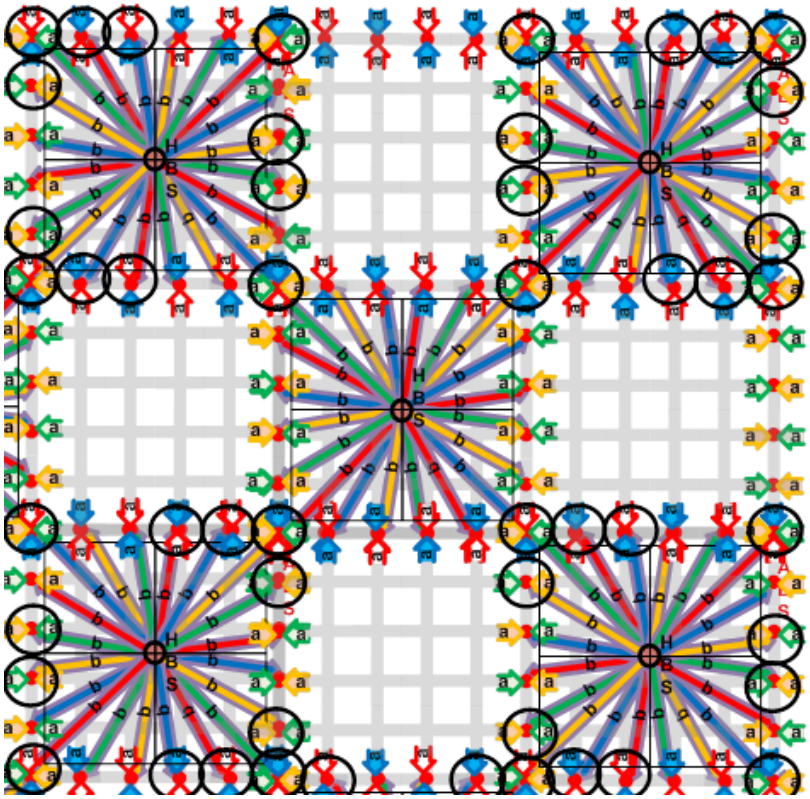

Figure 2-10: Multi-HBS frequency plan

Only 20 beams are used at the HBS in each cell to serve 20 HSSs in this case. Therefore, the ray-tracing results from UCL have been properly adjusted to fit the frequency plan as illustrated in section 2.2.1. A total of 4 channels (red, green, yellow, blue) are shared between the backhaul network and the access network. Thus, a total 40MHz frequency band is utilized in the simulation and the 40 MHz band is divided into 4 10 MHz channels. The results of the frequency planning approach will show the system capacity of in-band backhaul scenario.

30 OFDMA format subchannels are assumed within each 10 MHz channel. Multiple subchannels will be allocated to a user depending on the offered traffic and availability of frequency resource. Retransmission is assumed where a blocked transmission will backoff a random time. TDD duplexing is also used in the simulation and a 50%-50% split is assumed for the downlink and uplink.

2.6.1.2Multi-Beam Assisted MIMO

By using multi-beam assisted MIMO techniques, all the beams of a HBS will be processed jointly. In other words, only the active HBS beams from other cells contribute to the interference in the system. Thus, instead of assigning different frequency bands to different beams and ABSs, we assume that all the HBS beams in a cell use the same frequency channel. Figure 2-11 shows the frequency plan used in the simulation. Different

colours represent different 10MHz channels in the same way as explained in the previous section. Immediate neighbouring HBSs are not allowed to use the same frequency channel to further reduce the potential interference between HBS beams. Thus, in the Multi-Beam Assisted MIMO system, only 3 10MHz frequency band is utilized (Red, Yellow, Green) and 30 OFDMA format subchannels are assumed within each 10 MHz channel.

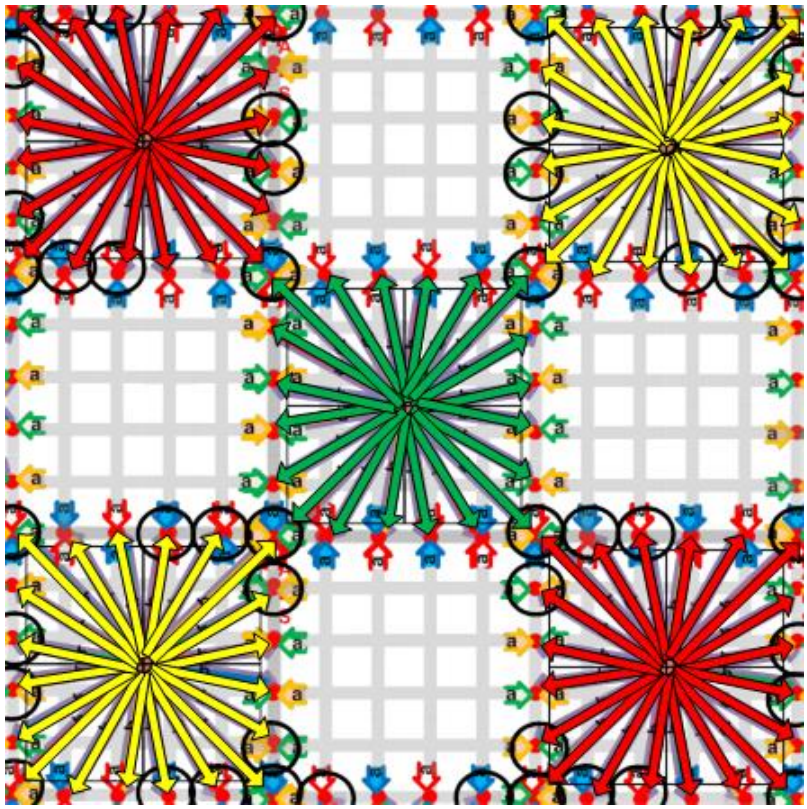

Figure 2-11: Multi-HBS Multi-Beam Assisted MIMO frequency plan

2.6.1.3Cognitive RRM

Spectrum sensing is a process where a Cognitive Radio scans the available frequency bands, estimating the interference level of each of them. Based on the interference estimation the cognitive device can then select the most appropriate frequency channel to use. This cognitive capability is one of the most distinguishing features of cognitive radio [13]. The spectrum awareness aspect helps capture the variations of the radio environment over a period of time or space. It provides the opportunity to fundamentally change the way we manage the radio frequency. Through this capability, the frequency opportunities will be identified distributedly, dynamically and autonomously. The available frequency band and the appropriate transmitting parameters can then be selected. This is the basis of the on-line interaction between cognitive radio and the unpredictable environment.

A low complexity spectrum sensing approach or a channel usage database is suggested in BuNGee to perform the frequency awareness process. Information of spectrum utilization is obtained either through a database or spectrum sensing. The frequency plan is completely removed in this case where the entire 40 MHz frequency band is available at all entities. Frequency resources are dynamically assigned purely based on the spectrum sensing measurements. The difference between the Spectrum Sensing based Dynamic Frequency Assignment (SSDFA) and the frequency planning approach is that before initializing the transmission on the targeted sub-channels, spectrum sensing is carried out on all available channels. Transmission will only be permitted when the interference level on the least-inference subchannel is below the interference threshold. It is assumed that the spectrum sensing is carried out at the receiver end of the wireless link. BuNGee is designed primarily for the dense city centre area where the propagation

environment is very complex. The utilization of directional antennas in such areas makes it possible that the received signal power and the interference power can vary significantly over a range of a few meters. Thus, spectrum sensing at the transmitter is not accurate enough to identify the interference level on the targeted channel. Spectrum sensing at the receiver end therefore is more desirable in this case.

2.6.1.4 Scheduling

A first come first serve scheduling scheme is assumed since the premier goal of the system-level simulation is to demonstrate the capacity of the system. More sophisticated scheduling schemes are likely to improve the fairness of the resource allocation between entities. However, it has virtually no impact on the overall system capacity. Thus, due to the complexity of the system-level simulator, we applied the low complexity first come first serve scheduling scheme. An MS is allowed to occupy more than 1 subchannel if multiple files are requested to be transmitted simultaneously. However, only 1 subchannel will be allocated to 1 file transmission in the simulation.

3. System Level Simulator

3.1 Simulator Structure

A two layer simulation has been developed to accurately model the BuNGee system. The first layer models the self-backhaul link between HBS and HSS. The second layer models the access link between ABS and MS. These two layers are connected together by a channel usage table and the aggregated traffic at HSS for downlink and ABS for the uplink. A 3D (user, time, frequency) channel usage table is designed to track the frequency utilization information in the simulation. The information of entities that are transmitting on the same frequency is available by examining this table, and then the interference can be determined by using an appropriate propagation model and antenna profiles.

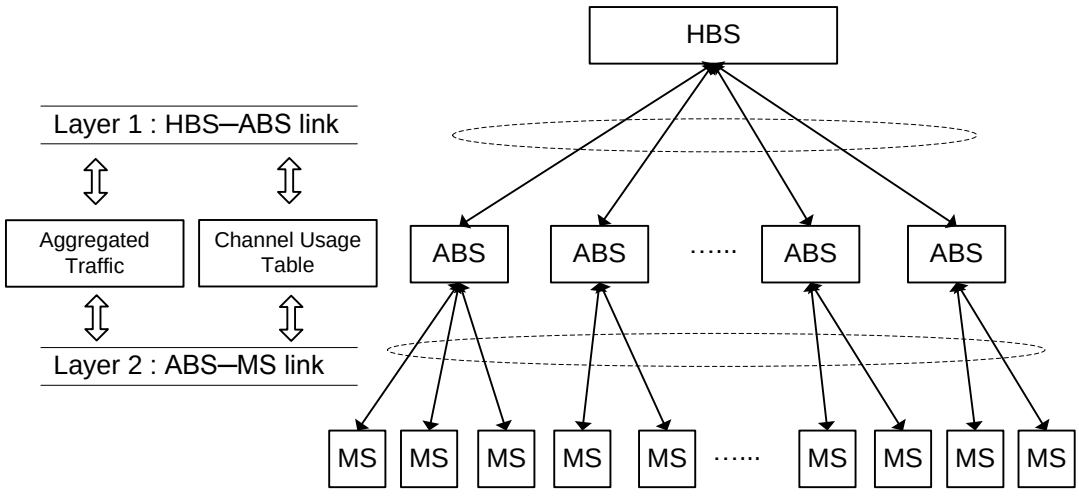

Figure 3-1: Simulation structure

A flowchart is also given in figure 3-2 to show the basic simulation process. The simulator will first generate the location of all entities within the service area. The simulator will check the departure of existing users and release channels no longer in use at the beginning of each trial, then a channel will be assigned to a requested file transmission based on certain RRM strategy. After that the transmission starts and the *SINR* level and throughput are measured on all existing links.

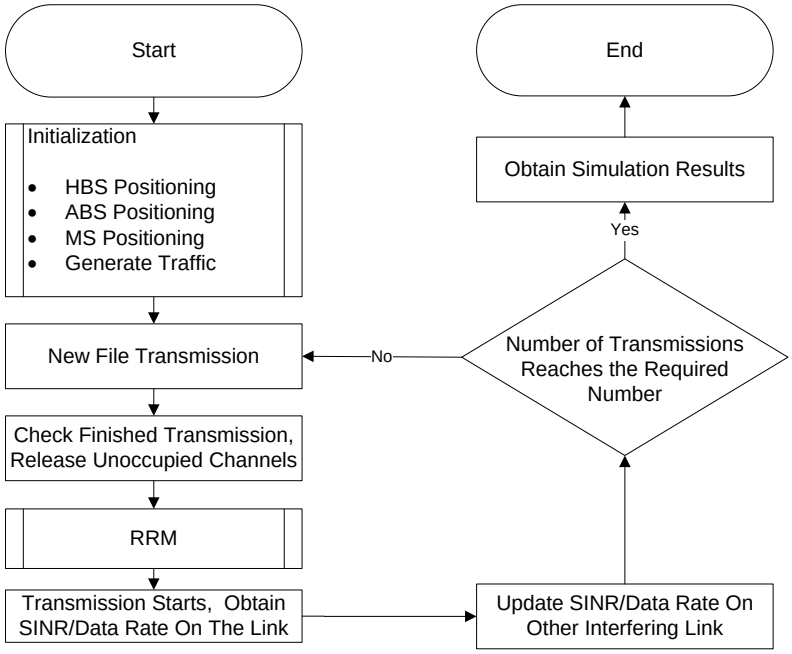

Figure 3-2: Simulation Flowchart

3.2 Modules

A modularized simulator has been designed in WP4 to maximize the flexibility and compatibility of the simulator with different techniques proposed in BuNGee. A wide range of advanced techniques have been proposed in BuNGee, covering issues in the physical layer, MAC layer and network layer. Combined with the complex architecture, these factors make the BuNGee system extremely difficult to model. Thus the modularized simulator has been developed in the format shown in Figure 3-3.

Different modules model different aspects of the system and all the modules can be modified separately without interfering with each other. In this way, the simulator can be updated relatively easily to address the development of different work packages within the BuNGee project.

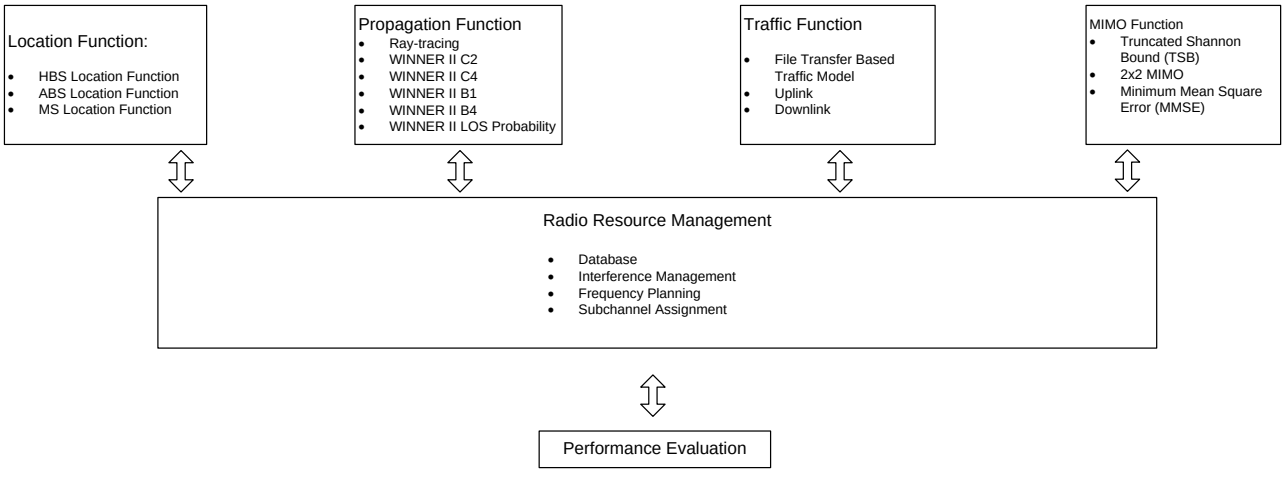

Figure 3-3: Simulator Modules

3.2.1 Location Function

The location function is a set of functions that model the physical environment where the BuNGee system is assumed to be placed. The location function will first generate a City-grid environment over a certain service area by defining the number of N-S streets, the number of E-W streets and the street width. Then according to the deployment strategy assumed, the location function will place the base stations at appropriate locations with a small random variation (within the street). The number of HBSs, the number of ABS per cell and their locations are also available to be defined in the simulation. Figure 3-4 shows the examples of the Square topology in 5-HBS and 9-HBS deployment scenario. The red squares are the HBSs, the black circles represent ABSs and the blue crosses are the crosses of the streets.

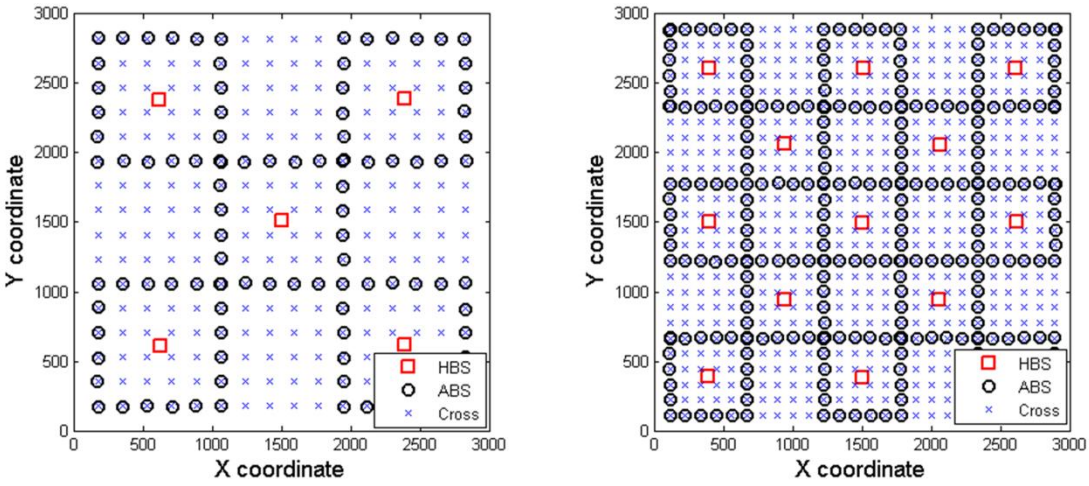

Figure 3-4: Example Square Topology plots with different number of HBSs

In the final simulation, the simulation scenario is defined by UoY and UCL jointly. A 5 HBS, 64 ABS/HSS scenario is applied that the location module is tailored to fit with the layout discussed in section 2.1 (shown in Figure 2-1). Figure 3-5 shows the final simulation scenario plot obtained from the simulator. It completely matches the proposed system environment shown in Figure 2-1. Both the outdoor MS scenario and the outdoor+indoor MS scenario are proposed to be simulated in the final simulation. Figure 3-6 and Figure 3-7 show these two scenarios respectively.

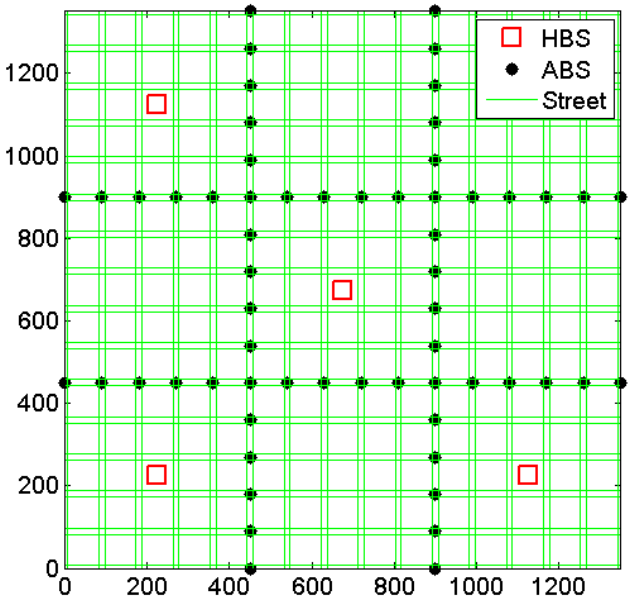

Figure 3-5: Final simulation scenario plot

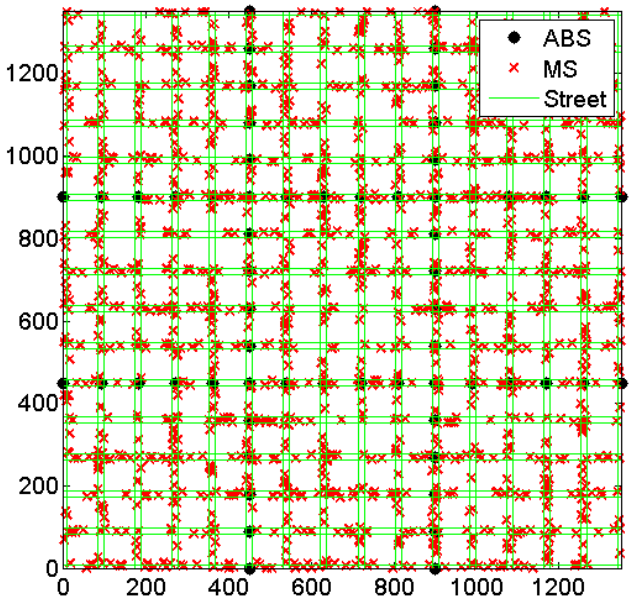

Figure 3-6: Final simulation scenario plot – outdoor MS only

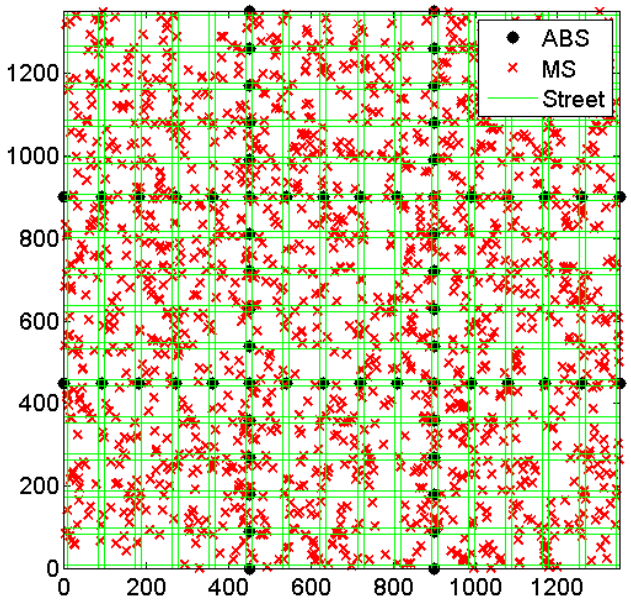

Figure 3-7: Final simulation scenario plot – outdoor + indoor MS

3.2.2 Propagation Function

The propagation function includes a set of tools developed in the simulator that model the propagation environment of the BuNGee system. UCL's ray-tracing model, WINNER II B1, WINNER II B4, WINNER II C2, WINNER II C4 are all included in this function set [2, 4]. Moreover, unlike the interim simulation in which

all links between same-street outdoor entities are assumed to be LOS (clearly too optimistic), two LOS probability estimation models are also developed to obtain the probability of LOS link for outdoor entities. The application of LOS probability models enables more accurate modelling of the physical environment. The average received signal strength of outdoor MSs is expected to be lower than the interim simulation in this case.

Backhaul network propagation measurements are taken by UCL's ray-tracing at fixed points where HBS/HSS are placed. A 64x64 lookup table is applied to obtain the path loss of either a signal or an interference path. Based on the location of the entities, when calculating the path loss for access network entities, most appropriate WINNER II model will be selected.

Another task of the propagation function is to obtain the right antenna gain values from the data provided by CASMA. Again for the backhaul network, this work has been carried out by UCL. However, the tools developed in the propagation function are able to calculate angles between any two entities, including the azimuth angle and the elevation angle. By using the 3D antenna profiles, the antenna gain of ABS/HBS can be obtained. An omni-directional antenna is assumed at the MS, and 0 dBi gain is also applied.

3.2.3 Traffic Function

The traffic function generates traffic for the MS, both downlink and uplink. As explained earlier, this link level file transfer-based traffic model generates file arrival time and file size at certain offered traffic levels. The interarrival time follows Negative Exponential distribution and the file size follows the Pareto distribution. In the simulation, offered traffic levels can be adjusted by changing the average file size and average inter-arrival time. The average file size is fixed at 1Mbits in this simulation. The size of the generated files in this case varies from few hundred kilobits to around 1.1 gigabits because of the 'long-tail' property of Pareto distribution. The offered traffic level is adjusted by changing the arrival rate of files. The mean interarrival time of files can be obtained by:

$$\overline{T}_{\text{int}} = 1/\lambda \tag{3-1}$$

where λ is the arrival rate of files. Retransmission is assumed: that is, that blocked file transmissions will backoff for a random time. The mean backoff time follows the Negative Exponential distribution and the mean backoff time is set equal to the mean interarrival time of files in the simulation:

$$\overline{T}_{backoff} = \overline{T}_{\text{int}} \tag{3-2}$$

3.2.4 MIMO Function

3.2.4.1Point-to-Point MIMO

Collaborative work has been carried out at UY between WP2 and WP4 to develop the MIMO function. To design our MIMO simulation module, i.e., the mapping from an average SINR value to a throughput value, we conduct offline numerical experiments. For a range of useful average SINR values (values that are likely to occur), typically from -5 to 40 dB and for 1 dB step size, we generate a number of 2x2 matrices with Rayleigh channel coefficients. We estimated that a set of 3000 matrices results in sufficiently accurate results. We apply the assumed MMSE linear detection for each of these matrix samples and obtain a value for the achievable rate under the TSB. Therefore for each average SINR value we create a vector containing throughput values (3000 samples in our current evaluation) which fully capture our assumptions and the effect of MIMO signal processing. These values describe the distribution of the achievable rate with MIMO. The obtained set of vectors is stored and made available to our BuNGee throughput simulator.

In the process of simulating the achievable throughput, we perform the following actions in every iteration:

1. For each wireless link we calculate the average SINR taking into account the path loss and shadowing of the useful and the interfering links.
2. For the obtained average SINR we choose the closest value of SINR for which we have an available MIMO throughput distribution (a vector of throughput values).

3. For the chosen average SINR value we select at random a throughput value from the corresponding vector.

In the system level simulation, a random throughput value will be randomly selected from the 3000 samples at a given SINR level, and then the transmitter is assumed to transmit data at the selected throughput level.

Antennas, Small-scale fading

As stated before we assume two antenna elements per HBS, ABS and MS. Therefore the dimension of the MIMO channel matrix per wireless link is 2x2. Furthermore we assume independent and identically distributed (iid) small-scale fading coefficients whose envelope follows the Rayleigh distribution (absence of line-of-sight). Therefore MIMO channels are assumed to be uncorrelated.

Parameters and TSB Look-up Table

The parameters of our BuNGee-specific TSB are *a* = 0.65, SNIRmin = 1.8 dB, SNIRmax = 21 dB and Thrmax = 4.5 bps/Hz. These parameters are chosen so that the integral of the BuNGee-specific AMC throughput curve matches that of the TSB in order to ensure that average throughput is matched. The BuNGee-specific TSB can be seen in the following figure (red curve) together with the achievable throughput of the BuNGee AMC codeset, which is the codeset used by the BuNGee project relating to WiMAX, and the pure Shannon bound.

Figure 3-8 compares the Shannon bound and truncated Shannon bound with the same MMSE post-processing SNR. TSB introduces the maximum throughput C_{max} which restricts the throughput of each data stream. Therefore, TSB constrains the overall MIMO throughput below 4.5x2=9 bps/Hz. The parameter a = 0.65 scales SB down and obtains TSB in low SNR region.

A typical look-up table for the link throughput against pre-processing SNR is given in Figure 3-9. The CDF is given for a range from -5 dB to 40 dB in steps of 1 dB. In system level simulations, the link throughput is obtained by looking-up the curves with a given pre-processing SNR. Not all the points in each curve need to be stored in the table, intermediate values can be obtained by interpolation.

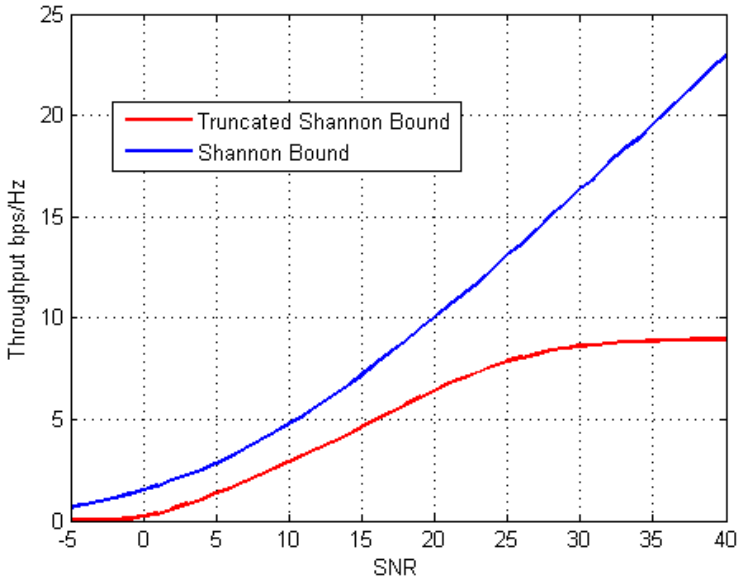

Figure 3-8: System capacity in terms of Shannon bound and truncated Shannon bound for a MIMO system with MMSE linear detector and Nt = Nr =2.

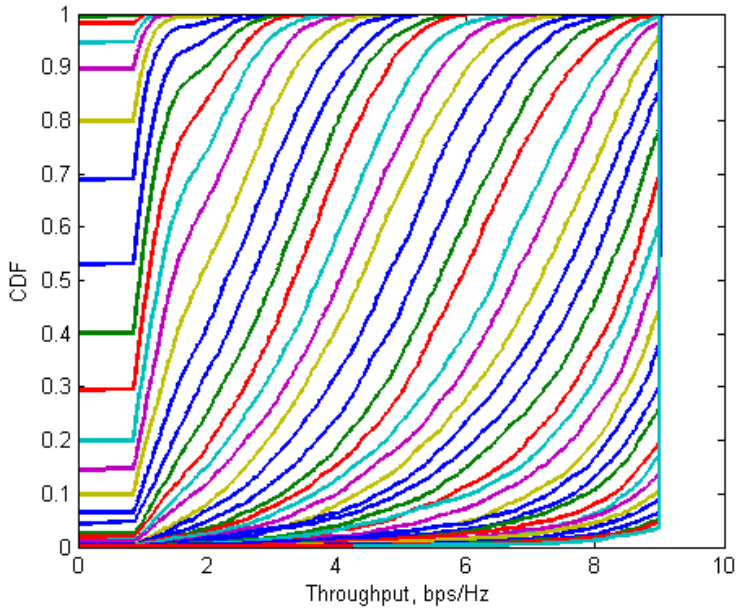

Figure 3-9: Throughput look-up table for system level simulator for MIMO system with Nt = Nr =2.

3.2.4.2Multi-Beam Assisted MIMO

A modeling approach similar to the point-to-point MIMO scenario is applied for the Multi-Beam Assisted MIMO links. For a range of useful average SINR values, from -5 to 40 dB and for 1 dB step size, we generate 3000 matrix results at each SINR level. These values describe the distribution of the achievable rate with Multi-beam assisted MIMO. Then for the backhaul network, we measure the SINR values of backhaul links and randomly obtain the data rate from the distribution we generated offline by assuming Multi-beam assisted MIMO at HBSs.

Figure 3-10 shows the average capacity of the ABSs under different MIMO detection techniques. Here all the ABSs are assumed with the same transmit power. Multi-beam assisted MIMO processing significantly outperforms single beam processing. The MMSE SIC generally has better performance than the linear MMSE detections. This is true especially when interference exists and the performance of linear MMSE downgrades. It can be seen that even in the presence of interference, the achievable capacity of MMSE SIC detection can be very close to the constraint of TSB at 9bps/Hz.

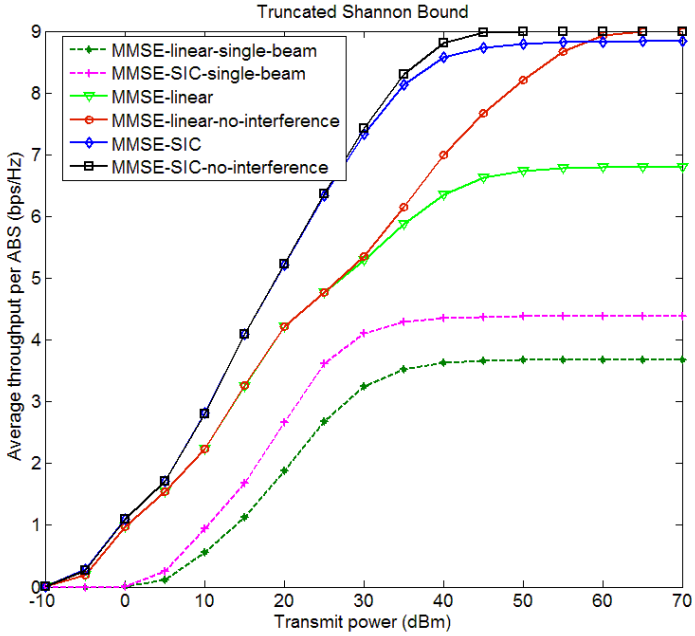

Figure 3-10: Averaged ABS capacity vs. ABS transmit power

Typical look-up tables used in the system level simulation with respect to the average link SINR are presented in Figure 3-11 and Figure 3-12. Linear MMSE detection is used to obtain the CDF. The results are obtained in the uplink for an SINR range from -5 dB to 40 dB with 3000 randomly generated channel matrices. In the simulation, we assume:

- All ABSs in the target cell have the same transmit power P_S;
- All interfering ABSs outside the target cell have the same transmit power P_{int};
- The noise level is fixed at σ_n^2, obtained from the noise figure in BuNGee;
- The interference to noise ratio (INR), averaged over all HBS beams, is fixed at 10 dB.

Before generating random channel coefficients and computing the resultant SINR, two parameters P_S and P_{int} should be calculated. Since the noise power and INR is fixed, the power of interference P_{int} can be calculated according to:

$$INR = \frac{P_{\text{int}} \sum_{m,n} G_{mn}^{\text{int}}}{\sigma_n^2 \bullet N} \tag{3-3}$$

where G_{mn}^{int} is the path loss from the mth interfering ABS to the nth beam at the HBS, m=1,…,M and n=1,…,N. The transmit power of the target ABSs P_S can be calculated based on the calculated P_{int} and the noise power, according to the following relation:

$$SINR = \frac{P_s \sum_{k,n} G_{kn}}{P_{\text{int}} \sum_{m,n} G_{mn}^{\text{int}} + \sigma_n^2 \bullet N} \tag{3-4}$$

where G_{kn} is the path loss from the kth target ABS to the nth beam and k=1,…,K. . It is important to mention that to reduce the complexity of simulation, we treat the inter-cell interference as noise, i.e., instead of generating random channel coefficients for interference channels, we take the average values according to the path loss. This simplification is reasonable for the Backhaul link in BuNGee as the number of interfering ABSs is relatively large.

Since the geometry of the backhaul link is fixed and the path losses of different data streams (ABSs) are different, each data stream has its own statistical characteristics, i.e., the mean and standard derivation of the data rate distribution at a given SINR. Therefore, it is important to retain all this information in the look-up tables used for determining the instant throughput in the system level simulation. An ideal way is to keep different look-up tables for different data streams. However, this significantly increases the complexity when extending the system level simulation from point to point MIMO processing to MBA MIMO processing.

Combined MBA-MIMO Data Rate Distribution

An alternative method which avoids significant increase of the simulation complexity is used in our work. In each simulation trial, the SINR of each data stream (ABS) after MIMO detection, to be applied to the TSB for computing the capacity, is computed based on the current channel coefficients. The attained data rates of all data streams are put into the look-up tables. For each SINR level, only one look-up table is produced. The mean value of this Combined MBA-MIMO data rate distribution is the same as the average mean value over all data streams; while the standard deviation is higher than that of any data stream. Hence, because the probability of low capacity (and hence blocking) is larger, this will lead to a pessimistic estimate of overall throughput density. The CDFs of the Combined MBA-MIMO data rate distribution are presented in Figure 3-11. The shape of the CDFs suggests that the result of aggregating the distributions of all ABS data streams is a mixture distribution, whose components correspond to the throughputs of different ABSs, and confirms that the result is likely to be pessimistic.

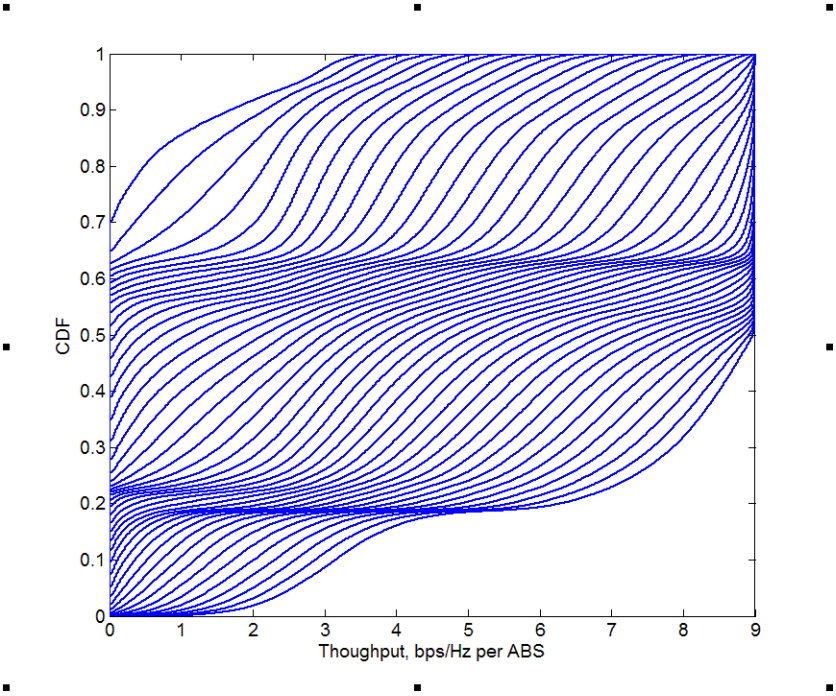

Figure 3-11: Backhaul link CDF for combined MBA-MIMO data rate distribution

Averaged MBA-MIMO Data Rate Distribution

A straightforward way of producing the look-up tables is to average the attained throughputs of different data streams in each simulation trial. At each SINR level, the mean of this averaged MBA-MIMO data rate distribution is the same as that of the Combined MBA-MIMO data rate distribution. However, the standard deviation is much smaller, i.e., when drawing random data rate values from the look-up tables, the probability of very low values is much lower, as can be seen in Figure 3-11 and Figure 3-12. In such a case, the system performance obtained is optimistic, which may be useful for providing an upper bound of the system performance.

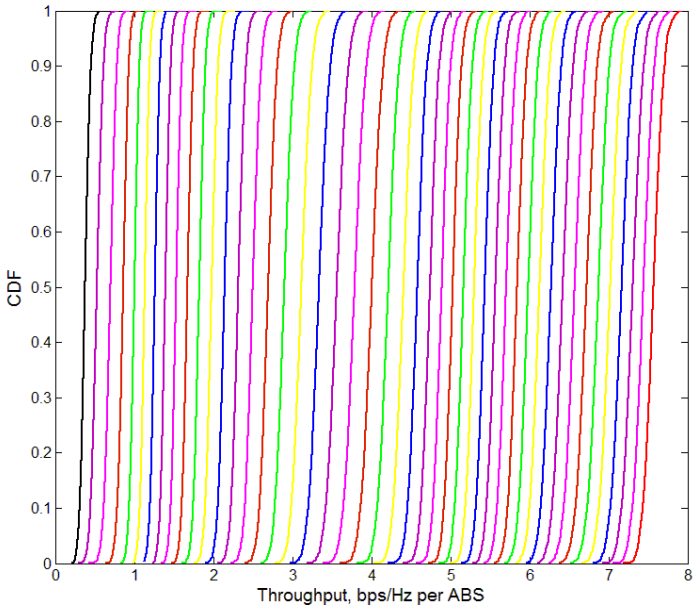

Figure 3-12: Backhaul link CDF for averaged MBA-MIMO data rate distribution.

3.2.5 Radio Resource Management Function

The RRM function is the main module of the simulator. All other functions are integrated with the RRM function to perform certain tasks. There are two main RRM approaches that have been simulated in the simulation as described in section 2.6. Here two flow charts are given to show the simulation process. The difference between these two approaches is the spectrum sensing part.

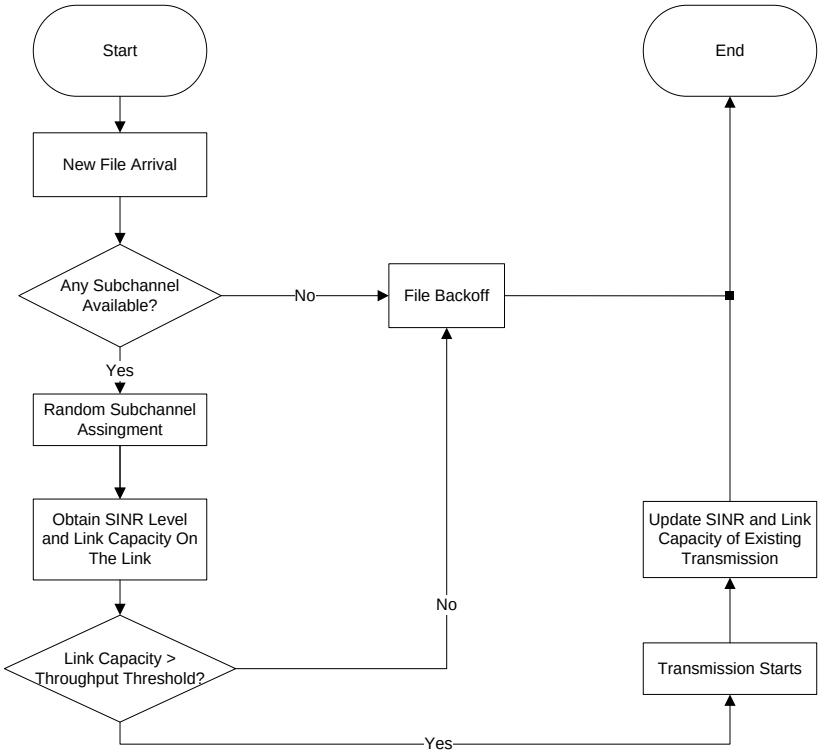

Figure 3-13: RRM algorithm: Frequency Planning

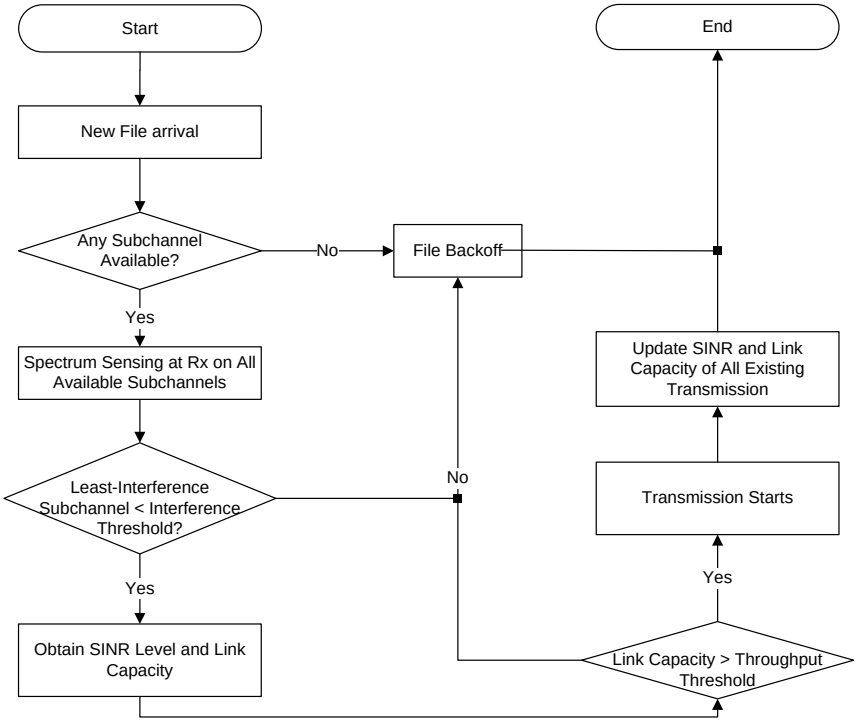

Figure 3-14: RRM algorithm: Pure Spectrum Sensing

Note that a throughput threshold has been used to check the quality of the wireless link instead of a *SINR* threshold. By applying MIMO, the achievable data rate at a certain *SINR* level is no longer a deterministic value. Instead, it is a variable that follows a distribution. Thus, a fixed *SINR* threshold which is traditionally used in such a scenario is no longer accurate enough. A throughput threshold of 0.86 bps/Hz is used in this case instead of the *SINR* threshold in the simulation.

4. Performance Evaluation

4.1 Performance Measures

In order to compare the system performance against the ambitious target of 1 Gbps/km^2, system throughput density is used as the major measurement in this simulation. The system throughput can be defined as:

Thr_s is the system throughput value defined as:

$$Thr_s = \frac{\sum_{i=1}^{N_u}\sum_{k=1}^{n_i}\sum_{t=0}^{T_k} Thr_{MIMO-TSB}(t)}{t_s} \cdot P_{TDD} \qquad (4\text{-}1)$$

$Thr_{MIMO\text{-}TSB}(t)$ is the throughput value of a link obtained at time t, and it is updated constantly in the simulation. T_k is the transmission time of the k^{th} file of an entity, and n_i is the total number of transmissions that have been finished by the i^{th} entity in the simulation. N_u is the total number of entities in the simulation. t_s is the simulation time and P_{TDD} is the percentage of time slots have been allocated to the DL or UL. A 50%-50% split TDD for DL and UL is assumed, therefore P_{TDD} = 0.5 for DL/UL in this case.

Throughput density can then be defined by:

$$Thr_D = Thr_s / A_s \tag{4-2}$$

where A_s is the service area.

Delay can be obtained by:

$$t_D = \frac{\sum_{i=1}^{N_u}\sum_{k=1}^{n_i}(t_T(k)+t_B(k))}{N_f} \tag{4-3}$$

where t_T is the transmission time of file k and t_B is the backoff time of file k. n_i is the total number of files that have been transmitted by the i^{th} entity in the simulation. N_u is the total number of entities in the simulation.

The probability of retry is also used in this simulation to describe the probability that the current file transmission request been rejected by the system. The probability of retry at time t is obtained by:

$$P_{retry}(t) = N_r(t)/N_a(t) \tag{4-4}$$

where $P_{retry}(t)$ is the probability of retry at time t. $N_r(t)$ is the total number of reject file transmissions of the system by time t, and $N_a(t)$ is the total number of file transmission requests (including retries) of the system by time t.

4.2 Simulation Results and Analysis

This section presents the results obtained from the simulation. Downlink and uplink results are all provided with the analysis of the system level performance. Results are given in forms of performance measures presented in the previous section.

4.2.1 Frequency Planning

4.2.1.1 Outdoor MS

An outdoor MS only scenario has been simulated in which 1500 MSs are uniformly distributed on the streets in the service area. The outdoor MSs are expected to be less affected by interference due to the isolation of building blocks. Figure 4-1 and Figure 4-2 show the system throughput density Thr_d defined in equation (4-2) and the delay performance t_D defined in equation (4-3) of the downlink and the uplink respectively. The end-to-end downlink throughput is about 0.65Gbps/km^2. For the uplink, the throughput density is about 0.4Gbps/km^2. Thus, an overall throughput density of 1.05Gbps/km^2 can be achieved in this scenario. The system becomes saturated when the offered traffic is above 2Gbps/km^2 for the downlink and 1Gbps/km2 for the uplink. The delay increases dramatically if we keep increasing the offered traffic level after these saturation points.

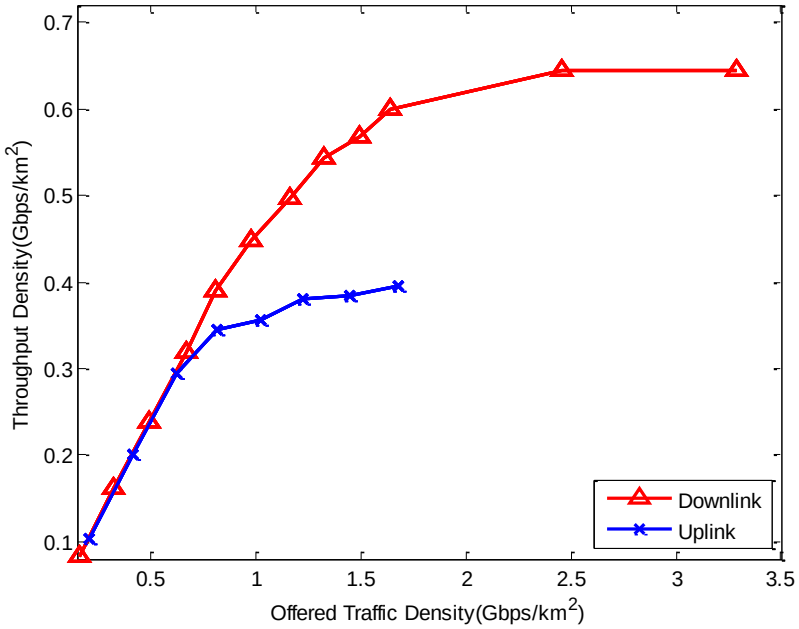

Figure 4-1: System throughput density versus system offered traffic density: Frequency Planning (outdoor MS only)

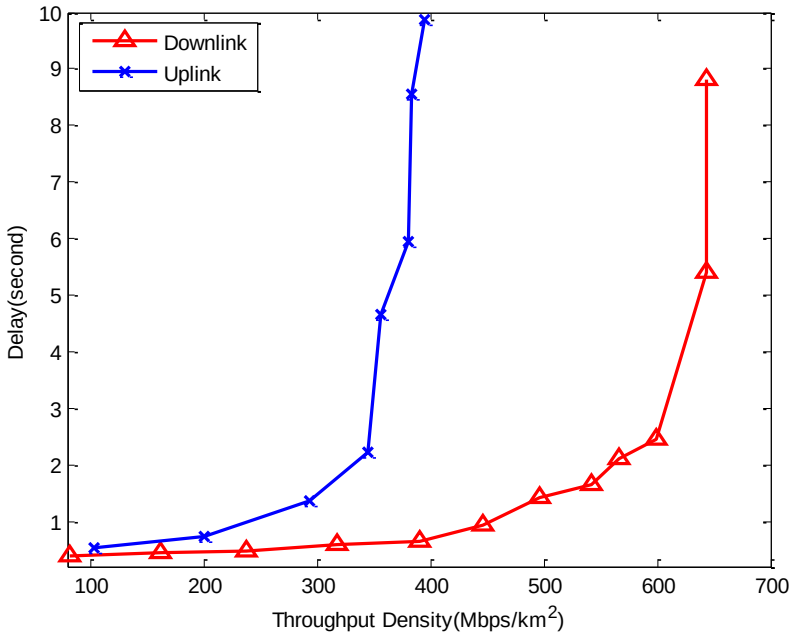

Figure 4-2: Delay versus system throughput density: Frequency Planning (outdoor MS only)

4.2.1.2Indoor+Outdoor MS

We have also simulated a scenario where MSs are uniformly distributed over the entire service area. Please note that MSs are assumed to be at street level only and no windows are assumed in the buildings (clearly a pessimistic case). The building layouts in most cities will in practice also mean that most users are closer to the streets than assumed here. All the indoor MSs are covered by the ABSs on streets, and no other approaches are assumed to provide indoor coverage, e.g. femto-cells. The propagation environment is very

harsh for the indoor MS in this case. The majority of the MSs are placed indoors when a uniform MS density distribution is used over the service area. Thus, the results provided in this section are useful in terms of understanding the worst case system performance of BuNGee.

We used exactly the same simulation setup and parameters as the outdoor MS scenario except the MS distribution. Figure 4-3 shows the system throughput density of the downlink and the uplink in the outdoor plus indoor MS scenario. A downlink throughput density of about 0.55Gbps/km^2 can be achieved. The uplink throughput density can be achieved at 0.3Gbps/km^2. Thus an overall throughput density of 0.85Gbps/km^2 can be reached under the worst case assumptions. The throughput density is below the targeted 1 Gbps/km^2 due to the insufficient coverage of in building MSs.

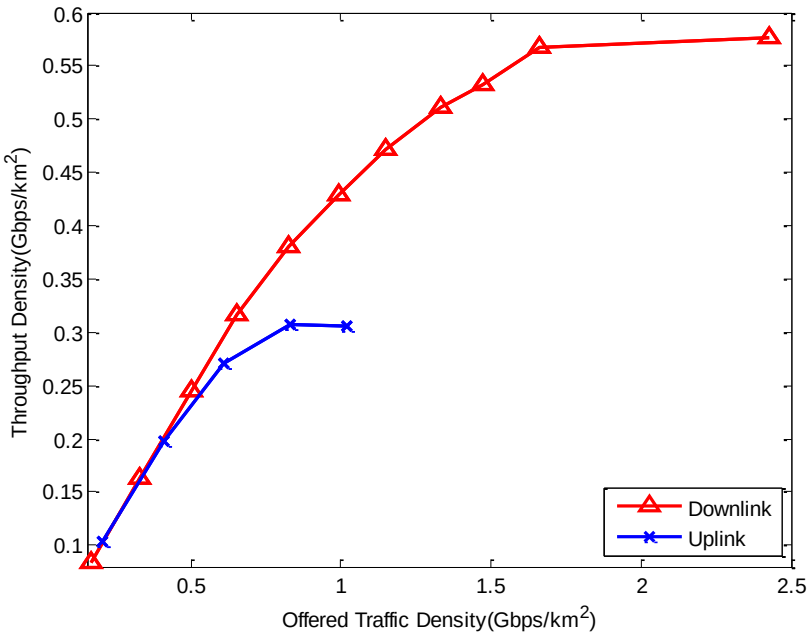

Figure 4-3: System throughput density versus system offered traffic density: Frequency Planning (outdoor + indoor MS)

Figure 4-4 shows the delay performance of the indoor plus outdoor MS scenario. Again, delay increases dramatically if we keep increasing the offered traffic level after these saturation points. The QoS measurements of the indoor+outdoor MS scenario are likely to be higher than the outdoor MS only scenario due to the poor signal reception of indoor MSs. Figure 4-5 to Figure 4-8 compare the QoS measurements of this two cases.

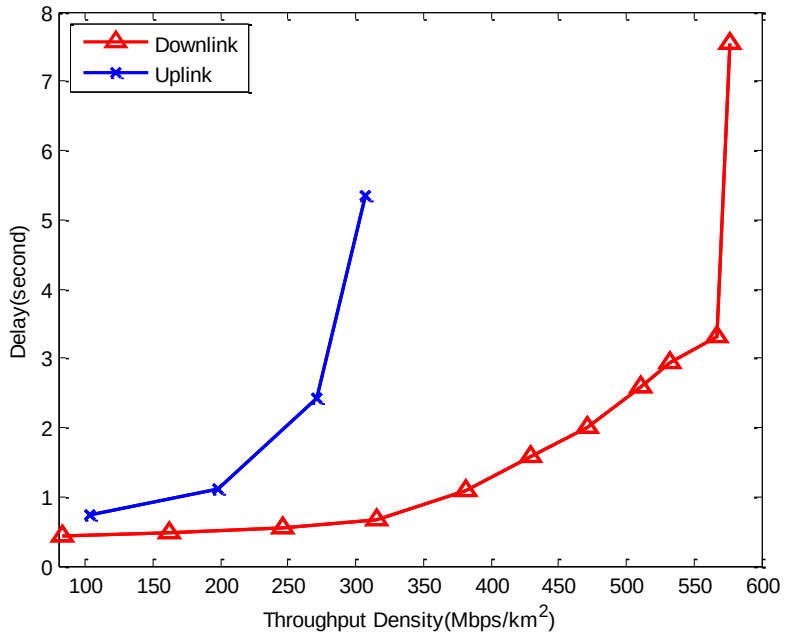

Figure 4-4: Delay versus system throughput density: Frequency Planning (outdoor + indoor MS)

Figure 4-5 and Figure 4-6 compare the probability of retry of the downlink and the uplink of the system under the two MS deployment assumptions respectively. It can be clearly seen that the outdoor+indoor MS approach suffers a higher level of system interruption than the outdoor MS only scenario, e.g. for the downlink, the retry probability of the outdoor+indoor MS scenario approximately double the figure of the outdoor MS only scenario when the offered traffic is higher than 0.8Gbps/km^2. Also the retry probability of the uplink in the outdoor+indoor MS scenario is about twice as high as the outdoor MS only scenario.

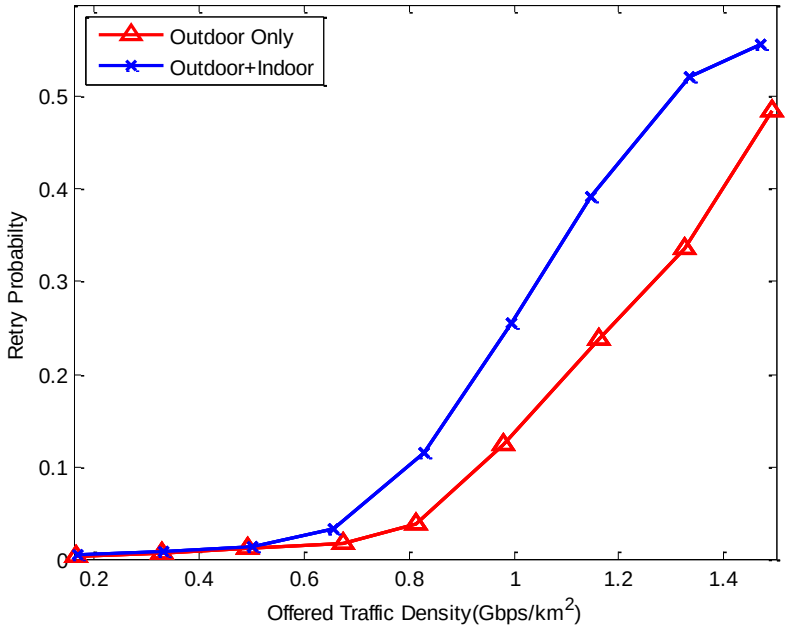

Figure 4-5: Probability of retry versus system offered traffic density: Frequency Planning (Downlink)

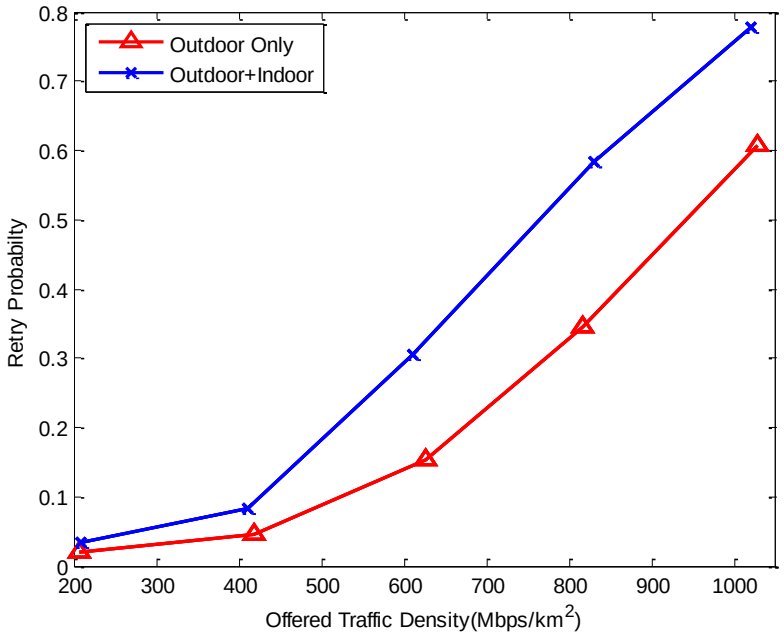

Figure 4-6: Probability of retry versus system offered traffic density: Frequency Planning (Uplink)

Figure 4-7 and Figure 4-8 compare the delay performance of the downlink and the uplink of the system respectively. It can be seen that the delay of outdoor+indoor MS scenario is higher than the indoor MS only scenario. The indoor MS only scenario the system can still transmit files with a satisfactory QoS measurement after the outdoor+indoor MS system has saturated. The delay of the outdoor+indoor MS scenario is about 7.5 seconds when the throughput density is about 0.55Gbps/km^2. The delay of the outdoor MS only scenario is significantly lower at the same point which is only about 2 second. The results of uplink are similar in that the system delay is approximately 10 seconds when the throughput density is around 300Mbps/km^2 for the outdoor+indoor MS scenario. The system delay of the outdoor MS only scenario is only about 2 second when the throughput density is 350Mbps/km^2. Thus the outdoor+indoor scenario not only achieves a higher overall throughput density, but also the QoS is much better in the simulation, especially when the offered traffic level is relatively higher.

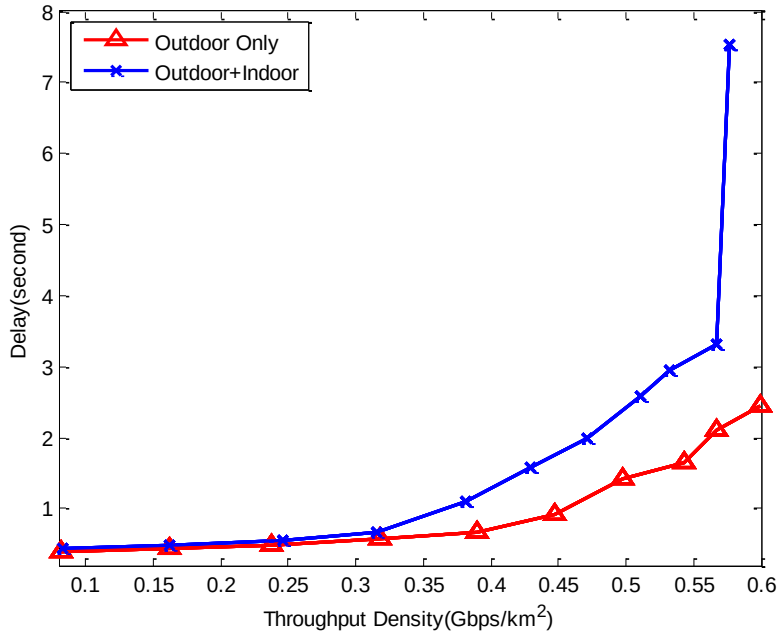

Figure 4-7: Delay versus system throughput density: Frequency Planning (Downlink)

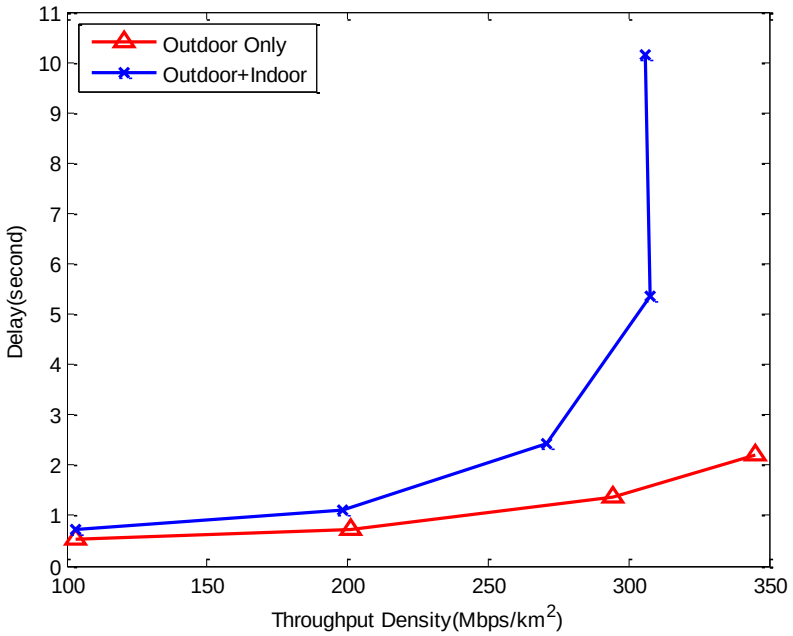

Figure 4-8: Delay versus system throughput density: Frequency Planning (Uplink)

4.2.1.3Multi-Beam Assisted MIMO

The BuNGee Multi-Beam Asisited MIMO techniques developed in WP2 has the potential to significantly improve the system capacity. By carrying out joint-beam processing at HBSs, the interference between the beams of a single HBS is no longer 'harmful'. Instead it contributes to the system in a positive way. Thus, same cell HBS beams are no longer interference sources and only the inter-cell interference are considered for the backhaul network. By introducing the frequency plan for the Multi-Beam Assisted MIMO approach (as shown in Figure 2-11), the interference of the backhaul network is not expected to be very high in this case because the immediate neighbouring HBSs use different frequency bands. The distance between two interfering HBS is long and the path loss is expected to be high.

An outdoor MS only scenario is assumed because it is not desirable if the access network is the 'bottleneck' of the system. Two different MBA-MIMO simulation techniques (as introduced in section 3.2.4.2) are applied to provide a more comprehensive analysis of the potential capacity of the MBA-MIMO based system: a pessimistic case which uses the combined MBA-MIMO data rate distribution and an optimistic case which takes advantage of the averaged MBA-MIMO data rate distribution. The optimistic case results are provided to show the upper bound of the MBA-MIMO based system capacity, and the much more pessimistic case provides a more accurate estimation of the achievable throughput density that allows us to confirm with confidence an achievable "headline" throughput density.

Combined MBA-MIMO Data Rate Distribution

Figure 4-9 and Figure 4-10 show the system performance of the combined MBA-MIMO data rate distribution approach. The highest end-to-end downlink throughput is about 1.05Gbps/km^2. For the uplink, the throughput density is about 0.95Gbps/km^2. Thus, an overall throughput density of approximately 2Gbps/km^2 can be achieved in this scenario. The overall system capacity has been significantly improved by applying Multi-Beam Assisted MIMO at HBSs. Considering the backhaul network only uses 3 10MHz channel, the Multi-Beam Assisted MIMO technique also has the potential to reduce the requirement for frequency resource.

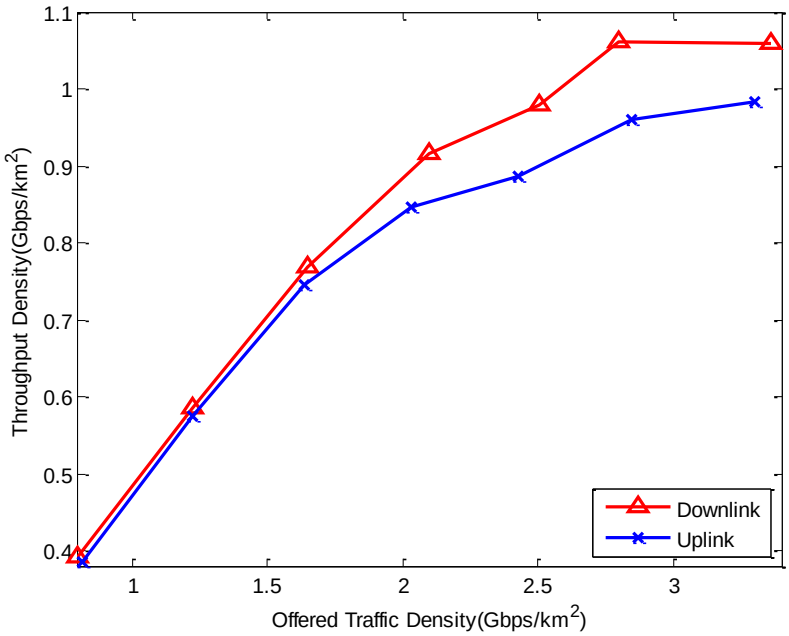

Figure 4-9: System throughput density versus system offered traffic density: MBA-MIMO (Combined MBA-MIMO Data Rate Distribution)

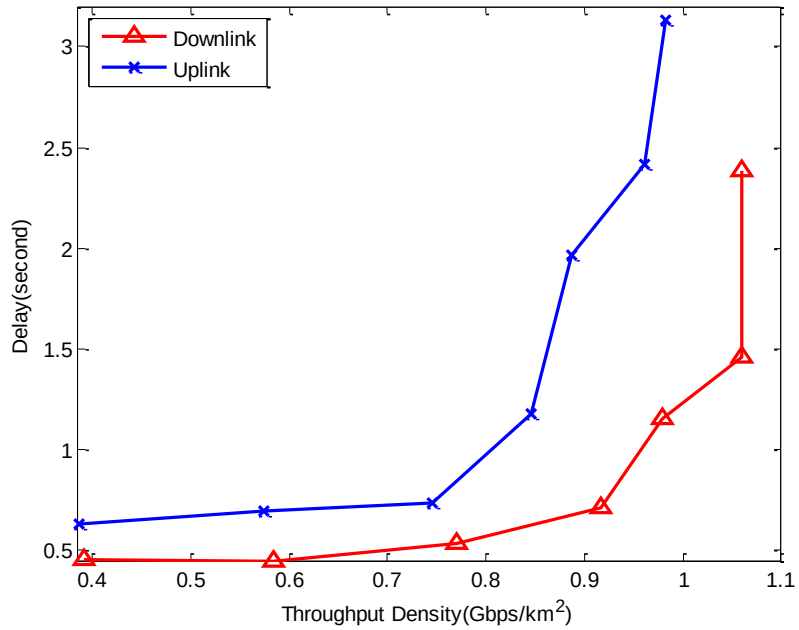

Figure 4-10: Delay versus system throughput density: MBA-MIMO (Combined MBA-MIMO Data Rate Distribution)

Averaged MBA-MIMO Data Rate Distribution

Figure ***4-11*** and Figure 4-12 illustrate the system performance of the more optimistic Averaged MBA-MIMO Data Rate Distribution approach. The highest end-to-end downlink throughput is about 1.2Gbps/km^2. For the uplink, the throughput density is about 1Gbps/km^2. Thus, an overall throughput density of 2.2Gbps/km^2 can be achieved in this scenario. Note that the results obtained by using the averaged MBA-MIMO data rate

distribution are only intended to indicate the upper bound of the potential improvement by using MBA-MIMO. The results provided previously in the combined MBA-MIMO data rate distribution section are more accurate hence more appropriate to be used as the 'headline' achievable system capacity.

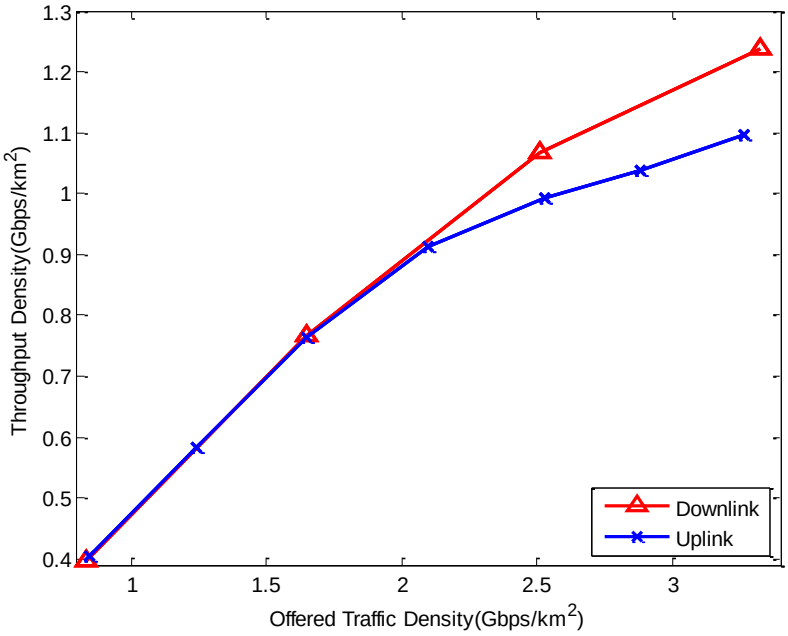

Figure** 4-11**: System throughput density versus system offered traffic density: MBA-MIMO (Averaged MBA-MIMO Data Rate Distribution)

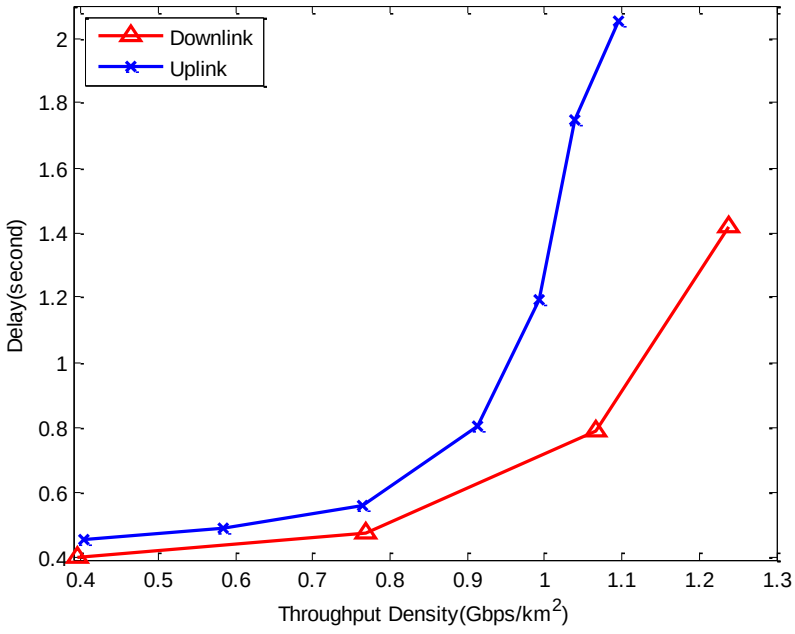

Figure 4-12: Delay versus system throughput density: MBA-MIMO (Averaged MBA-MIMO Data Rate Distribution)

4.3 Cognitive Radio Based Approach

Cognitive radio based dynamic resource management approach is able to completely remove the requirement for the frequency plan. The frequency resource is allocated dynamically based on the spectrum sensing measurements. Thus the RRM complexity, in terms of planning, is significantly reduced. The indoor+outdoor MS scenario is assumed because the coverage of the pure frequency planning approach provided to the indoor MSs is poor, if no further means of indoor coverage (e.g. femto-cells) are assumed. It is useful to understand whether the cognitive radio could improve the system performance in such situation.

Figure 4-13 shows the system throughput density performance of the cognitive radio approach. It can be seen that a downlink throughput density of 530Mbps/km^2 and an uplink throughput density of 320 Mbps/km^2 have been achieved. An overall throughput density of 850 Mbps/km^2 can be achieved. Note that the system delay is kept to a very low level as shown in Figure 4-14 all through the simulation until the system saturates when the offered traffic is above 1.2Gbps/km^2 for the downlink and 0.8Gbps/km^2 for the uplink..

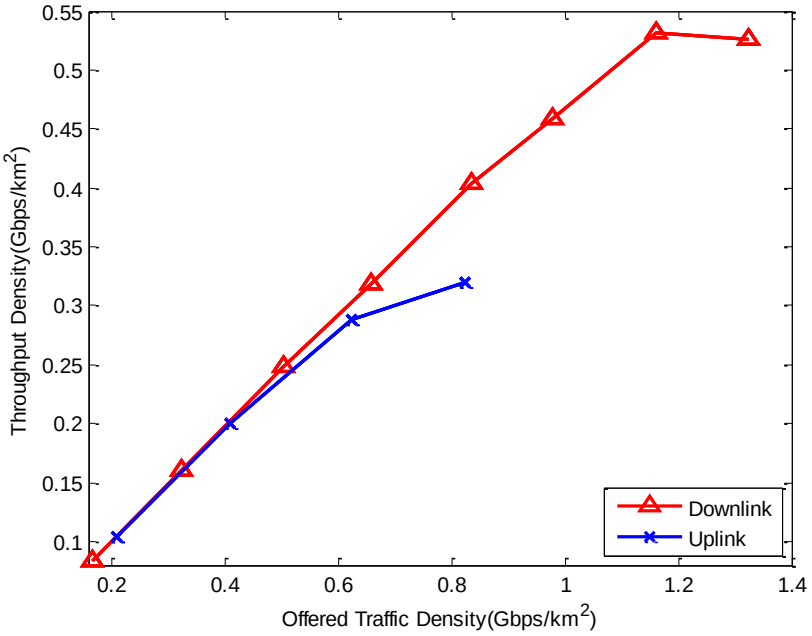

Figure 4-13: System throughput density versus system offered traffic density: Cognitive Radio (outdoor + indoor MS)

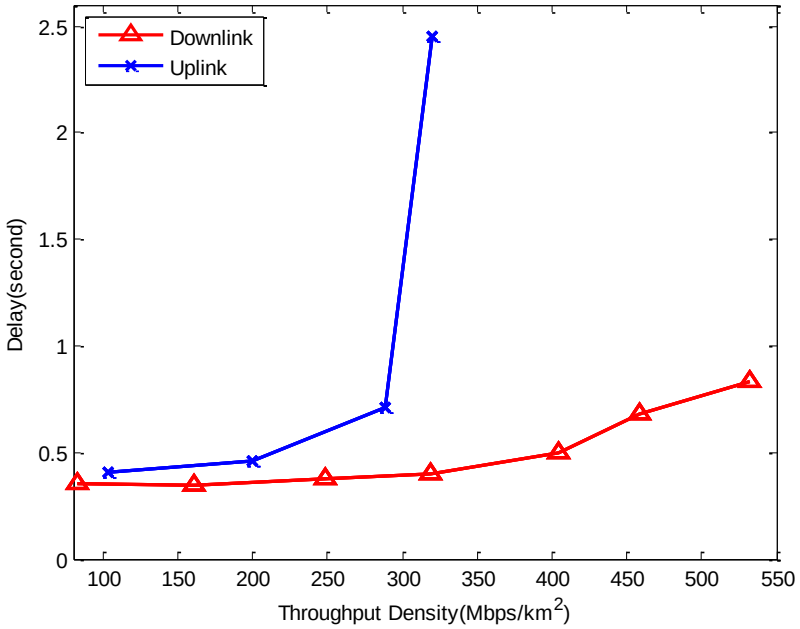

Figure 4-14: Delay versus system throughput density: Cognitive Radio (outdoor + indoor MS)

Although the overall system throughput density of the cognitive radio approach is broadly the same as with the frequency planning approach under the harsh outdoor+indoor MS assumption, the system delay and retry probability are expected to be significantly lower. Figure ***4-15*** and Figure 4-16 compare the retry probability of the downlink and the uplink of the system respectively. The retry probability of the cognitive radio approach is significantly lower than the frequency planning approach, e.g. the DL retry probability of the cognitive radio approach is only around 7% when the offered traffic density is 1.2Gbps/km^2. However, the retry probability of the frequency planning approach is about 40% at the same offered traffic level. Note that the retry probability is almost zero on both the DL and the UL when the offered traffic is below 1Gbps/km^2 and 600Mbps/km^2 respectively, meaning that the all requested files transmissions are accepted by the system.

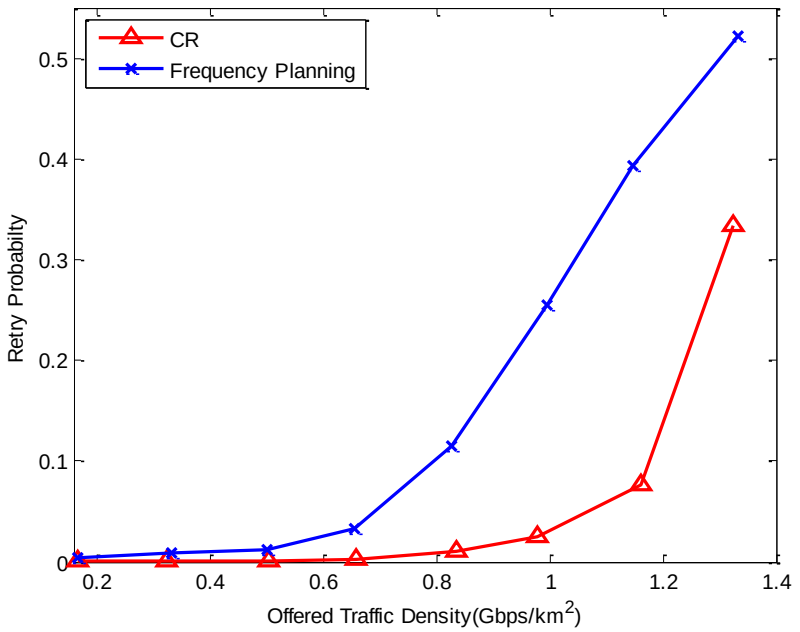

Figure** 4-15**: Probability of retry versus system offered traffic density: Downlink (CR and Frequency Planning)

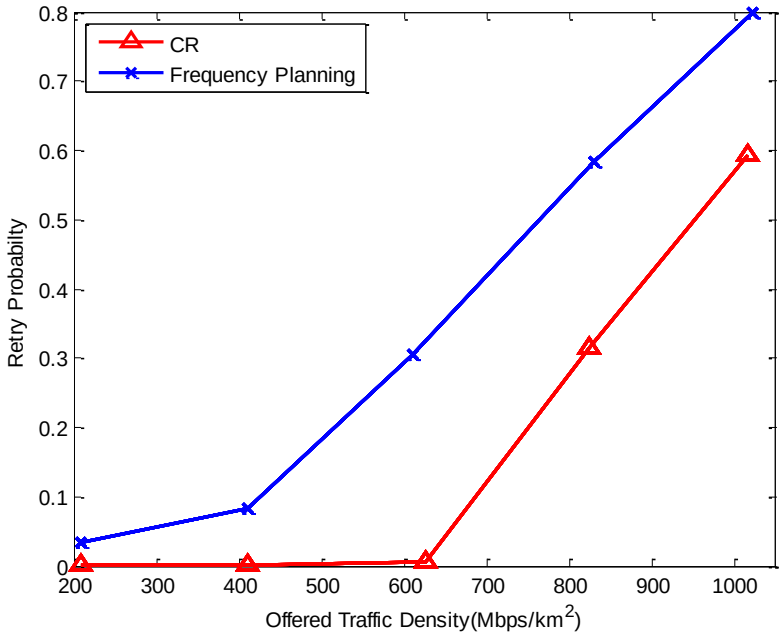

Figure 4-16: Probability of retry versus system offered traffic density: Uplink (CR and Frequency Planning)

Figure 4-17 and Figure 4-18 compares the system delay of cognitive radio approach and the frequency planning approach. The system delay of the cognitive radio approach is significantly lower than the frequency planning approach, as there are fewer retries at the same level of traffic. The cognitive radio approach not only reduces the RRM complexity, but also transmits files with significantly improved QoS measurements.

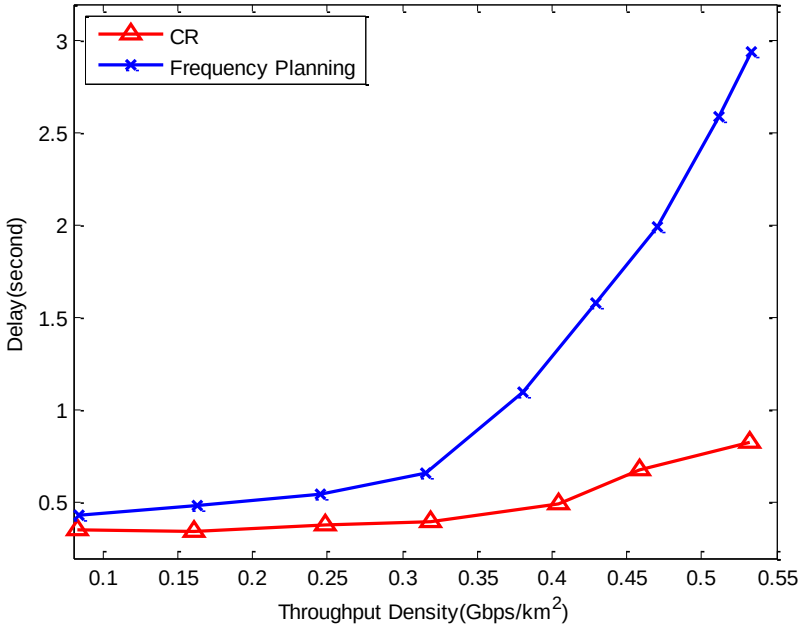

Figure 4-17: Delay performance versus system throughput density: Downlink (CR and Frequency Planning)

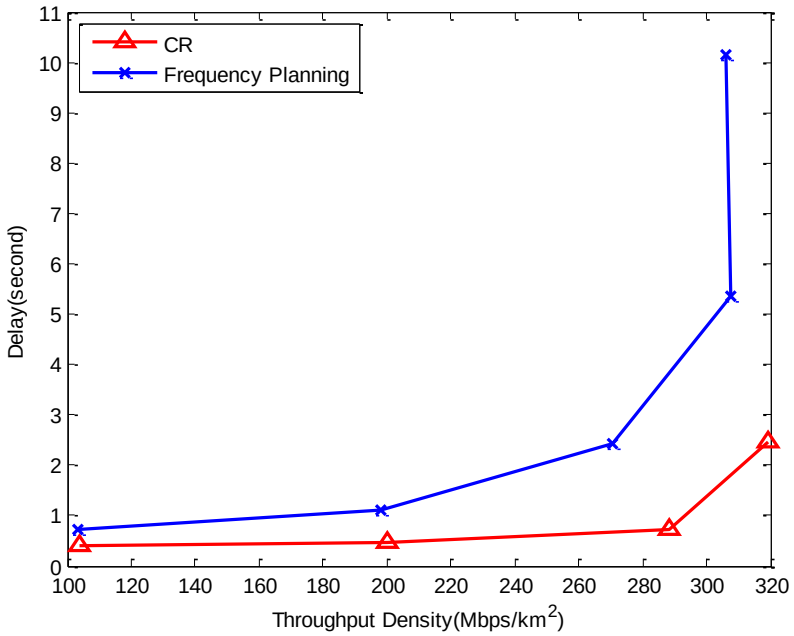

Figure 4-18: Delay performance versus system throughput density: Uplink (CR and Frequency Planning)

5. Conclusions

The D4.1.2 system-level simulation provides indications of the system capacity. A two layer simulator has been developed to capture the features of BuNGee's two-hop architecture. A modularized structure has been used in designing the simulator that the compatibility of the simulator with different techniques proposed to BuNGee is maximized. A number of modules are developed to model different aspects of the system, including the location function, traffic function, propagation function, MIMO function and RRM function.

The square topology has been modelled in the simulation. The backhaul network propagation environment has been simulated by UCL and the results are used in the system-level simulation. The propagation models applied to estimate the path loss between entities in the access network of BuNGee are WINNER II B1, WINNER II B4, WINNER II C2 and WINNER II C4. 3D antenna patterns of HBS antenna, HSS antenna and ABS antenna are provided by CASMA. Moreover, the collaborative work at UY between WP2 and WP4 has been used to develop a MIMO function, with both of the point-to-point MIMO and Multi-Beam Assisted MIMO techniques developed by WP2 incorporated into the system-level simulation.

Two RRM approaches are simulated in the simulation: frequency planning, and a basic cognitive radio approach. In the frequency planning approach, if we assume only outdoor MSs and point-to-point MIMO are taking place, the overall throughput density is 1.05 Gbps/km^2, which is above the 1Gbps/km^2 target. However, if the MSs are uniformly distributed in the service area (outdoor MS plus indoor MS), the overall throughput density is about 0.85 Gbps/km^2. Moreover, the QoS is relatively poor, with the retry probability about 50% higher both downlink and uplink when the offered traffic is above 0.7Gbps/km^2 and 0.4Gbps/km^2 respectively. This is because the poor signal reception of indoor users. It is assumed that all the indoor MSs are covered by the ABSs on streets, and no other approaches are assumed to provide indoor coverage, e.g. femto-cells. The propagation environment is very harsh for the indoor MS in this case.

The Multi-Beam Assisted MIMO (MBA-MIMO) techniques have also been modelled in the street MS only scenario. In a pessimistic scenario where the combined MBA-MIMO data rate distribution is used to estimate the link capacity, a downlink throughput density of 1.05Gbps/km^2 and an uplink throughput density of 0.95Gbps/km^2 can be achieved. The overall throughput is boosted to around 2Gbps/km^2. Considering the backhaul network only uses only 75% of the available frequency band, the improvement is significant. In a more optimistic scenario where the averaged MBA-MIMO data rate distribution is applied, the downlink throughput density is reached at 1.2Gbps/km^2 and an uplink throughput density of 1Gbps/km^2 is achieved. Thus, an overall throughput of 2.2Gbps/km^2 is achieved in the optimistic scenario. This figure shows the upper bond of the potential improvement that can be achieved by applying MBA-MIMO at the backhaul network.

Finally a basic cognitive radio approach has been modelled where a spectrum sensing function is assumed at the receiver. The cognitive radio approach is able to reduce the RRM complexity by completely removes the requirement for frequency plan. The basic cognitive radio is able to significantly improve the QoS of the system in the indoor+outdoor MS scenario while achieving a similar 0.85Gbps/km^2.

A number of approaches have been simulated in this simulation and the system performances are evaluated and compared. It is clear that the 1Gbps/km^2 can be achieved by applying the advanced techniques developed in BuNGee. The throughput density can be achieved as high as 2Gbps/km^2 by applying Multi-Beam Assisted MIMO. Even in the worst case scenario where the majority of the MS are deployed indoor with no means of dedicated indoor coverage, the overall achievable throughput density can still be achieved around 0.85Gbps/km^2. If dedicated approaches are assumed to provide indoor coverage, e.g. femto-cells, the 1Gbps/km^2 can be reached even in the worst case scenario.

6. Appendix

6.1 Simulation Parameters

Table 6-1: Simulation parameters

Parameter	Value
Deployment	Square topology
Deployment area dimension	1350m*1350m
Number of streets in one dimension	16
Street width	15 m
Building block size	75m*75m
Number of building blocks per cell	25
Service area size	1.8225 km^2 (1350m*1350m)
Number of HBS	5
Number of ABS	64
Number of MS	1500(800per km^2)
HBS antenna pattern	19 dBi -21 dBi
HSS antenna pattern	13 dBi
ABS antenna pattern	17 dBi
HBS antenna height	25m
HSS, ABS antenna height	5m
MS antenna height	1.5m
MS antenna	Omnidirectional antenna
HBS transmission power	37dBm
HSS transmission power	27dBm
ABS transmission power	37dBm
MS transmission power	23dBm
Carrier frequency	3.5 GHz
Number of Channels	4 (10 MHz each channel)
Throughput threshold	0.86 bps/Hz
Lognormal shadowing	6dB
Noise floor	-114 dbm/MHz
HBS - HSS propagation model	Ray-tracing based channel model
ABS - MS propagation model	WINNER II B1, WINNER II B4
HBS-MS propagation model	WINNER II C2, WINNER II C4
RRM	Frequency planning Cognitive Radio
MIMO	TSB + MIMO(MMSE) Multi-Beam Assisted MIMO
Traffic	File transfer model
Duplexing	TDD (50%-50% split for Downlink and Uplink)

6.2 UCL Multi-HBS Interference Results (HBS3, HBS5)

Table 6-2: Received powers from HBS5 in the coverage area of HBS1

	Beam1	Beam2	Beam3	Beam4	Beam5	Beam6	Beam7	Beam8	Beam9	Beam10	Beam11	Beam12
HSS1	-168.4	-172.0	-179.8	-167.6	-162.7	-150.7	-153.1	-156.0	-149.4	-161.8	-168.4	-175.9
HSS2	-157.1	-168.4	-164.4	-158.1	-161.8	-160.0	-149.7	-142.9	-139.4	-151.0	-158.2	-169.0
HSS3	-163.3	-172.1	-167.6	-161.6	-156.8	-153.8	-162.1	-145.8	-144.5	-156.9	-163.8	-177.2
HSS4	-157.2	-168.0	-165.4	-157.9	-160.4	-150.8	-148.6	-142.7	-143.5	-155.8	-162.1	-171.3
HSS5	-153.1	-166.5	-161.9	-151.6	-153.3	-155.1	-147.8	-135.0	-139.5	-155.9	-160.4	-167.2
HSS6	-159.4	-182.6	-162.4	-153.7	-153.6	-169.2	-157.9	-136.6	-146.2	-165.0	-166.9	-166.4
HSS7	-182.9	-184.4	-188.9	-176.5	-176.8	-161.6	-170.0	-172.9	-163.9	-172.0	-182.8	-184.8
HSS8	-132.7	-150.0	-140.1	-164.6	-155.5	-143.9	-137.3	-135.0	-123.8	-125.8	-140.4	-140.9
HSS9	-133.8	-150.0	-141.2	-150.3	-151.8	-147.6	-131.4	-135.5	-111.5	-123.7	-152.6	-146.5
HSS10	-190.9	-198.3	-197.7	-187.3	-189.6	-202.1	-177.0	-179.7	-172.2	-159.5	-161.7	-171.5
HSS11	-177.1	-177.5	-178.0	-177.5	-172.2	-178.5	-160.9	-161.8	-151.2	-142.1	-134.8	-165.7

Table 6-3: Received powers from HBS5 in the coverage area of HBS2

	Beam1	Beam2	Beam3	Beam4	Beam5	Beam6	Beam7	Beam8	Beam9	Beam10	Beam11	Beam12
HSS12	-164.3	-166.9	-167.1	-156.4	-150.0	-153.2	-156.1	-163.7	-173.2	-169.4	-179.0	-175.3
HSS13	-161.2	-160.7	-163.2	-153.7	-143.6	-146.2	-147.1	-155.2	-166.4	-162.8	-172.3	-168.8
HSS14	-166.0	-169.3	-169.1	-159.6	-155.3	-146.4	-144.6	-154.0	-163.3	-162.5	-171.6	-168.9
HSS15	-175.6	-180.8	-174.8	-173.9	-176.1	-151.2	-145.7	-156.8	-166.7	-163.5	-174.3	-169.8
HSS16	-164.6	-163.3	-161.9	-161.2	-151.0	-145.3	-147.5	-151.3	-161.1	-158.3	-167.5	-164.7
HSS17	-162.2	-160.6	-160.4	-163.9	-148.8	-140.7	-146.7	-153.1	-164.8	-160.6	-168.4	-166.4
HSS18	-158.3	-155.9	-156.0	-159.2	-148.5	-140.0	-142.3	-179.9	-164.3	-154.3	-163.7	-160.7
HSS19	-165.0	-160.8	-161.0	-168.6	-158.7	-156.3	-146.5	-152.8	-159.9	-159.5	-167.9	-165.8
HSS20	-166.8	-159.4	-160.3	-159.6	-168.0	-167.9	-143.6	-143.7	-151.8	-155.6	-164.8	-161.5
HSS21	-174.4	-162.7	-164.4	-156.1	-161.4	-150.9	-155.1	-149.5	-149.3	-155.5	-165.3	-161.2
HSS22	-174.6	-169.8	-172.0	-158.9	-162.1	-153.4	-149.7	-141.5	-153.7	-160.8	-169.9	-165.9

Table 6-4: Received powers from HBS5 in the coverage area of HBS3

	Beam1	Beam2	Beam3	Beam4	Beam5	Beam6	Beam7	Beam8	Beam9	Beam10	Beam11	Beam12
HSS23	-125.7	-148.8	-126.8	-115.5	-116.7	-134.8	-128.6	-111.2	-118.2	-138.6	-140.3	-140.2
HSS24	-137.9	-152.7	-162.5	-118.3	-123.8	-128.4	-119.0	-111.6	-130.7	-136.1	-143.1	-136.5
HSS25	-158.7	-149.0	-151.9	-137.0	-140.3	-132.2	-118.5	-120.1	-133.5	-142.9	-150.3	-146.5
HSS26	-144.3	-138.9	-139.4	-144.3	-141.1	-141.2	-114.0	-127.0	-130.6	-133.6	-144.4	-139.9
HSS27	-143.0	-140.5	-140.4	-142.2	-133.7	-122.5	-116.9	-156.6	-144.2	-136.7	-147.4	-143.4
HSS28	-143.7	-141.9	-140.9	-139.0	-131.5	-119.0	-118.2	-135.8	-146.1	-139.3	-148.6	-146.1
HSS29	-145.4	-144.4	-142.4	-143.8	-132.0	-114.4	-117.9	-131.1	-140.4	-139.6	-147.8	-145.9
HSS30	-143.3	-146.4	-146.2	-138.3	-133.9	-110.9	-118.5	-128.8	-137.8	-137.7	-146.3	-144.0
HSS31	-147.6	-143.3	-152.6	-140.0	-125.5	-120.1	-134.2	-141.5	-153.4	-148.5	-158.1	-154.2

HSS32	-135.2	-132.3	-141.8	-130.0	-109.4	-115.7	-137.3	-131.4	-114.5	-120.3	-133.5	-138.7
HSS33	-134.5	-137.1	-125.3	-117.0	-107.5	-134.3	-127.7	-118.5	-114.8	-132.7	-127.0	-124.0
HSS34	-171.1	-167.8	-160.7	-156.1	-133.4	-149.2	-172.6	-154.0	-148.9	-156.5	-159.2	-156.5
HSS35	-156.2	-152.5	-163.6	-149.5	-128.3	-135.2	-157.7	-150.3	-145.0	-156.9	-159.3	-157.0
HSS36	-151.7	-149.0	-154.2	-143.7	-129.8	-131.4	-141.1	-148.1	-159.0	-151.1	-156.4	-154.4
HSS37	-156.9	-161.5	-159.0	-151.6	-146.6	-124.4	-131.4	-141.7	-151.1	-149.8	-159.4	-155.3
HSS38	-153.9	-152.7	-151.9	-150.2	-140.0	-124.0	-126.3	-140.2	-151.0	-147.6	-156.9	-153.6
HSS39	-154.3	-148.7	-149.2	-152.3	-151.1	-148.5	-123.1	-135.3	-141.8	-144.4	-154.1	-150.6
HSS40	-154.7	-156.9	-160.2	-146.1	-148.9	-140.2	-127.0	-126.8	-138.3	-145.4	-156.4	-150.5
HSS41	-150.4	-170.4	-159.0	-147.2	-145.8	-144.8	-136.2	-128.0	-149.8	-151.3	-164.4	-154.5
HSS42	-156.0	-165.1	-182.0	-155.7	-155.9	-157.8	-152.1	-133.5	-150.5	-164.6	-183.2	-161.9

Table 6-5: Received powers from HBS5 in the coverage area of HBS4

	Beam1	**Beam2**	**Beam3**	**Beam4**	**Beam5**	**Beam6**	**Beam7**	**Beam8**	**Beam9**	**Beam10**	**Beam11**	**Beam12**
HSS43	-167.5	-168.3	-161.2	-154.1	-144.8	-164.7	-167.4	-156.1	-154.3	-173.2	-166.6	-159.0
HSS44	-153.1	-154.7	-145.4	-136.2	-130.4	-152.0	-154.2	-161.0	-154.0	-167.0	-171.1	-177.5
HSS45	-154.4	-157.0	-148.1	-136.8	-134.7	-150.9	-161.7	-159.9	-159.8	-167.4	-173.9	-182.9
HSS46	-162.3	-165.6	-156.6	-143.8	-144.5	-158.4	-154.6	-156.9	-171.9	-183.5	-185.6	-184.4
HSS47	-154.8	-158.4	-149.0	-135.8	-136.8	-152.2	-158.7	-166.3	-163.5	-166.1	-172.1	-184.5
HSS48	-164.1	-164.5	-158.2	-145.7	-145.6	-147.1	-158.0	-166.5	-170.2	-174.7	-183.1	-186.8
HSS49	-143.6	-126.5	-133.7	-149.8	-153.5	-158.4	-193.6	-166.6	-160.2	-153.9	-150.5	-165.7
HSS50	-171.6	-170.6	-164.2	-172.0	-182.8	-184.8	-201.3	-187.5	-193.2	-179.9	-184.2	-177.0
HSS51	-139.0	-136.2	-123.0	-125.8	-140.4	-140.9	-178.9	-148.6	-139.7	-125.4	-144.2	-156.0
HSS52	-130.3	-134.8	-110.0	-123.7	-152.5	-146.5	-177.6	-148.1	-138.6	-127.0	-139.8	-149.1
HSS53	-177.6	-181.6	-173.5	-159.6	-161.8	-171.5	-190.7	-185.4	-190.0	-185.1	-195.0	-191.3

Table 6-6: Received powers from HBS5 in the coverage area of HBS5

	Beam1	**Beam2**	**Beam3**	**Beam4**	**Beam5**	**Beam6**	**Beam7**	**Beam8**	**Beam9**	**Beam10**	**Beam11**	**Beam12**
HSS54	-155.4	-153.8	-184.8	-132.8	-142.0	-139.4	-132.9	-130.8	-130.5	-130.0	-120.8	-110.7
HSS55	-144.0	-139.8	-163.9	-121.8	-130.9	-128.7	-123.6	-124.0	-124.7	-116.0	-106.4	-98.8
HSS56	-120.4	-128.0	-143.7	-114.8	-123.4	-122.5	-114.1	-115.5	-107.9	-95.8	-91.3	-93.2
HSS57	-116.3	-115.2	-128.9	-107.2	-101.0	-98.5	-92.6	-93.2	-97.8	-111.6	-118.9	-120.1
HSS58	-128.8	-118.9	-145.5	-122.5	-114.0	-112.7	-102.1	-110.2	-119.1	-123.7	-133.1	-129.9
HSS59	-139.7	-137.8	-137.5	-136.7	-127.5	-117.2	-114.2	-135.8	-152.3	-137.0	-146.2	-143.4
HSS60	-126.8	-127.7	-128.5	-120.1	-111.7	-102.0	-108.2	-113.8	-122.7	-125.9	-119.6	-130.1
HSS61	-115.9	-117.1	-109.4	-98.4	-93.1	-94.6	-96.4	-102.5	-106.0	-111.7	-116.1	-120.1
HSS62	-91.6	-89.9	-93.2	-106.0	-112.9	-117.7	-114.1	-122.6	-121.6	-114.5	-115.6	-114.4
HSS63	-100.4	-110.7	-119.7	-121.5	-130.9	-127.6	-121.9	-132.1	-141.3	-141.7	-130.9	-124.6
HSS64	-109.3	-128.0	-138.3	-132.7	-141.9	-139.1	-126.8	-143.9	-154.7	-153.1	-143.9	-131.3

Table 6-7: Received powers from HBS3 in the coverage area of HBS1

	Beam1	Beam2	Beam3	Beam4	Beam5	Beam6	Beam7	Beam8	Beam9	Beam10	Beam11	Beam12
HSS1	-163.5	-174.3	-180.6	-162.2	-168.8	-171.5	-165.6	-164.5	-154.3	-145.6	-134.9	-167.2
HSS2	-171.3	-177.2	-167.8	-156.0	-167.0	-164.2	-166.1	-163.9	-165.8	-156.2	-133.6	-149.2
HSS3	-165.1	-208.3	-170.6	-151.2	-160.3	-158.5	-154.8	-151.5	-159.8	-149.5	-128.3	-135.2
HSS4	-172.2	-174.9	-171.2	-150.4	-157.9	-157.3	-152.2	-149.5	-154.6	-143.7	-129.8	-127.3
HSS5	-172.3	-167.0	-167.3	-149.1	-158.1	-155.7	-158.9	-169.2	-158.9	-151.6	-146.6	-124.4
HSS6	-173.6	-173.4	-171.1	-153.0	-161.4	-160.0	-153.8	-150.7	-150.5	-151.9	-142.8	-135.2
HSS7	-175.3	-179.7	-178.0	-149.8	-159.4	-156.7	-156.5	-149.4	-150.2	-152.3	-151.1	-148.4
HSS8	-167.2	-172.4	-169.9	-152.1	-160.9	-158.9	-153.2	-152.1	-148.9	-145.2	-148.6	-140.1
HSS9	-169.1	-179.1	-174.7	-157.3	-165.5	-165.8	-150.6	-152.8	-148.6	-146.3	-146.0	-144.8
HSS10	-173.9	-187.6	-180.2	-164.9	-173.0	-168.8	-158.8	-158.0	-151.9	-153.2	-157.0	-158.2
HSS11	-181.9	-178.8	-189.2	-168.2	-174.1	-163.1	-151.3	-160.1	-159.0	-152.0	-152.5	-169.4

Table 6-8: Received powers from HBS3 in the coverage area of HBS2

	Beam1	Beam2	Beam3	Beam4	Beam5	Beam6	Beam7	Beam8	Beam9	Beam10	Beam11	Beam12
HSS12	-162.4	-162.9	-152.8	-145.7	-135.1	-167.2	-159.2	-156.6	-156.9	-166.7	-169.1	-163.9
HSS13	-171.1	-167.8	-160.7	-156.1	-133.4	-149.2	-172.6	-154.0	-148.9	-156.5	-159.2	-156.5
HSS14	-156.2	-152.5	-163.6	-149.5	-128.3	-135.2	-157.7	-150.3	-145.0	-156.9	-159.3	-157.0
HSS15	-151.7	-149.0	-154.2	-143.7	-129.8	-127.3	-141.1	-148.1	-159.0	-151.1	-156.4	-154.4
HSS16	-156.9	-161.5	-159.0	-151.6	-146.6	-124.4	-131.4	-141.7	-151.1	-149.8	-159.4	-155.3
HSS17	-153.7	-150.9	-150.7	-152.0	-142.9	-135.3	-127.4	-156.9	-158.7	-149.2	-158.3	-156.0
HSS18	-154.3	-148.7	-149.2	-152.3	-151.1	-148.5	-123.1	-135.3	-141.8	-144.4	-154.1	-150.6
HSS19	-155.5	-151.7	-149.3	-145.2	-148.6	-140.2	-127.0	-126.7	-138.3	-145.5	-156.4	-150.4
HSS20	-151.3	-152.2	-149.4	-146.3	-146.0	-144.8	-136.2	-128.0	-149.8	-151.3	-164.0	-154.4
HSS21	-158.9	-156.1	-152.6	-153.2	-157.0	-158.2	-151.9	-133.5	-150.5	-166.6	-174.4	-162.6
HSS22	-151.4	-161.0	-159.4	-152.0	-152.5	-169.4	-157.4	-135.5	-144.3	-165.9	-166.4	-166.4

Table 6-9: Received powers from HBS3 in the coverage area of HBS3

	Beam1	Beam2	Beam3	Beam4	Beam5	Beam6	Beam7	Beam8	Beam9	Beam10	Beam11	Beam12
HSS23	-157.1	-157.7	-156.4	-135.3	-144.9	-141.2	-135.2	-133.4	-133.4	-137.0	-123.7	-114.9
HSS24	-157.8	-142.2	-148.1	-125.4	-133.7	-132.0	-128.3	-127.6	-131.1	-119.5	-108.7	-101.2
HSS25	-127.2	-134.6	-134.0	-127.0	-134.5	-141.2	-118.4	-118.5	-109.5	-98.3	-96.3	-93.3
HSS26	-119.2	-123.4	-128.3	-121.0	-110.6	-101.7	-108.6	-99.5	-102.9	-119.6	-127.9	-128.7
HSS27	-135.4	-124.9	-129.9	-129.7	-138.7	-123.2	-105.6	-112.5	-118.2	-123.9	-133.7	-130.6
HSS28	-139.2	-137.0	-135.8	-133.4	-124.5	-111.6	-112.7	-128.1	-136.9	-134.2	-142.8	-141.3
HSS29	-127.2	-126.2	-129.7	-119.6	-108.7	-101.3	-112.3	-120.2	-132.9	-130.2	-122.8	-131.7
HSS30	-118.4	-117.8	-109.7	-98.3	-96.3	-93.3	-104.6	-110.1	-126.2	-129.7	-131.2	-135.5
HSS31	-107.4	-99.7	-104.0	-119.9	-128.0	-128.8	-131.2	-132.6	-132.7	-117.5	-121.6	-123.6

HSS32	-105.3	-114.3	-119.0	-123.9	-133.7	-130.6	-127.7	-135.2	-146.7	-141.0	-131.1	-126.8
HSS33	-113.3	-127.5	-135.7	-134.2	-142.8	-141.4	-128.2	-145.4	-155.0	-152.4	-146.6	-133.5
HSS34	-113.7	-121.2	-135.4	-130.2	-123.0	-131.8	-124.9	-133.0	-141.8	-150.3	-164.3	-148.0
HSS35	-104.1	-112.4	-127.7	-129.8	-131.2	-135.4	-121.5	-115.3	-119.7	-129.3	-128.9	-123.1
HSS36	-130.6	-132.9	-133.3	-117.5	-121.6	-123.6	-143.2	-143.8	-133.8	-119.5	-116.7	-129.2
HSS37	-126.5	-134.5	-145.3	-140.9	-131.1	-126.8	-161.3	-150.8	-157.6	-131.5	-137.3	-138.1
HSS38	-128.1	-147.2	-156.4	-152.3	-146.5	-133.4	-152.5	-151.3	-150.1	-135.6	-143.4	-142.8
HSS39	-125.7	-131.8	-141.1	-150.3	-164.3	-148.0	-162.0	-142.0	-146.6	-125.2	-133.5	-131.8
HSS40	-124.4	-114.4	-121.0	-129.3	-128.9	-123.1	-127.4	-134.5	-134.5	-127.2	-134.4	-141.9
HSS41	-146.2	-145.0	-132.5	-119.4	-116.6	-129.2	-119.5	-124.3	-129.9	-121.0	-110.7	-101.6
HSS42	-160.4	-151.1	-157.6	-131.9	-137.4	-138.3	-137.3	-124.5	-129.6	-129.8	-138.9	-123.2

Table 6-10: Received powers from HBS3 in the coverage area of HBS4

	Beam1	**Beam2**	**Beam3**	**Beam4**	**Beam5**	**Beam6**	**Beam7**	**Beam8**	**Beam9**	**Beam10**	**Beam11**	**Beam12**
HSS43	-127.1	-139.8	-150.4	-147.7	-157.0	-153.7	-145.5	-166.8	-182.7	-174.2	-167.0	-161.2
HSS44	-123.1	-137.9	-143.6	-144.4	-154.1	-150.6	-146.5	-155.6	-165.4	-168.0	-161.3	-148.0
HSS45	-126.2	-127.6	-138.0	-145.5	-156.3	-150.3	-155.3	-161.1	-174.1	-167.5	-155.0	-155.3
HSS46	-134.5	-128.3	-146.0	-151.2	-164.0	-154.4	-175.8	-170.8	-170.3	-180.2	-155.3	-166.1
HSS47	-148.1	-133.5	-155.5	-166.8	-174.1	-162.5	-169.7	-173.8	-169.3	-174.2	-160.2	-181.3
HSS48	-163.3	-135.1	-146.3	-165.9	-166.4	-166.0	-166.5	-180.6	-168.3	-166.9	-159.7	-177.3
HSS49	-159.3	-157.9	-159.6	-172.2	-179.7	-178.1	-200.3	-165.0	-179.8	-176.0	-177.2	-187.3
HSS50	-182.9	-153.9	-150.5	-159.9	-160.1	-161.1	-166.9	-161.1	-176.1	-170.3	-178.3	-181.0
HSS51	-162.2	-149.8	-145.9	-157.4	-159.4	-156.9	-158.5	-155.8	-171.3	-164.1	-170.7	-174.8
HSS52	-142.8	-149.2	-160.4	-151.3	-156.5	-154.4	-151.9	-155.9	-164.9	-172.8	-181.3	-169.6
HSS53	-132.5	-142.1	-151.7	-149.8	-159.4	-155.3	-145.9	-164.4	-169.3	-180.3	-171.2	-164.9

Table 6-11: Received powers from HBS3 in the coverage area of HBS5

	Beam1	**Beam2**	**Beam3**	**Beam4**	**Beam5**	**Beam6**	**Beam7**	**Beam8**	**Beam9**	**Beam10**	**Beam11**	**Beam12**
HSS54	-159.8	-164.2	-177.8	-169.6	-178.0	-188.3	-163.9	-175.2	-182.6	-162.2	-168.8	-171.6
HSS55	-171.1	-161.1	-172.8	-169.8	-178.3	-182.0	-173.8	-177.3	-168.9	-156.1	-167.2	-164.2
HSS56	-159.7	-155.7	-173.3	-164.1	-170.5	-174.9	-166.3	-193.1	-171.7	-151.1	-160.0	-158.3
HSS57	-152.7	-155.2	-165.2	-173.0	-181.7	-169.6	-175.1	-173.7	-171.3	-150.3	-157.7	-157.1
HSS58	-146.2	-161.2	-167.3	-180.3	-171.2	-164.8	-170.9	-166.9	-166.9	-148.9	-157.9	-155.5
HSS59	-145.7	-158.8	-168.1	-184.6	-170.5	-149.1	-175.7	-176.4	-173.0	-152.7	-161.2	-159.8
HSS60	-145.7	-155.4	-164.9	-168.0	-161.3	-147.9	-173.7	-176.1	-176.8	-149.6	-159.1	-156.5
HSS61	-153.7	-160.1	-172.6	-167.5	-155.0	-155.4	-167.8	-173.1	-170.8	-151.9	-160.8	-158.7
HSS62	-169.7	-170.5	-169.4	-180.3	-155.3	-166.2	-169.5	-180.7	-175.5	-157.1	-165.4	-165.6
HSS63	-173.1	-173.5	-169.4	-175.3	-160.3	-184.9	-173.8	-186.3	-177.5	-163.4	-180.4	-172.2
HSS64	-168.0	-181.1	-169.6	-166.0	-159.8	-179.1	-197.4	-190.9	-181.7	-171.4	-180.4	-182.0

6.3 Extended Ray-Tracing Results

Table 6-12: Received powers from 11 beams HBS1

	Beam1	Beam2	Beam3	Beam4	Beam5	Beam6	Beam7	Beam8	Beam9	Beam10	Beam11
HSS1	-110.7	-120.8	-130	-130.5	-130.8	-132.9	-142	-132.8	-184.8	-153.8	-155.4
HSS2	-98.8	-106.4	-116	-124.7	-124	-123.6	-130.9	-121.8	-163.9	-139.8	-144
HSS3	-93.2	-91.3	-95.8	-107.9	-115.5	-114.1	-123.4	-114.8	-143.7	-128	-120.4
HSS4	-120.1	-118.9	-111.6	-97.8	-93.2	-92.6	-101	-107.2	-128.9	-115.2	-116.3
HSS5	-129.9	-133.1	-123.7	-119.1	-110.2	-102.1	-114	-122.5	-145.5	-118.9	-128.8
HSS6	-143.4	-146.2	-137	-152.3	-135.8	-114.2	-127.5	-136.7	-137.5	-137.8	-139.7
HSS7	-130.1	-119.6	-125.9	-122.7	-113.8	-108.2	-111.7	-120.1	-128.5	-127.7	-126.8
HSS8	-120.1	-116.1	-111.7	-106	-102.5	-96.4	-93.1	-98.4	-109.4	-117.1	-115.9
HSS9	-114.4	-115.6	-114.5	-121.6	-122.6	-114.1	-112.9	-106	-93.2	-89.9	-91.6
HSS10	-124.6	-130.9	-141.7	-141.3	-132.1	-121.9	-130.9	-121.5	-119.7	-110.7	-100.4
HSS11	-131.3	-143.9	-153.1	-154.7	-143.9	-126.8	-141.9	-132.7	-138.3	-128	-109.3
HSS12	-175.9	-168.4	-161.8	-149.4	-156	-153.1	-162.7	-167.6	-179.8	-172	-168.4
HSS13	-169	-158.2	-151	-139.4	-142.9	-149.7	-161.8	-158.1	-164.4	-168.4	-157.1
HSS14	-177.2	-163.8	-156.9	-144.5	-145.8	-162.1	-156.8	-161.6	-167.6	-172.1	-163.3
HSS15	-171.3	-162.1	-155.8	-143.5	-142.7	-148.6	-160.4	-157.9	-165.4	-168	-157.2
HSS16	-167.2	-160.4	-155.9	-139.5	-135	-147.8	-153.3	-151.6	-161.9	-166.5	-153.1
HSS17	-166.4	-166.9	-165	-146.2	-136.6	-157.9	-153.6	-153.7	-162.4	-182.6	-159.4
HSS18	-184.8	-182.8	-172	-163.9	-172.9	-170	-176.8	-176.5	-188.9	-184.4	-182.9
HSS19	-140.9	-140.4	-125.8	-123.8	-135	-137.3	-155.5	-164.6	-140.1	-150	-132.7
HSS20	-146.5	-152.6	-123.7	-111.5	-135.5	-131.4	-151.8	-150.3	-141.2	-150	-133.8
HSS21	-171.5	-161.7	-159.5	-172.2	-179.7	-177	-189.6	-187.3	-197.7	-198.3	-190.9
HSS22	-165.7	-134.8	-142.1	-151.2	-161.8	-160.9	-172.2	-177.5	-178	-177.5	-177.1
HSS23	-153.6	-156.9	-147.6	-151	-140.2	-126.3	-140	-150.2	-151.9	-152.7	-153.9
HSS24	-150.6	-154.1	-144.4	-141.8	-135.3	-123.1	-151.1	-152.3	-149.2	-148.7	-154.3
HSS25	-150.5	-156.4	-145.4	-138.3	-126.8	-127	-148.9	-146.1	-160.2	-156.9	-154.7
HSS26	-154.5	-164.4	-151.3	-149.8	-128	-136.2	-145.8	-147.2	-159	-170.4	-150.4
HSS27	-161.9	-183.2	-164.6	-150.5	-133.5	-152.1	-155.9	-155.7	-182	-165.1	-156
HSS28	-140.2	-140.3	-138.6	-118.2	-111.2	-128.6	-116.7	-115.5	-126.8	-148.8	-125.7
HSS29	-136.5	-143.1	-136.1	-130.7	-111.6	-119	-123.8	-118.3	-162.5	-152.7	-137.9
HSS30	-146.5	-150.3	-142.9	-133.5	-120.1	-118.5	-140.3	-137	-151.9	-149	-158.7
HSS31	-139.9	-144.4	-133.6	-130.6	-127	-114	-141.1	-144.3	-139.4	-138.9	-144.3
HSS32	-143.4	-147.4	-136.7	-144.2	-156.6	-116.9	-133.7	-142.2	-140.4	-140.5	-143
HSS33	-146.1	-148.6	-139.3	-146.1	-135.8	-118.2	-131.5	-139	-140.9	-141.9	-143.7
HSS34	-145.9	-147.8	-139.6	-140.4	-131.1	-117.9	-132	-143.8	-142.4	-144.4	-145.4
HSS35	-144	-146.3	-137.7	-137.8	-128.8	-118.5	-133.9	-138.3	-146.2	-146.4	-143.3
HSS36	-154.2	-158.1	-148.5	-153.4	-141.5	-134.2	-125.5	-140	-152.6	-143.3	-147.6
HSS37	-138.7	-133.5	-120.3	-114.5	-131.4	-137.3	-109.4	-130	-141.8	-132.3	-135.2

HSS38	-124	-127	-132.7	-114.8	-118.5	-127.7	-107.5	-117	-125.3	-137.1	-134.5
HSS39	-156.5	-159.2	-156.5	-148.9	-154	-172.6	-133.4	-156.1	-160.7	-167.8	-171.1
HSS40	-157	-159.3	-156.9	-145	-150.3	-157.7	-128.3	-149.5	-163.6	-152.5	-156.2
HSS41	-154.4	-156.4	-151.1	-159	-148.1	-141.1	-129.8	-143.7	-154.2	-149	-151.7
HSS42	-155.3	-159.4	-149.8	-151.1	-141.7	-131.4	-146.6	-151.6	-159	-161.5	-156.9
HSS43	-166.4	-168.4	-160.6	-164.8	-153.1	-146.7	-148.8	-163.9	-160.4	-160.6	-162.2
HSS44	-160.7	-163.7	-154.3	-164.3	-179.9	-142.3	-148.5	-159.2	-156	-155.9	-158.3
HSS45	-165.8	-167.9	-159.5	-159.9	-152.8	-146.5	-158.7	-168.6	-161	-160.8	-165
HSS46	-161.5	-164.8	-155.6	-151.8	-143.7	-143.6	-168	-159.6	-160.3	-159.4	-166.8
HSS47	-161.2	-165.3	-155.5	-149.3	-149.5	-155.1	-161.4	-156.1	-164.4	-162.7	-174.4
HSS48	-165.9	-169.9	-160.8	-153.7	-141.5	-149.7	-162.1	-158.9	-172	-169.8	-174.6
HSS49	-175.3	-179	-169.4	-173.2	-163.7	-156.1	-150	-156.4	-167.1	-166.9	-164.3
HSS50	-168.8	-172.3	-162.8	-166.4	-155.2	-147.1	-143.6	-153.7	-163.2	-160.7	-161.2
HSS51	-168.9	-171.6	-162.5	-163.3	-154	-144.6	-155.3	-159.6	-169.1	-169.3	-166
HSS52	-169.8	-174.3	-163.5	-166.7	-156.8	-145.7	-176.1	-173.9	-174.8	-180.8	-175.6
HSS53	-164.7	-167.5	-158.3	-161.1	-151.3	-147.5	-151	-161.2	-161.9	-163.3	-164.6
HSS54	-165.7	-150.5	-153.9	-160.2	-166.6	-193.6	-153.5	-149.8	-133.7	-126.5	-143.6
HSS55	-177	-184.2	-179.9	-193.2	-187.5	-201.3	-182.8	-172	-164.2	-170.6	-171.6
HSS56	-156	-144.2	-125.4	-139.7	-148.6	-178.9	-140.4	-125.8	-123	-136.2	-139
HSS57	-149.1	-139.8	-127	-138.6	-148.1	-177.6	-152.5	-123.7	-110	-134.8	-130.3
HSS58	-191.3	-195	-185.1	-190	-185.4	-190.7	-161.8	-159.6	-173.5	-181.6	-177.6
HSS59	-159	-166.6	-173.2	-154.3	-156.1	-167.4	-144.8	-154.1	-161.2	-168.3	-167.5
HSS60	-177.5	-171.1	-167	-154	-161	-154.2	-130.4	-136.2	-145.4	-154.7	-153.1
HSS61	-182.9	-173.9	-167.4	-159.8	-159.9	-161.7	-134.7	-136.8	-148.1	-157	-154.4
HSS62	-184.4	-185.6	-183.5	-171.9	-156.9	-154.6	-144.5	-143.8	-156.6	-165.6	-162.3
HSS63	-184.5	-172.1	-166.1	-163.5	-166.3	-158.7	-136.8	-135.8	-149	-158.4	-154.8
HSS64	-186.8	-183.1	-174.7	-170.2	-166.5	-158	-145.6	-145.7	-158.2	-164.5	-164.1

Table 6-13: Received powers from 11 beams HBS2

	Beam12	**Beam13**	**Beam14**	**Beam15**	**Beam16**	**Beam17**	**Beam18**	**Beam19**	**Beam20**	**Beam21**	**Beam22**
HSS1	-165.7	-150.5	-153.9	-160.2	-166.6	-193.6	-153.5	-149.8	-133.7	-126.5	-143.6
HSS2	-177	-184.2	-179.9	-193.2	-187.5	-201.3	-182.8	-172	-164.2	-170.6	-171.6
HSS3	-156	-144.2	-125.4	-139.7	-148.6	-178.9	-140.4	-125.8	-123	-136.2	-139
HSS4	-149.1	-139.8	-127	-138.6	-148.1	-177.6	-152.5	-123.7	-110	-134.8	-130.3
HSS5	-191.3	-195	-185.1	-190	-185.4	-190.7	-161.8	-159.6	-173.5	-181.6	-177.6
HSS6	-159	-166.6	-173.2	-154.3	-156.1	-167.4	-144.8	-154.1	-161.2	-168.3	-167.5
HSS7	-177.5	-171.1	-167	-154	-161	-154.2	-130.4	-136.2	-145.4	-154.7	-153.1
HSS8	-182.9	-173.9	-167.4	-159.8	-159.9	-161.7	-134.7	-136.8	-148.1	-157	-154.4
HSS9	-184.4	-185.6	-183.5	-171.9	-156.9	-154.6	-144.5	-143.8	-156.6	-165.6	-162.3
HSS10	-184.5	-172.1	-166.1	-163.5	-166.3	-158.7	-136.8	-135.8	-149	-158.4	-154.8

HSS11	-186.8	-183.1	-174.7	-170.2	-166.5	-158	-145.6	-145.7	-158.2	-164.5	-164.1
HSS12	-110.7	-120.8	-130	-130.5	-130.8	-132.9	-142	-132.8	-184.8	-153.8	-155.4
HSS13	-98.8	-106.4	-116	-124.7	-124	-123.6	-130.9	-121.8	-163.9	-139.8	-144
HSS14	-93.2	-91.3	-95.8	-107.9	-115.5	-114.1	-123.4	-114.8	-143.7	-128	-120.4
HSS15	-120.1	-118.9	-111.6	-97.8	-93.2	-92.6	-101	-107.2	-128.9	-115.2	-116.3
HSS16	-129.9	-133.1	-123.7	-119.1	-110.2	-102.1	-114	-122.5	-145.5	-118.9	-128.8
HSS17	-143.4	-146.2	-137	-152.3	-135.8	-114.2	-127.5	-136.7	-137.5	-137.8	-139.7
HSS18	-130.1	-119.6	-125.9	-122.7	-113.8	-108.2	-111.7	-120.1	-128.5	-127.7	-126.8
HSS19	-120.1	-116.1	-111.7	-106	-102.5	-96.4	-93.1	-98.4	-109.4	-117.1	-115.9
HSS20	-114.4	-115.6	-114.5	-121.6	-122.6	-114.1	-112.9	-106	-93.2	-89.9	-91.6
HSS21	-124.6	-130.9	-141.7	-141.3	-132.1	-121.9	-130.9	-121.5	-119.7	-110.7	-100.4
HSS22	-131.3	-143.9	-153.1	-154.7	-143.9	-126.8	-141.9	-132.7	-138.3	-128	-109.3
HSS23	-124	-127	-132.7	-114.8	-118.5	-127.7	-107.5	-117	-125.3	-137.1	-134.5
HSS24	-156.5	-159.2	-156.5	-148.9	-154	-172.6	-133.4	-156.1	-160.7	-167.8	-171.1
HSS25	-157	-159.3	-156.9	-145	-150.3	-157.7	-128.3	-149.5	-163.6	-152.5	-156.2
HSS26	-154.4	-156.4	-151.1	-159	-148.1	-141.1	-129.8	-143.7	-154.2	-149	-151.7
HSS27	-155.3	-159.4	-149.8	-151.1	-141.7	-131.4	-146.6	-151.6	-159	-161.5	-156.9
HSS28	-153.6	-156.9	-147.6	-151	-140.2	-126.3	-140	-150.2	-151.9	-152.7	-153.9
HSS29	-150.6	-154.1	-144.4	-141.8	-135.3	-123.1	-151.1	-152.3	-149.2	-148.7	-154.3
HSS30	-150.5	-156.4	-145.4	-138.3	-126.8	-127	-148.9	-146.1	-160.2	-156.9	-154.7
HSS31	-154.5	-164.4	-151.3	-149.8	-128	-136.2	-145.8	-147.2	-159	-170.4	-150.4
HSS32	-161.9	-183.2	-164.6	-150.5	-133.5	-152.1	-155.9	-155.7	-182	-165.1	-156
HSS33	-140.2	-140.3	-138.6	-118.2	-111.2	-128.6	-116.7	-115.5	-126.8	-148.8	-125.7
HSS34	-136.5	-143.1	-136.1	-130.7	-111.6	-119	-123.8	-118.3	-162.5	-152.7	-137.9
HSS35	-146.5	-150.3	-142.9	-133.5	-120.1	-118.5	-140.3	-137	-151.9	-149	-158.7
HSS36	-139.9	-144.4	-133.6	-130.6	-127	-114	-141.1	-144.3	-139.4	-138.9	-144.3
HSS37	-143.4	-147.4	-136.7	-144.2	-156.6	-116.9	-133.7	-142.2	-140.4	-140.5	-143
HSS38	-146.1	-148.6	-139.3	-146.1	-135.8	-118.2	-131.5	-139	-140.9	-141.9	-143.7
HSS39	-145.9	-147.8	-139.6	-140.4	-131.1	-117.9	-132	-143.8	-142.4	-144.4	-145.4
HSS40	-144	-146.3	-137.7	-137.8	-128.8	-118.5	-133.9	-138.3	-146.2	-146.4	-143.3
HSS41	-154.2	-158.1	-148.5	-153.4	-141.5	-134.2	-125.5	-140	-152.6	-143.3	-147.6
HSS42	-138.7	-133.5	-120.3	-114.5	-131.4	-137.3	-109.4	-130	-141.8	-132.3	-135.2
HSS43	-166.4	-166.9	-165	-146.2	-136.6	-157.9	-153.6	-153.7	-162.4	-182.6	-159.4
HSS44	-184.8	-182.8	-172	-163.9	-172.9	-170	-176.8	-176.5	-188.9	-184.4	-182.9
HSS45	-140.9	-140.4	-125.8	-123.8	-135	-137.3	-155.5	-164.6	-140.1	-150	-132.7
HSS46	-146.5	-152.6	-123.7	-111.5	-135.5	-131.4	-151.8	-150.3	-141.2	-150	-133.8
HSS47	-171.5	-161.7	-159.5	-172.2	-179.7	-177	-189.6	-187.3	-197.7	-198.3	-190.9
HSS48	-165.7	-134.8	-142.1	-151.2	-161.8	-160.9	-172.2	-177.5	-178	-177.5	-177.1
HSS49	-175.9	-168.4	-161.8	-149.4	-156	-153.1	-162.7	-167.6	-179.8	-172	-168.4
HSS50	-169	-158.2	-151	-139.4	-142.9	-149.7	-161.8	-158.1	-164.4	-168.4	-157.1
HSS51	-177.2	-163.8	-156.9	-144.5	-145.8	-162.1	-156.8	-161.6	-167.6	-172.1	-163.3

HSS52	-171.3	-162.1	-155.8	-143.5	-142.7	-148.6	-160.4	-157.9	-165.4	-168	-157.2
HSS53	-167.2	-160.4	-155.9	-139.5	-135	-147.8	-153.3	-151.6	-161.9	-166.5	-153.1
HSS54	-175.3	-179	-169.4	-173.2	-163.7	-156.1	-150	-156.4	-167.1	-166.9	-164.3
HSS55	-168.8	-172.3	-162.8	-166.4	-155.2	-147.1	-143.6	-153.7	-163.2	-160.7	-161.2
HSS56	-168.9	-171.6	-162.5	-163.3	-154	-144.6	-155.3	-159.6	-169.1	-169.3	-166
HSS57	-169.8	-174.3	-163.5	-166.7	-156.8	-145.7	-176.1	-173.9	-174.8	-180.8	-175.6
HSS58	-164.7	-167.5	-158.3	-161.1	-151.3	-147.5	-151	-161.2	-161.9	-163.3	-164.6
HSS59	-166.4	-168.4	-160.6	-164.8	-153.1	-146.7	-148.8	-163.9	-160.4	-160.6	-162.2
HSS60	-160.7	-163.7	-154.3	-164.3	-179.9	-142.3	-148.5	-159.2	-156	-155.9	-158.3
HSS61	-165.8	-167.9	-159.5	-159.9	-152.8	-146.5	-158.7	-168.6	-161	-160.8	-165
HSS62	-161.5	-164.8	-155.6	-151.8	-143.7	-143.6	-168	-159.6	-160.3	-159.4	-166.8
HSS63	-161.2	-165.3	-155.5	-149.3	-149.5	-155.1	-161.4	-156.1	-164.4	-162.7	-174.4
HSS64	-165.9	-169.9	-160.8	-153.7	-141.5	-149.7	-162.1	-158.9	-172	-169.8	-174.6

Table 6-14: Received powers from beam 1-10 of HBS3

	Beam23	**Beam24**	**Beam25**	**Beam26**	**Beam27**	**Beam28**	**Beam29**	**Beam30**	**Beam31**	**Beam32**
HSS1	-167.2	-134.9	-145.6	-154.3	-164.5	-165.6	-168.8	-162.2	-180.6	-174.3
HSS2	-149.2	-133.6	-156.2	-165.8	-163.9	-166.1	-167	-156	-167.8	-177.2
HSS3	-135.2	-128.3	-149.5	-159.8	-151.5	-154.8	-160.3	-151.2	-170.6	-208.3
HSS4	-127.3	-129.8	-143.7	-154.6	-149.5	-152.2	-157.9	-150.4	-171.2	-174.9
HSS5	-124.4	-146.6	-151.6	-158.9	-169.2	-158.9	-158.1	-149.1	-167.3	-167
HSS6	-135.2	-142.8	-151.9	-150.5	-150.7	-153.8	-161.4	-153	-171.1	-173.4
HSS7	-148.4	-151.1	-152.3	-150.2	-149.4	-156.5	-159.4	-149.8	-178	-179.7
HSS8	-140.1	-148.6	-145.2	-148.9	-152.1	-153.2	-160.9	-152.1	-169.9	-172.4
HSS9	-144.8	-146	-146.3	-148.6	-152.8	-150.6	-165.5	-157.3	-174.7	-179.1
HSS10	-158.2	-157	-153.2	-151.9	-158	-158.8	-173	-164.9	-180.2	-187.6
HSS11	-169.4	-152.5	-152	-159	-160.1	-151.3	-174.1	-168.2	-189.2	-178.8
HSS12	-163.9	-169.1	-166.7	-156.9	-156.6	-159.2	-135.1	-145.7	-152.8	-162.9
HSS13	-156.5	-159.2	-156.5	-148.9	-154	-172.6	-133.4	-156.1	-160.7	-167.8
HSS14	-157	-159.3	-156.9	-145	-150.3	-157.7	-128.3	-149.5	-163.6	-152.5
HSS15	-154.4	-156.4	-151.1	-159	-148.1	-141.1	-129.8	-143.7	-154.2	-149
HSS16	-155.3	-159.4	-149.8	-151.1	-141.7	-131.4	-146.6	-151.6	-159	-161.5
HSS17	-156	-158.3	-149.2	-158.7	-156.9	-127.4	-142.9	-152	-150.7	-150.9
HSS18	-150.6	-154.1	-144.4	-141.8	-135.3	-123.1	-151.1	-152.3	-149.2	-148.7
HSS19	-150.4	-156.4	-145.5	-138.3	-126.7	-127	-148.6	-145.2	-149.3	-151.7
HSS20	-154.4	-164	-151.3	-149.8	-128	-136.2	-146	-146.3	-149.4	-152.2
HSS21	-162.6	-174.4	-166.6	-150.5	-133.5	-151.9	-157	-153.2	-152.6	-156.1
HSS22	-166.4	-166.4	-165.9	-144.3	-135.5	-157.4	-152.5	-152	-159.4	-161
HSS23	-114.9	-123.7	-137	-133.4	-133.4	-135.2	-144.9	-135.3	-156.4	-157.7
HSS24	-101.2	-108.7	-119.5	-131.1	-127.6	-128.3	-133.7	-125.4	-148.1	-142.2

HSS25	-93.3	-96.3	-98.3	-109.5	-118.5	-118.4	-134.5	-127	-134	-134.6
HSS26	-128.7	-127.9	-119.6	-102.9	-99.5	-108.6	-110.6	-121	-128.3	-123.4
HSS27	-130.6	-133.7	-123.9	-118.2	-112.5	-105.6	-138.7	-129.7	-129.9	-124.9
HSS28	-141.3	-142.8	-134.2	-136.9	-128.1	-112.7	-124.5	-133.4	-135.8	-137
HSS29	-131.7	-122.8	-130.2	-132.9	-120.2	-112.3	-108.7	-119.6	-129.7	-126.2
HSS30	-135.5	-131.2	-129.7	-126.2	-110.1	-104.6	-96.3	-98.3	-109.7	-117.8
HSS31	-123.6	-121.6	-117.5	-132.7	-132.6	-131.2	-128	-119.9	-104	-99.7
HSS32	-126.8	-131.1	-141	-146.7	-135.2	-127.7	-133.7	-123.9	-119	-114.3
HSS33	-133.5	-146.6	-152.4	-155	-145.4	-128.2	-142.8	-134.2	-135.7	-127.5
HSS34	-148	-164.3	-150.3	-141.8	-133	-124.9	-123	-130.2	-135.4	-121.2
HSS35	-123.1	-128.9	-129.3	-119.7	-115.3	-121.5	-131.2	-129.8	-127.7	-112.4
HSS36	-129.2	-116.7	-119.5	-133.8	-143.8	-143.2	-121.6	-117.5	-133.3	-132.9
HSS37	-138.1	-137.3	-131.5	-157.6	-150.8	-161.3	-131.1	-140.9	-145.3	-134.5
HSS38	-142.8	-143.4	-135.6	-150.1	-151.3	-152.5	-146.5	-152.3	-156.4	-147.2
HSS39	-131.8	-133.5	-125.2	-146.6	-142	-162	-164.3	-150.3	-141.1	-131.8
HSS40	-141.9	-134.4	-127.2	-134.5	-134.5	-127.4	-128.9	-129.3	-121	-114.4
HSS41	-101.6	-110.7	-121	-129.9	-124.3	-119.5	-116.6	-119.4	-132.5	-145
HSS42	-123.2	-138.9	-129.8	-129.6	-124.5	-137.3	-137.4	-131.9	-157.6	-151.1
HSS43	-161.2	-167	-174.2	-182.7	-166.8	-145.5	-157	-147.7	-150.4	-139.8
HSS44	-148	-161.3	-168	-165.4	-155.6	-146.5	-154.1	-144.4	-143.6	-137.9
HSS45	-155.3	-155	-167.5	-174.1	-161.1	-155.3	-156.3	-145.5	-138	-127.6
HSS46	-166.1	-155.3	-180.2	-170.3	-170.8	-175.8	-164	-151.2	-146	-128.3
HSS47	-181.3	-160.2	-174.2	-169.3	-173.8	-169.7	-174.1	-166.8	-155.5	-133.5
HSS48	-177.3	-159.7	-166.9	-168.3	-180.6	-166.5	-166.4	-165.9	-146.3	-135.1
HSS49	-187.3	-177.2	-176	-179.8	-165	-200.3	-179.7	-172.2	-159.6	-157.9
HSS50	-181	-178.3	-170.3	-176.1	-161.1	-166.9	-160.1	-159.9	-150.5	-153.9
HSS51	-174.8	-170.7	-164.1	-171.3	-155.8	-158.5	-159.4	-157.4	-145.9	-149.8
HSS52	-169.6	-181.3	-172.8	-164.9	-155.9	-151.9	-156.5	-151.3	-160.4	-149.2
HSS53	-164.9	-171.2	-180.3	-169.3	-164.4	-145.9	-159.4	-149.8	-151.7	-142.1
HSS54	-171.6	-168.8	-162.2	-182.6	-175.2	-163.9	-178	-169.6	-177.8	-164.2
HSS55	-164.2	-167.2	-156.1	-168.9	-177.3	-173.8	-178.3	-169.8	-172.8	-161.1
HSS56	-158.3	-160	-151.1	-171.7	-193.1	-166.3	-170.5	-164.1	-173.3	-155.7
HSS57	-157.1	-157.7	-150.3	-171.3	-173.7	-175.1	-181.7	-173	-165.2	-155.2
HSS58	-155.5	-157.9	-148.9	-166.9	-166.9	-170.9	-171.2	-180.3	-167.3	-161.2
HSS59	-159.8	-161.2	-152.7	-173	-176.4	-175.7	-170.5	-184.6	-168.1	-158.8
HSS60	-156.5	-159.1	-149.6	-176.8	-176.1	-173.7	-161.3	-168	-164.9	-155.4
HSS61	-158.7	-160.8	-151.9	-170.8	-173.1	-167.8	-155	-167.5	-172.6	-160.1
HSS62	-165.6	-165.4	-157.1	-175.5	-180.7	-169.5	-155.3	-180.3	-169.4	-170.5
HSS63	-172.2	-180.4	-163.4	-177.5	-186.3	-173.8	-160.3	-175.3	-169.4	-173.5
HSS64	-182	-180.4	-171.4	-181.7	-190.9	-197.4	-159.8	-166	-169.6	-181.1

Table 6-15: Received powers from beam 11-20 of HBS3

	Beam32	Beam33	Beam34	Beam35	Beam36	Beam37	Beam38	Beam39	Beam40	Beam41	Beam42
HSS1	-174.3	-163.5	-177.2	-176	-179.8	-165	-200.3	-179.7	-172.2	-159.6	-157.9
HSS2	-177.2	-171.3	-178.3	-170.3	-176.1	-161.1	-166.9	-160.1	-159.9	-150.5	-153.9
HSS3	-208.3	-165.1	-170.7	-164.1	-171.3	-155.8	-158.5	-159.4	-157.4	-145.9	-149.8
HSS4	-174.9	-172.2	-181.3	-172.8	-164.9	-155.9	-151.9	-156.5	-151.3	-160.4	-149.2
HSS5	-167	-172.3	-171.2	-180.3	-169.3	-164.4	-145.9	-159.4	-149.8	-151.7	-142.1
HSS6	-173.4	-173.6	-167	-174.2	-182.7	-166.8	-145.5	-157	-147.7	-150.4	-139.8
HSS7	-179.7	-175.3	-161.3	-168	-165.4	-155.6	-146.5	-154.1	-144.4	-143.6	-137.9
HSS8	-172.4	-167.2	-155	-167.5	-174.1	-161.1	-155.3	-156.3	-145.5	-138	-127.6
HSS9	-179.1	-169.1	-155.3	-180.2	-170.3	-170.8	-175.8	-164	-151.2	-146	-128.3
HSS10	-187.6	-173.9	-160.2	-174.2	-169.3	-173.8	-169.7	-174.1	-166.8	-155.5	-133.5
HSS11	-178.8	-181.9	-159.7	-166.9	-168.3	-180.6	-166.5	-166.4	-165.9	-146.3	-135.1
HSS12	-162.9	-162.4	-168.8	-162.2	-182.6	-175.2	-163.9	-178	-169.6	-177.8	-164.2
HSS13	-167.8	-171.1	-167.2	-156.1	-168.9	-177.3	-173.8	-178.3	-169.8	-172.8	-161.1
HSS14	-152.5	-156.2	-160	-151.1	-171.7	-193.1	-166.3	-170.5	-164.1	-173.3	-155.7
HSS15	-149	-151.7	-157.7	-150.3	-171.3	-173.7	-175.1	-181.7	-173	-165.2	-155.2
HSS16	-161.5	-156.9	-157.9	-148.9	-166.9	-166.9	-170.9	-171.2	-180.3	-167.3	-161.2
HSS17	-150.9	-153.7	-161.2	-152.7	-173	-176.4	-175.7	-170.5	-184.6	-168.1	-158.8
HSS18	-148.7	-154.3	-159.1	-149.6	-176.8	-176.1	-173.7	-161.3	-168	-164.9	-155.4
HSS19	-151.7	-155.5	-160.8	-151.9	-170.8	-173.1	-167.8	-155	-167.5	-172.6	-160.1
HSS20	-152.2	-151.3	-165.4	-157.1	-175.5	-180.7	-169.5	-155.3	-180.3	-169.4	-170.5
HSS21	-156.1	-158.9	-180.4	-163.4	-177.5	-186.3	-173.8	-160.3	-175.3	-169.4	-173.5
HSS22	-161	-151.4	-180.4	-171.4	-181.7	-190.9	-197.4	-159.8	-166	-169.6	-181.1
HSS23	-157.7	-157.1	-146.6	-152.4	-155	-145.4	-128.2	-142.8	-134.2	-135.7	-127.5
HSS24	-142.2	-157.8	-164.3	-150.3	-141.8	-133	-124.9	-123	-130.2	-135.4	-121.2
HSS25	-134.6	-127.2	-128.9	-129.3	-119.7	-115.3	-121.5	-131.2	-129.8	-127.7	-112.4
HSS26	-123.4	-119.2	-116.7	-119.5	-133.8	-143.8	-143.2	-121.6	-117.5	-133.3	-132.9
HSS27	-124.9	-135.4	-137.3	-131.5	-157.6	-150.8	-161.3	-131.1	-140.9	-145.3	-134.5
HSS28	-137	-139.2	-143.4	-135.6	-150.1	-151.3	-152.5	-146.5	-152.3	-156.4	-147.2
HSS29	-126.2	-127.2	-133.5	-125.2	-146.6	-142	-162	-164.3	-150.3	-141.1	-131.8
HSS30	-117.8	-118.4	-134.4	-127.2	-134.5	-134.5	-127.4	-128.9	-129.3	-121	-114.4
HSS31	-99.7	-107.4	-110.7	-121	-129.9	-124.3	-119.5	-116.6	-119.4	-132.5	-145
HSS32	-114.3	-105.3	-138.9	-129.8	-129.6	-124.5	-137.3	-137.4	-131.9	-157.6	-151.1
HSS33	-127.5	-113.3	-123.7	-137	-133.4	-133.4	-135.2	-144.9	-135.3	-156.4	-157.7
HSS34	-121.2	-113.7	-108.7	-119.5	-131.1	-127.6	-128.3	-133.7	-125.4	-148.1	-142.2
HSS35	-112.4	-104.1	-96.3	-98.3	-109.5	-118.5	-118.4	-134.5	-127	-134	-134.6
HSS36	-132.9	-130.6	-127.9	-119.6	-102.9	-99.5	-108.6	-110.6	-121	-128.3	-123.4
HSS37	-134.5	-126.5	-133.7	-123.9	-118.2	-112.5	-105.6	-138.7	-129.7	-129.9	-124.9
HSS38	-147.2	-128.1	-142.8	-134.2	-136.9	-128.1	-112.7	-124.5	-133.4	-135.8	-137
HSS39	-131.8	-125.7	-122.8	-130.2	-132.9	-120.2	-112.3	-108.7	-119.6	-129.7	-126.2

HSS40	-114.4	-124.4	-131.2	-129.7	-126.2	-110.1	-104.6	-96.3	-98.3	-109.7	-117.8
HSS41	-145	-146.2	-121.6	-117.5	-132.7	-132.6	-131.2	-128	-119.9	-104	-99.7
HSS42	-151.1	-160.4	-131.1	-141	-146.7	-135.2	-127.7	-133.7	-123.9	-119	-114.3
HSS43	-139.8	-127.1	-142.8	-151.9	-150.5	-150.7	-153.8	-161.4	-153	-171.1	-173.4
HSS44	-137.9	-123.1	-151.1	-152.3	-150.2	-149.4	-156.5	-159.4	-149.8	-178	-179.7
HSS45	-127.6	-126.2	-148.6	-145.2	-148.9	-152.1	-153.2	-160.9	-152.1	-169.9	-172.4
HSS46	-128.3	-134.5	-146	-146.3	-148.6	-152.8	-150.6	-165.5	-157.3	-174.7	-179.1
HSS47	-133.5	-148.1	-157	-153.2	-151.9	-158	-158.8	-173	-164.9	-180.2	-187.6
HSS48	-135.1	-163.3	-152.5	-152	-159	-160.1	-151.3	-174.1	-168.2	-189.2	-178.8
HSS49	-157.9	-159.3	-134.9	-145.6	-154.3	-164.5	-165.6	-168.8	-162.2	-180.6	-174.3
HSS50	-153.9	-182.9	-133.6	-156.2	-165.8	-163.9	-166.1	-167	-156	-167.8	-177.2
HSS51	-149.8	-162.2	-128.3	-149.5	-159.8	-151.5	-154.8	-160.3	-151.2	-170.6	-208.3
HSS52	-149.2	-142.8	-129.8	-143.7	-154.6	-149.5	-152.2	-157.9	-150.4	-171.2	-174.9
HSS53	-142.1	-132.5	-146.6	-151.6	-158.9	-169.2	-158.9	-158.1	-149.1	-167.3	-167
HSS54	-164.2	-159.8	-169.1	-166.7	-156.9	-156.6	-159.2	-135.1	-145.7	-152.8	-162.9
HSS55	-161.1	-171.1	-159.2	-156.5	-148.9	-154	-172.6	-133.4	-156.1	-160.7	-167.8
HSS56	-155.7	-159.7	-159.3	-156.9	-145	-150.3	-157.7	-128.3	-149.5	-163.6	-152.5
HSS57	-155.2	-152.7	-156.4	-151.1	-159	-148.1	-141.1	-129.8	-143.7	-154.2	-149
HSS58	-161.2	-146.2	-159.4	-149.8	-151.1	-141.7	-131.4	-146.6	-151.6	-159	-161.5
HSS59	-158.8	-145.7	-158.3	-149.2	-158.7	-156.9	-127.4	-142.9	-152	-150.7	-150.9
HSS60	-155.4	-145.7	-154.1	-144.4	-141.8	-135.3	-123.1	-151.1	-152.3	-149.2	-148.7
HSS61	-160.1	-153.7	-156.4	-145.5	-138.3	-126.7	-127	-148.6	-145.2	-149.3	-151.7
HSS62	-170.5	-169.7	-164	-151.3	-149.8	-128	-136.2	-146	-146.3	-149.4	-152.2
HSS63	-173.5	-173.1	-174.4	-166.6	-150.5	-133.5	-151.9	-157	-153.2	-152.6	-156.1
HSS64	-181.1	-168	-166.4	-165.9	-144.3	-135.5	-157.4	-152.5	-152	-159.4	-161

Table 6-16: Received powers from 11 beams of HBS4

	Beam43	**Beam44**	**Beam45**	**Beam46**	**Beam47**	**Beam48**	**Beam49**	**Beam50**	**Beam51**	**Beam52**	**Beam53**
HSS1	-156.1	-150	-156.4	-167.1	-166.9	-164.3	-175.3	-179	-169.4	-173.2	-163.7
HSS2	-147.1	-143.6	-153.7	-163.2	-160.7	-161.2	-168.8	-172.3	-162.8	-166.4	-155.2
HSS3	-144.6	-155.3	-159.6	-169.1	-169.3	-166	-168.9	-171.6	-162.5	-163.3	-154
HSS4	-145.7	-176.1	-173.9	-174.8	-180.8	-175.6	-169.8	-174.3	-163.5	-166.7	-156.8
HSS5	-147.5	-151	-161.2	-161.9	-163.3	-164.6	-164.7	-167.5	-158.3	-161.1	-151.3
HSS6	-146.7	-148.8	-163.9	-160.4	-160.6	-162.2	-166.4	-168.4	-160.6	-164.8	-153.1
HSS7	-142.3	-148.5	-159.2	-156	-155.9	-158.3	-160.7	-163.7	-154.3	-164.3	-179.9
HSS8	-146.5	-158.7	-168.6	-161	-160.8	-165	-165.8	-167.9	-159.5	-159.9	-152.8
HSS9	-143.6	-168	-159.6	-160.3	-159.4	-166.8	-161.5	-164.8	-155.6	-151.8	-143.7
HSS10	-155.1	-161.4	-156.1	-164.4	-162.7	-174.4	-161.2	-165.3	-155.5	-149.3	-149.5
HSS11	-149.7	-162.1	-158.9	-172	-169.8	-174.6	-165.9	-169.9	-160.8	-153.7	-141.5
HSS12	-193.6	-153.5	-149.8	-133.7	-126.5	-143.6	-165.7	-150.5	-153.9	-160.2	-166.6

HSS13	-201.3	-182.8	-172	-164.2	-170.6	-171.6	-177	-184.2	-179.9	-193.2	-187.5
HSS14	-178.9	-140.4	-125.8	-123	-136.2	-139	-156	-144.2	-125.4	-139.7	-148.6
HSS15	-177.6	-152.5	-123.7	-110	-134.8	-130.3	-149.1	-139.8	-127	-138.6	-148.1
HSS16	-190.7	-161.8	-159.6	-173.5	-181.6	-177.6	-191.3	-195	-185.1	-190	-185.4
HSS17	-167.4	-144.8	-154.1	-161.2	-168.3	-167.5	-159	-166.6	-173.2	-154.3	-156.1
HSS18	-154.2	-130.4	-136.2	-145.4	-154.7	-153.1	-177.5	-171.1	-167	-154	-161
HSS19	-161.7	-134.7	-136.8	-148.1	-157	-154.4	-182.9	-173.9	-167.4	-159.8	-159.9
HSS20	-154.6	-144.5	-143.8	-156.6	-165.6	-162.3	-184.4	-185.6	-183.5	-171.9	-156.9
HSS21	-158.7	-136.8	-135.8	-149	-158.4	-154.8	-184.5	-172.1	-166.1	-163.5	-166.3
HSS22	-158	-145.6	-145.7	-158.2	-164.5	-164.1	-186.8	-183.1	-174.7	-170.2	-166.5
HSS23	-118.2	-131.5	-139	-140.9	-141.9	-143.7	-146.1	-148.6	-139.3	-146.1	-135.8
HSS24	-117.9	-132	-143.8	-142.4	-144.4	-145.4	-145.9	-147.8	-139.6	-140.4	-131.1
HSS25	-118.5	-133.9	-138.3	-146.2	-146.4	-143.3	-144	-146.3	-137.7	-137.8	-128.8
HSS26	-134.2	-125.5	-140	-152.6	-143.3	-147.6	-154.2	-158.1	-148.5	-153.4	-141.5
HSS27	-137.3	-109.4	-130	-141.8	-132.3	-135.2	-138.7	-133.5	-120.3	-114.5	-131.4
HSS28	-127.7	-107.5	-117	-125.3	-137.1	-134.5	-124	-127	-132.7	-114.8	-118.5
HSS29	-172.6	-133.4	-156.1	-160.7	-167.8	-171.1	-156.5	-159.2	-156.5	-148.9	-154
HSS30	-157.7	-128.3	-149.5	-163.6	-152.5	-156.2	-157	-159.3	-156.9	-145	-150.3
HSS31	-141.1	-129.8	-143.7	-154.2	-149	-151.7	-154.4	-156.4	-151.1	-159	-148.1
HSS32	-131.4	-146.6	-151.6	-159	-161.5	-156.9	-155.3	-159.4	-149.8	-151.1	-141.7
HSS33	-126.3	-140	-150.2	-151.9	-152.7	-153.9	-153.6	-156.9	-147.6	-151	-140.2
HSS34	-123.1	-151.1	-152.3	-149.2	-148.7	-154.3	-150.6	-154.1	-144.4	-141.8	-135.3
HSS35	-127	-148.9	-146.1	-160.2	-156.9	-154.7	-150.5	-156.4	-145.4	-138.3	-126.8
HSS36	-136.2	-145.8	-147.2	-159	-170.4	-150.4	-154.5	-164.4	-151.3	-149.8	-128
HSS37	-152.1	-155.9	-155.7	-182	-165.1	-156	-161.9	-183.2	-164.6	-150.5	-133.5
HSS38	-128.6	-116.7	-115.5	-126.8	-148.8	-125.7	-140.2	-140.3	-138.6	-118.2	-111.2
HSS39	-119	-123.8	-118.3	-162.5	-152.7	-137.9	-136.5	-143.1	-136.1	-130.7	-111.6
HSS40	-118.5	-140.3	-137	-151.9	-149	-158.7	-146.5	-150.3	-142.9	-133.5	-120.1
HSS41	-114	-141.1	-144.3	-139.4	-138.9	-144.3	-139.9	-144.4	-133.6	-130.6	-127
HSS42	-116.9	-133.7	-142.2	-140.4	-140.5	-143	-143.4	-147.4	-136.7	-144.2	-156.6
HSS43	-114.2	-127.5	-136.7	-137.5	-137.8	-139.7	-143.4	-146.2	-137	-152.3	-135.8
HSS44	-108.2	-111.7	-120.1	-128.5	-127.7	-126.8	-130.1	-119.6	-125.9	-122.7	-113.8
HSS45	-96.4	-93.1	-98.4	-109.4	-117.1	-115.9	-120.1	-116.1	-111.7	-106	-102.5
HSS46	-114.1	-112.9	-106	-93.2	-89.9	-91.6	-114.4	-115.6	-114.5	-121.6	-122.6
HSS47	-121.9	-130.9	-121.5	-119.7	-110.7	-100.4	-124.6	-130.9	-141.7	-141.3	-132.1
HSS48	-126.8	-141.9	-132.7	-138.3	-128	-109.3	-131.3	-143.9	-153.1	-154.7	-143.9
HSS49	-132.9	-142	-132.8	-184.8	-153.8	-155.4	-110.7	-120.8	-130	-130.5	-130.8
HSS50	-123.6	-130.9	-121.8	-163.9	-139.8	-144	-98.8	-106.4	-116	-124.7	-124
HSS51	-114.1	-123.4	-114.8	-143.7	-128	-120.4	-93.2	-91.3	-95.8	-107.9	-115.5
HSS52	-92.6	-101	-107.2	-128.9	-115.2	-116.3	-120.1	-118.9	-111.6	-97.8	-93.2
HSS53	-102.1	-114	-122.5	-145.5	-118.9	-128.8	-129.9	-133.1	-123.7	-119.1	-110.2

HSS54	-153.1	-162.7	-167.6	-179.8	-172	-168.4	-175.9	-168.4	-161.8	-149.4	-156
HSS55	-149.7	-161.8	-158.1	-164.4	-168.4	-157.1	-169	-158.2	-151	-139.4	-142.9
HSS56	-162.1	-156.8	-161.6	-167.6	-172.1	-163.3	-177.2	-163.8	-156.9	-144.5	-145.8
HSS57	-148.6	-160.4	-157.9	-165.4	-168	-157.2	-171.3	-162.1	-155.8	-143.5	-142.7
HSS58	-147.8	-153.3	-151.6	-161.9	-166.5	-153.1	-167.2	-160.4	-155.9	-139.5	-135
HSS59	-157.9	-153.6	-153.7	-162.4	-182.6	-159.4	-166.4	-166.9	-165	-146.2	-136.6
HSS60	-170	-176.8	-176.5	-188.9	-184.4	-182.9	-184.8	-182.8	-172	-163.9	-172.9
HSS61	-137.3	-155.5	-164.6	-140.1	-150	-132.7	-140.9	-140.4	-125.8	-123.8	-135
HSS62	-131.4	-151.8	-150.3	-141.2	-150	-133.8	-146.5	-152.6	-123.7	-111.5	-135.5
HSS63	-177	-189.6	-187.3	-197.7	-198.3	-190.9	-171.5	-161.7	-159.5	-172.2	-179.7
HSS64	-160.9	-172.2	-177.5	-178	-177.5	-177.1	-165.7	-134.8	-142.1	-151.2	-161.8

Table 6-17: Received powers from 11 beams of HBS5

	Beam54	**Beam55**	**Beam56**	**Beam57**	**Beam58**	**Beam59**	**Beam60**	**Beam61**	**Beam62**	**Beam63**	**Beam64**
HSS1	-175.9	-168.4	-161.8	-149.4	-156	-153.1	-162.7	-167.6	-179.8	-172	-168.4
HSS2	-169	-158.2	-151	-139.4	-142.9	-149.7	-161.8	-158.1	-164.4	-168.4	-157.1
HSS3	-177.2	-163.8	-156.9	-144.5	-145.8	-162.1	-156.8	-161.6	-167.6	-172.1	-163.3
HSS4	-171.3	-162.1	-155.8	-143.5	-142.7	-148.6	-160.4	-157.9	-165.4	-168	-157.2
HSS5	-167.2	-160.4	-155.9	-139.5	-135	-147.8	-153.3	-151.6	-161.9	-166.5	-153.1
HSS6	-166.4	-166.9	-165	-146.2	-136.6	-157.9	-153.6	-153.7	-162.4	-182.6	-159.4
HSS7	-184.8	-182.8	-172	-163.9	-172.9	-170	-176.8	-176.5	-188.9	-184.4	-182.9
HSS8	-140.9	-140.4	-125.8	-123.8	-135	-137.3	-155.5	-164.6	-140.1	-150	-132.7
HSS9	-146.5	-152.6	-123.7	-111.5	-135.5	-131.4	-151.8	-150.3	-141.2	-150	-133.8
HSS10	-171.5	-161.7	-159.5	-172.2	-179.7	-177	-189.6	-187.3	-197.7	-198.3	-190.9
HSS11	-165.7	-134.8	-142.1	-151.2	-161.8	-160.9	-172.2	-177.5	-178	-177.5	-177.1
HSS12	-175.3	-179	-169.4	-173.2	-163.7	-156.1	-150	-156.4	-167.1	-166.9	-164.3
HSS13	-168.8	-172.3	-162.8	-166.4	-155.2	-147.1	-143.6	-153.7	-163.2	-160.7	-161.2
HSS14	-168.9	-171.6	-162.5	-163.3	-154	-144.6	-155.3	-159.6	-169.1	-169.3	-166
HSS15	-169.8	-174.3	-163.5	-166.7	-156.8	-145.7	-176.1	-173.9	-174.8	-180.8	-175.6
HSS16	-164.7	-167.5	-158.3	-161.1	-151.3	-147.5	-151	-161.2	-161.9	-163.3	-164.6
HSS17	-166.4	-168.4	-160.6	-164.8	-153.1	-146.7	-148.8	-163.9	-160.4	-160.6	-162.2
HSS18	-160.7	-163.7	-154.3	-164.3	-179.9	-142.3	-148.5	-159.2	-156	-155.9	-158.3
HSS19	-165.8	-167.9	-159.5	-159.9	-152.8	-146.5	-158.7	-168.6	-161	-160.8	-165
HSS20	-161.5	-164.8	-155.6	-151.8	-143.7	-143.6	-168	-159.6	-160.3	-159.4	-166.8
HSS21	-161.2	-165.3	-155.5	-149.3	-149.5	-155.1	-161.4	-156.1	-164.4	-162.7	-174.4
HSS22	-165.9	-169.9	-160.8	-153.7	-141.5	-149.7	-162.1	-158.9	-172	-169.8	-174.6
HSS23	-140.2	-140.3	-138.6	-118.2	-111.2	-128.6	-116.7	-115.5	-126.8	-148.8	-125.7
HSS24	-136.5	-143.1	-136.1	-130.7	-111.6	-119	-123.8	-118.3	-162.5	-152.7	-137.9
HSS25	-146.5	-150.3	-142.9	-133.5	-120.1	-118.5	-140.3	-137	-151.9	-149	-158.7
HSS26	-139.9	-144.4	-133.6	-130.6	-127	-114	-141.1	-144.3	-139.4	-138.9	-144.3

HSS27	-143.4	-147.4	-136.7	-144.2	-156.6	-116.9	-133.7	-142.2	-140.4	-140.5	-143
HSS28	-146.1	-148.6	-139.3	-146.1	-135.8	-118.2	-131.5	-139	-140.9	-141.9	-143.7
HSS29	-145.9	-147.8	-139.6	-140.4	-131.1	-117.9	-132	-143.8	-142.4	-144.4	-145.4
HSS30	-144	-146.3	-137.7	-137.8	-128.8	-118.5	-133.9	-138.3	-146.2	-146.4	-143.3
HSS31	-154.2	-158.1	-148.5	-153.4	-141.5	-134.2	-125.5	-140	-152.6	-143.3	-147.6
HSS32	-138.7	-133.5	-120.3	-114.5	-131.4	-137.3	-109.4	-130	-141.8	-132.3	-135.2
HSS33	-124	-127	-132.7	-114.8	-118.5	-127.7	-107.5	-117	-125.3	-137.1	-134.5
HSS34	-156.5	-159.2	-156.5	-148.9	-154	-172.6	-133.4	-156.1	-160.7	-167.8	-171.1
HSS35	-157	-159.3	-156.9	-145	-150.3	-157.7	-128.3	-149.5	-163.6	-152.5	-156.2
HSS36	-154.4	-156.4	-151.1	-159	-148.1	-141.1	-129.8	-143.7	-154.2	-149	-151.7
HSS37	-155.3	-159.4	-149.8	-151.1	-141.7	-131.4	-146.6	-151.6	-159	-161.5	-156.9
HSS38	-153.6	-156.9	-147.6	-151	-140.2	-126.3	-140	-150.2	-151.9	-152.7	-153.9
HSS39	-150.6	-154.1	-144.4	-141.8	-135.3	-123.1	-151.1	-152.3	-149.2	-148.7	-154.3
HSS40	-150.5	-156.4	-145.4	-138.3	-126.8	-127	-148.9	-146.1	-160.2	-156.9	-154.7
HSS41	-154.5	-164.4	-151.3	-149.8	-128	-136.2	-145.8	-147.2	-159	-170.4	-150.4
HSS42	-161.9	-183.2	-164.6	-150.5	-133.5	-152.1	-155.9	-155.7	-182	-165.1	-156
HSS43	-159	-166.6	-173.2	-154.3	-156.1	-167.4	-144.8	-154.1	-161.2	-168.3	-167.5
HSS44	-177.5	-171.1	-167	-154	-161	-154.2	-130.4	-136.2	-145.4	-154.7	-153.1
HSS45	-182.9	-173.9	-167.4	-159.8	-159.9	-161.7	-134.7	-136.8	-148.1	-157	-154.4
HSS46	-184.4	-185.6	-183.5	-171.9	-156.9	-154.6	-144.5	-143.8	-156.6	-165.6	-162.3
HSS47	-184.5	-172.1	-166.1	-163.5	-166.3	-158.7	-136.8	-135.8	-149	-158.4	-154.8
HSS48	-186.8	-183.1	-174.7	-170.2	-166.5	-158	-145.6	-145.7	-158.2	-164.5	-164.1
HSS49	-165.7	-150.5	-153.9	-160.2	-166.6	-193.6	-153.5	-149.8	-133.7	-126.5	-143.6
HSS50	-177	-184.2	-179.9	-193.2	-187.5	-201.3	-182.8	-172	-164.2	-170.6	-171.6
HSS51	-156	-144.2	-125.4	-139.7	-148.6	-178.9	-140.4	-125.8	-123	-136.2	-139
HSS52	-149.1	-139.8	-127	-138.6	-148.1	-177.6	-152.5	-123.7	-110	-134.8	-130.3
HSS53	-191.3	-195	-185.1	-190	-185.4	-190.7	-161.8	-159.6	-173.5	-181.6	-177.6
HSS54	-110.7	-120.8	-130	-130.5	-130.8	-132.9	-142	-132.8	-184.8	-153.8	-155.4
HSS55	-98.8	-106.4	-116	-124.7	-124	-123.6	-130.9	-121.8	-163.9	-139.8	-144
HSS56	-93.2	-91.3	-95.8	-107.9	-115.5	-114.1	-123.4	-114.8	-143.7	-128	-120.4
HSS57	-120.1	-118.9	-111.6	-97.8	-93.2	-92.6	-101	-107.2	-128.9	-115.2	-116.3
HSS58	-129.9	-133.1	-123.7	-119.1	-110.2	-102.1	-114	-122.5	-145.5	-118.9	-128.8
HSS59	-143.4	-146.2	-137	-152.3	-135.8	-114.2	-127.5	-136.7	-137.5	-137.8	-139.7
HSS60	-130.1	-119.6	-125.9	-122.7	-113.8	-108.2	-111.7	-120.1	-128.5	-127.7	-126.8
HSS61	-120.1	-116.1	-111.7	-106	-102.5	-96.4	-93.1	-98.4	-109.4	-117.1	-115.9
HSS62	-114.4	-115.6	-114.5	-121.6	-122.6	-114.1	-112.9	-106	-93.2	-89.9	-91.6
HSS63	-124.6	-130.9	-141.7	-141.3	-132.1	-121.9	-130.9	-121.5	-119.7	-110.7	-100.4
HSS64	-131.3	-143.9	-153.1	-154.7	-143.9	-126.8	-141.9	-132.7	-138.3	-128	-109.3

7. Bibliography

[1] M. Goldhamer, *et al.* BuNGee D1.2 Baseline RRM & JointAccess/Self-Backhaul Protocols. 2011.

[2] P. Kyosti, *et al.*, "IST-WINNER D1.1.2 WINNER II Channel Models," Available: https://www.ist-winner.org/WINNER2-Deliverables/D1.1.2v1.1.pdf2007.

[3] P. Hemphill and M. Ware, "BuNGee D2.2 Final Reprot on BuNGee Antenna," 2011.

[4] N. Khan, *et al.*, "BuNGee D2.1 Final BuNGee Channel Models," UCL2011.

[5] Z. Kowalczyk, *et al.*, "BuNGee D1.1 Functional BuNGee Specs, Economic model, Energy efficiency & Frequency Bands " 2010.

[6] T. Jiang, *et al.* BuNGee D4.1.1 Interim Simulation. 2011.

[7] I. E. Telatar, "Capacity of multi-antenna Gaussian channels," *European Transactions on Telecommunications,* vol. 10, pp. 585-595, Nov. 1999.

[8] A. G. Burr, "Bounds and estimates of the uplink capacity of cellular systems," in *Vehicular Technology Conference, 1994 IEEE 44th*, Jun. 1994, pp. 1480-1484 vol.3.

[9] M. Chiani, "Introducing erasures in decision-feedback equalization to reduce error propagation," *Communications, IEEE Transactions on,* vol. 45, pp. 757-760, July 1997.

[10] P. Li and R. C. d. Lamare, "Adaptive Decision-Feedback Detection With Constellation Constraints for MIMO Systems," *Vehicular Technology, IEEE Transactions on,* vol. 61, pp. 853-859, Feb. 2012.

[11] P. Li, R. C. d. Lamare, and R. Fa, "Multiple Feedback Successive Interference Cancellation Detection for Multiuser MIMO Systems," *IEEE Transactions on Wireless Communications,* vol. 10, pp. 2434-2439, Aug. 2011.

[12] M. Goldhamer, "Frequency Planning," in *5th BuNGee Project Meeting*, 2010.

[13] S. Haykin, "Cognitive Radio: Brain-Empowered Wireless Communications," *IEEE Journal on selected areas in communications,* vol. 23, pp. 201-220, Feb, 2005

8. Release History

Please give details in the table below about successive releases:

Release number	Date	Comments	Dissemination of this release (task level, WP/SP level, Project Office Manager, Steering Committee, etc)
0.0.1	22/05/2012		Document submitted to the BuNGee Consortium
1.0.0	07/06/2012		Document submitted to EC